

Robust Fully-Asynchronous Methods for Distributed Training over General Architecture

Zehan Zhu¹, Ye Tian², Yan Huang¹, Jinming Xu^{1†}, Shibo He¹

Abstract—Perfect synchronization in distributed machine learning problems is inefficient and even impossible due to the existence of latency, package losses and stragglers. We propose a Robust Fully-Asynchronous Stochastic Gradient Tracking method (R-FAST), where each device performs local computation and communication at its own pace without any form of synchronization. Different from existing asynchronous distributed algorithms, R-FAST can eliminate the impact of data heterogeneity across devices and allow for packet losses by employing a robust gradient tracking strategy that relies on properly designed auxiliary variables for tracking and buffering the overall gradient vector. More importantly, the proposed method utilizes two spanning-tree graphs for communication so long as both share at least one common root, enabling flexible designs in communication architectures. We show that R-FAST converges in expectation to a neighborhood of the optimum with a geometric rate for smooth and strongly convex objectives; and to a stationary point with a sublinear rate for general non-convex settings. Extensive experiments demonstrate that R-FAST runs 1.5-2 times faster than synchronous benchmark algorithms, such as Ring-AllReduce and D-PSGD, while still achieving comparable accuracy, and outperforms existing asynchronous SOTA algorithms, such as AD-PSGD and OSGP, especially in the presence of stragglers.

Index Terms—Distributed machine learning, fully-asynchronous methods, spanning-tree topology.

I. INTRODUCTION

IN the past decade, deep learning [1] has shown great success in various fields, such as computer vision [2], natural language processing [3], autonomous driving [4]. Training modern deep neural networks to desirable accuracy usually requires an enormous number of training samples, which results in significant consumption of computing resources. Multiple computing devices can thus be employed to accelerate such large-scale training tasks [5]. In particular, one consider solving the following distributed stochastic optimization problem via a group of workers:

$$\min_{x \in \mathbb{R}^p} F(x) \triangleq \sum_{i=1}^n \left(f_i(x) \triangleq \mathbb{E}_{\zeta_i \sim \mathcal{D}_i} [l(x; \zeta_i)] \right), \quad (1)$$

where \mathcal{D}_i denotes the distribution of sample ζ_i locally stored at node i and $l(\cdot)$ denotes the local loss function. This setting also covers the empirical risk minimization (ERM) problems with \mathcal{D}_i being the local training dataset. The workers are connected over a communication network for information

exchange. Collaboratively, all workers seek the global optimal parameter x minimizing the global loss function F .

The stochastic gradient descent (SGD) is a commonly used technique for solving the above large-scale training problem [6]–[8]. However, standard SGD is not scaling well to large data sets due to its inherently sequential way of updating [9]. In particular, parallel and distributed architectures are employed for large-scale training using SGD, e.g., Parallel SGD [10], [11] which has a parameter server responsible for aggregating gradients from clients and updating model parameters; Ring-AllReduce SGD [12], [13] which computes the exact average of gradients via a ring network in a decentralized manner; and Distributed SGD [14], D² [15], DSGT [16], S-AB [17] that rely on approximate averaging of model parameters via certain gossip protocols over a peer-to-peer network. These abovementioned algorithms need to rely on perfect synchronization during frequent communications, which limits their application to real scenarios where one usually observes the presence of stragglers and high latency of the network communication channel due to limited bandwidth [18], [19].

Asynchronous parallel and distributed algorithms have thus been proposed to overcome the above drawback [20]. The existing works, however, usually impose stringent conditions on their asynchronous models, e.g., updating according to specific activating rules [21], requiring real-time information mixing among a subset of nodes [22], and computing at the same pace for all nodes [23]. Besides, they rely on certain architecture for communication, such as undirected graphs [22] or fixed strongly connected digraphs [24], [25], which limits the underlying network structure. Moreover, they usually suffer from the deteriorating effect on the convergence performance caused by data heterogeneity across computing devices [22], [23] and can not effectively deal with unpredictable packet losses [22]–[24].

In this paper, we propose a Robust Fully-Asynchronous Stochastic Gradient Tracking method (termed R-FAST) to address all the above identified issues. Our main contributions are summarized as follows:

- 1) **New robust fully asynchronous algorithms over general architectures.** The proposed R-FAST method allows each node to perform the local communication and computation at its own pace, without any form of synchronization and imposing no restriction on the arriving order of communication messages. Besides, R-FAST avoids the deteriorating effect from data heterogeneity on the convergence rate, and allows for package losses thanks to the introduced robust gradient tracking scheme. More importantly, R-FAST works on general communication

¹Z. Zhu, Y. Huang, J. Xu and S. He (12032045, huangyan5616, jimmyxu, s18he@zju.edu.cn) are with the College of Control Science and Engineering, Zhejiang University, Hangzhou 310027, China. ²Y. Tian (yetianf@amazon.com) is currently with Amazon, NY 10018, USA, and his work of this paper is done prior to him joining Amazon.

[†]Correspondence to jimmyxu@zju.edu.cn.

graphs containing spanning trees that share at least one common root, which enables flexible design of the underlying network architecture, including PS, Ring and Gossip structure as special cases.

- 2) **Provable convergence guarantee.** We prove that R-FAST converges linearly in expectation to a neighborhood of the optimal solution, for strongly convex objectives and finds a stationary point at a rate of $\mathcal{O}(1/\sqrt{K})$ for non-convex objectives. Our proof relies on a properly designed augmented system to account for unpredictable delays and package losses. Different from [17], [26], we carry out the analysis over a properly chosen time period in which common root nodes of two spanning-tree graphs will be activated at least once, ensuring the contraction property for strongly convex cases. For non-convex cases, we develop a new decent lemma leveraging *two-time-scale techniques* that allow us to build an inequality within a properly chosen time window, yielding a valid decent towards the stationary point.
- 3) **Extensive experimental evaluations.** Experiments of training logistic regression model on MNIST dataset show that the proposed R-FAST algorithm can work over general network architectures such as binary-tree, line, and directed ring structures. In addition, large-scale image classification tasks of training ResNet50 on ImageNet dataset show that R-FAST converges 1.5-2 times faster than the synchronous algorithms while enjoys higher testing accuracy than the well-known asynchronous algorithms such as AD-PSGD [22] and OSGP [23], especially in the presence of a straggler. Moreover, we show the good scalability of R-FAST in the number of nodes.

II. RELATED WORK

A. On Asynchronous Model

Parallel schemes where there is a center (e.g., parameter server) responsible for aggregating gradients and updating model parameters have been widely employed for the parallel update of SGD, and corresponding asynchronous versions have been proposed recently. For example, Recht *et al.* [27] designed an asynchronous algorithm called HOGWILD!, where different processors have access to a shared memory that can be overwritten at any time. Duchi *et al.* [28] proposed an A-PSGD algorithm that allows the central parameter server to use stale gradients received from clients to update model parameters. Dean *et al.* [9] developed a DistBelief framework based on which they designed Downpour SGD where the model replicas run independently of each other and the parameter server maintains the current model parameters. Building on A-PSGD, Lian *et al.* [29] studied two asynchronous parallel implementations of SGD for non-convex problems and established a sublinear rate of $\mathcal{O}(1/\sqrt{K})$. To obtain better performance, Zhang *et al.* [30] proposed staleness-aware async-SGD, where the central server keeps track of the staleness associated with each gradient computation and adjusts the learning rate according to the staleness value. To deal with both the issues of stale gradients and non-IID data, Zhou *et al.* [31] proposed an asynchronous algorithm

termed WKAFL, where the central server assigns each of the first K received stale gradients with a weight based on its cosine similarity with respect to the estimated global unbiased gradient. The above asynchronous parallel schemes, however, rely on a center to aggregate gradients from clients, which may become the potential bottleneck due to high communication burden and suffer from the single point failure [22].

To address the above issues, numerous decentralized optimization algorithms are proposed for training deep neural networks, and some form of asynchrony are allowed. For instance, Ram *et al.* [21] proposed an asynchronous decentralized algorithm based on gossip protocols where each worker wakes up randomly according to the local Poisson clock and selects a neighbor to exchange parameters, while no any communication delay is allowed which calls for certain coordination among the workers. Lian *et al.* [22] developed an asynchronous decentralized algorithm, termed AD-PSGD, which allows for using stale gradients for update. However, they consider only undirected graph and requires real-time communication and information mixing among a group of agents at each iteration assuming the frequency of updating for each worker is known a priori, which imposes a key challenge for synchronization. To make it applicable to general digraphs, Assran *et al.* [23] proposed SGP based on push-sum protocol [32] and developed an asynchronous variant OSGP which allows for communication delays but requires all agents perform computation at the same pace. Building on SGP, Spiridonoff *et al.* [33] developed RASGP which enables each agent updating at its own pace, but requires all messages arriving in the order they were sent. There has been also some other efforts attempting to decompose the operation of exact average of all workers (c.f., AllReduce [12]) into a series of exact average of a subset of nodes [18], [34]. In particular, they use Partial-Reduce primitive instead of AllReduce primitive to compute the exact average whenever a bunch of nodes finish updating, thus accounting for computing heterogeneity among workers but still require blocking for synchronization among that bunch of nodes. To sum up, these abovementioned asynchronous distributed algorithms usually assume stringent conditions on their asynchronous models and thus can not be implemented in a *fully asynchronous* manner.

B. On Robustness

Existing asynchronous methods usually suffer from certain robustness issues due to data heterogeneity across computing devices, package losses and strict requirement on the underlying network architecture. For instance, the algorithms in [22], [23] suffer from the deteriorating effect on their convergence rates due to data heterogeneity across computing devices. To cope with such issue, Zhang *et al.* [24] proposed an asynchronous APPG algorithm which can alleviate the effect of data heterogeneity leveraging gradient tracking scheme [16], [17], [35]–[37] that corrects the gradient descent direction over time, but works only for deterministic problems and does not allow for package losses. The aforementioned RASGP [33] can handle packet losses but the result therein is established only for strongly convex objectives. The recently proposed

ASY-SONATA algorithm [25] can deal with both the issues of data heterogeneity and package loss, but works only for deterministic optimization problems. Kungurtsev *et al.* [38] extended the ASY-SONATA algorithm to consider stochastic gradient update and established a sublinear rate merely for nonconvex objective functions.

To the best of our knowledge, most decentralized optimization algorithms are only applicable to doubly stochastic weight matrices which are, indeed, not easy to design or even impossible for certain graphs [39]. The aforementioned algorithms [24], [38] based on gradient tracking strategy can work on two separate weight matrices (i.e., one being row stochastic and the other column stochastic) but require the two corresponding subgraphs to be both strongly-connected. Push-Pull methods [26] relax the above requirements and can work on two separate subgraphs as long as both contain a spanning tree and share a common root. This property admits great flexibility in designing the underlying network architecture, including popular structures such as Parameter Server, Ring and Gossip. However, similar to APPG, Push-Pull methods work only for deterministic optimization problems.

III. PRELIMINARY

A. Network Model

We consider that all workers cooperate to solve Problem (1) over a network modeled as a directed graph $\mathcal{G} = (\mathcal{V}, \mathcal{E})$ where $\mathcal{V} = \{1, 2, \dots, n\}$ denotes the set of nodes and $\mathcal{E} \subset \mathcal{V} \times \mathcal{V}$ denotes the set of edges/communication links. Let $\mathcal{G}(M)$ denote the graph induced by a non-negative matrix $M \in \mathbb{R}^{n \times n}$ such that $(j, i) \in \mathcal{E}(M)$ if and only if $M_{ij} > 0$. We use $\mathcal{N}_i^{\text{in}}(M) \triangleq \{j \mid M_{ij} > 0, j \in \mathcal{V}\}$ and $\mathcal{N}_i^{\text{out}}(M) \triangleq \{j \mid M_{ji} > 0, j \in \mathcal{V}\}$ to denote the sets of in-neighbors and out-neighbors that node i can communicate with.

B. Push-Pull Protocol

The proposed algorithm is developed based on synchronous push-pull algorithm proposed in [40], which has been recently employed to solve the ERM problem (1) over general digraphs [26]. The update of each agent i is as follows

$$x_i^{t+1} = \sum_{j=1}^n w_{ij} (x_j^t - \gamma^t z_j^t) \quad (2a)$$

$$z_i^{t+1} = \sum_{j=1}^n a_{ij} z_j^t + \nabla f_i(x_i^{t+1}) - \nabla f_i(x_i^t) \quad (2b)$$

with $z_i^0 = \nabla f_i(x_i^0)$ for $\forall i \in \mathcal{V}$. In (2), x_i^t and z_i^t are two estimates maintained by node i for the global optimal decision variable and the global gradient $\frac{1}{n} \nabla F$, respectively. It relies on two properly designed weight matrices for information exchange among nodes, that is, each node i uses $W \triangleq [w_{ij}]_{n \times n}$ to pull information of the decision variable from its in-neighbors $j \in \mathcal{N}_i^{\text{in}}(W)$ for reaching consensus, while using $A \triangleq [a_{ij}]_{n \times n}$ to push gradient information to its out-neighbors $j \in \mathcal{N}_i^{\text{out}}(A)$ for tracking the global gradient. To ensure the convergence of the update (2), the following assumptions are imposed on the two weight matrices as well as their induced graphs [26].

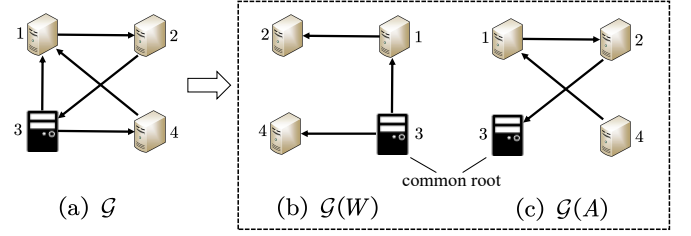


Figure 1. Illustration of a directed graph constructed by two spanning trees.

Assumption 1 (On the weight matrices). Let $M \in \mathbb{R}^{n \times n}$ denote either A or W . We have:

- i) $M_{ii} > 0, \forall i \in \mathcal{V}$; and $\min \{M_{ij} \mid M_{ij} > 0\} \geq \bar{m} > 0$.
- ii) W is row-stochastic and A is column-stochastic, i.e., $W\mathbf{1} = \mathbf{1}$ and $\mathbf{1}^\top A = \mathbf{1}^\top$.

Assumption 2 (On the induced graphs). The graph $\mathcal{G}(W)$ and $\mathcal{G}(A^\top)$ each contains at least one spanning tree, and at least one pair of the spanning trees of $\mathcal{G}(W)$ and $\mathcal{G}(A^\top)$ share a common root. That is, $\mathcal{R} \triangleq \mathcal{R}_W \cap \mathcal{R}_{A^\top} \neq \emptyset$ and $r \triangleq |\mathcal{R}| \geq 1$, where \mathcal{R}_W (resp. \mathcal{R}_{A^\top}) denotes the set of roots of all possible spanning trees in the graph $\mathcal{G}(W)$ (resp. $\mathcal{G}(A^\top)$).

Remark 1. Assumption 2 imposes a minimum requirement to guarantee an unobstructed information flow among nodes while most existing distributed/decentralized algorithms [16], [17], [24], [37] require every communication graph to be strongly connected, which limits the possibility in architecture design. For instance, the digraph \mathcal{G} with 4 nodes as shown in Figure 1(a) does not permit a doubly stochastic weight matrix [39], but can be split into two sub-graphs $\mathcal{G}(W)$ and $\mathcal{G}(A)$ (c.f., Figure 1(b) and 1(c)). Clearly, both of $\mathcal{G}(W)$ and $\mathcal{G}(A^\top)$ contain a spanning tree, and they share a common root – node 3. The information flow can thus happen between any pair of nodes via the hub node 3.

IV. THE PROPOSED R-FAST ALGORITHM

In this section, we present the proposed R-FAST method which employs three key schemes to allow it to be implemented in a fully asynchronous manner and enhance its robustness and efficiency, which are depicted as follows:

- i) **Fully-Asynchronous mechanism.** Each node performs autonomous computation and communication at its own pace without any synchronization;
- ii) **Communication over spanning trees.** Nodes exchange messages over two subgraphs $\mathcal{G}(W)$ and $\mathcal{G}(A)$ induced by the weight matrices W and A respectively, so long as each contains a spanning tree and both have at least one common root;
- iii) **Robust gradient tracking.** We employ the standard gradient tracking scheme to track the global gradient. Additionally, we introduce the auxiliary running-sum variable ρ_{ji} accumulating the tracking variable z_i (up to some scaling factor) and the buffer variable $\bar{\rho}_{ij}$ to tackle package losses.

Now, we proceed to the specific implementation of the algorithm, as summarized in Algorithm 1. It depicts the updates of any node, from a local perspective. Being *blind* to the progress of the entire system, every node i maintains a local iteration counter t_i (the subscript i is omitted from i 's local view to simplify notation), and updates at its own pace in a fully asynchronous way.

Algorithm 1 Robust Fully Asynchronous Stochastic Gradient Tracking (R-FAST)

- 1: **Initialization:** $x_i^0 \in \mathbb{R}^p$, $z_i^0 = \nabla f_i(x_i^0; \zeta_i^0)$, $\tau_{v,ij}^0 = \tau_{\rho,ij}^0 = 0$, $v_i^0 = \rho_{ij}^0 = \tilde{\rho}_{ij}^0 = 0$, $t = 0$.
 - 2: **While:** each node i asynchronously **do**
 - 3: (S1) **Perform local descent:** $v_i^{t+1} = x_i^t - \gamma^t z_i^t$
 - 4: (S2) **Process received messages:**
 - 5: a) $x_i^{t+1} = w_{ii}v_i^{t+1} + \sum_{j \in \mathcal{N}_i^{\text{in}}(W)} w_{ij}v_j^{\tau_{v,ij}^t}$
 - 6: with $\tau_{v,ij}^t$ being the largest local iteration stamp received from $j \in \mathcal{N}_i^{\text{in}}(W)$
 - 7: b) $z_i^{t+\frac{1}{2}} = z_i^t + \sum_{j \in \mathcal{N}_i^{\text{in}}(A)} \left(\rho_{ij}^{\tau_{\rho,ij}^t} - \tilde{\rho}_{ij}^t \right) + \nabla f_i(x_i^{t+1}; \zeta_i^{t+1}) - \nabla f_i(x_i^t; \zeta_i^t)$
 - 8: with $\tau_{\rho,ij}^t$ being the largest local iteration stamp received from $j \in \mathcal{N}_i^{\text{in}}(A)$
 - 9: c) $z_i^{t+1} = a_{ii}z_i^{t+\frac{1}{2}}$; $\rho_{ji}^{t+1} = \rho_{ji}^t + a_{ji}z_i^{t+\frac{1}{2}}$
 - 10: (S3) **Send information to its out-neighbors:**
 - 11: a) Send $(t+1, v_i^{t+1})$ to every $j \in \mathcal{N}_i^{\text{out}}(W)$
 - 12: b) Send $(t+1, \rho_{ji}^{t+1})$ to every $j \in \mathcal{N}_i^{\text{out}}(A)$
 - 13: (S4) **Update buffer:** $\tilde{\rho}_{ij}^{t+1} = \rho_{ij}^{\tau_{\rho,ij}^t}$, $\forall j \in \mathcal{N}_i^{\text{in}}(A)$
 - 14: (S5) **Increase local iteration counter:** $t = t + 1$
 - 15: **end**
-

The algorithm is constituted by three main steps: **i) Local descent.** With z_i^t being a proxy to the stochastic $\nabla F(\cdot)$, each agent i firstly performs an approximate stochastic gradient descent on x_i^t at (S1), generating the intermediate result v_i^{t+1} . The agent will then communicate with its neighbors over the two directed sub-graphs $\mathcal{G}(W)$ and $\mathcal{G}(A)$ in order to: 1) force consensus on v_i^{t+1} to form the next estimate x_i^{t+1} , and 2) update the gradient tracking variable z_i^t . **ii) Local communication for consensus and gradient-tracking.** At step (S2, a), the agent forms x_i^{t+1} as a weighted average of its most recent v_i^{t+1} and the v variables received from its in-neighbors, using the weights w_{ij} . For any v_j variable from $j \in \mathcal{N}_i^{\text{in}}(W)$, agent i will not be able to understand the extent of how outdated v_j currently is. However, among all v_j variables being available to i , agent i is able to pick up the most updated one, because each agent attaches its local iteration counter for any information packet it sends out. Thus we use $\tau_{v,ij}^t$ to denote j 's largest local iteration counter attached to the v_j variable, which is picked up by agent i when forming x_i^{t+1} . Regarding the update of z variables, we adopt the robust tracking method from [25]. Agent i maintains variables ρ_{ji} as the running sum of z_i (up to some scaling factor) over time for each out-neighbor $j \in \mathcal{N}_i^{\text{out}}(A)$, and also a buffer variable $\tilde{\rho}_{ij}$ for each in-neighbor $j \in \mathcal{N}_i^{\text{in}}(A)$. It picks up the most updated ρ_{ij} for each $j \in \mathcal{N}_i^{\text{in}}(A)$ among all the

available. The index notation $\tau_{\rho,ij}^t$ possesses the same logic as $\tau_{v,ij}^t$, but for the ρ variable now. The difference $\rho_{ij}^{\tau_{\rho,ij}^t} - \tilde{\rho}_{ij}^t$ captures the sum of the scaled z_j variables generated by j but unseen by i until i 's t -th local iteration. In addition, it samples a random local gradient $\nabla f_i(x_i^{t+1}; \zeta_i^{t+1})$ at x_i^{t+1} . With all the information ready, agent i generates $z_i^{t+1/2}$ at (S2, b), through adding the new gradient sample $\nabla f_i(x_i^{t+1}; \zeta_i^{t+1})$ while clearing out the old $\nabla f_i(x_i^t; \zeta_i^t)$. Afterwards, $z_i^{t+1/2}$ is used to update z_i^{t+1} and ρ_{ji}^{t+1} respectively at step (S2, c). **iii) Update the buffer variables.** After sending the information packets to its out-neighbors at (S3), agent i set the buffer variable $\tilde{\rho}$ as most recently consumed ρ variable at step (S4). Lastly, it increase the local iteration counter at (S5). Thanks to the introduction of robust gradient tracking scheme, the proposed algorithm is able to deal with unpredictable package loss due to the fact the running-sum variable ρ maintains all the historical information regarding the gradient z .

Algorithm 2 Robust Fully Asynchronous Stochastic gradient Tracking (R-FAST, Global View)

- Initialization:** $x_i^0 \in \mathbb{R}^p$, $z_i^0 = \nabla f_i(x_i^0; \zeta_i^0)$, $v_i^0 = \rho_{ij}^0 = \tilde{\rho}_{ij}^0 = 0$; $\rho_{ij}^\ell = v_i^\ell = 0$, $\forall \ell \in \{-D, -D+1, \dots, 0\}$; $t_i^0 = k = 0$
- While:** a termination criterion is not met **do**
- (S.0) **Pick:** $i^k, d_{v,j}^k$ for $\forall j \in \mathcal{N}_i^{\text{in}}(W)$, $d_{\rho,j}^k$ for $\forall j \in \mathcal{N}_i^{\text{in}}(A)$
- (S.1) **Perform local descent:** $v_{i^k}^{k+1} = x_{i^k}^k - \gamma^k z_{i^k}^k$
- (S.2) **Process received messages:**
- a) $x_{i^k}^{k+1} = w_{i^k i^k} v_{i^k}^{k+1} + \sum_{j \in \mathcal{N}_{i^k}^{\text{in}}(W)} w_{i^k j} v_j^{k-d_{v,j}^k}$
- b) $z_{i^k}^{k+\frac{1}{2}} = z_{i^k}^k + \sum_{j \in \mathcal{N}_{i^k}^{\text{in}}(A)} \left(\rho_{i^k j}^{k-d_{\rho,j}^k} - \tilde{\rho}_{i^k j}^k \right) + \nabla f_{i^k}(x_{i^k}^{k+1}; \zeta_{i^k}^{k+1}) - \nabla f_{i^k}(x_{i^k}^k; \zeta_{i^k}^k)$
- c) $z_{i^k}^{k+1} = a_{i^k i^k} z_{i^k}^{k+\frac{1}{2}}$, $\rho_{ji^k}^{k+1} = \rho_{ji^k}^k + a_{ji^k} z_{i^k}^{k+\frac{1}{2}}$, $\forall j \in \mathcal{N}_{i^k}^{\text{out}}(A)$
- (S.3) **Send information to out-neighbors:**
- a) Send $(t_{i^k}^k + 1, v_{i^k}^{k+1})$ to every $j \in \mathcal{N}_{i^k}^{\text{out}}(W)$
- b) Send $(t_{i^k}^k + 1, \rho_{ji^k}^{k+1})$ to every $j \in \mathcal{N}_{i^k}^{\text{out}}(A)$
- (S.4) **Update buffer:** $\tilde{\rho}_{i^k j}^{k+1} = \rho_{i^k j}^{k-d_{\rho,j}^k}$, $\forall j \in \mathcal{N}_{i^k}^{\text{in}}(A)$
- (S.5) **Increase iteration counter:**
- a) $t_{i^k}^k = t_{i^k}^k + 1$
- b) Untouched state variables shift to state $k+1$ while keeping the same value
- c) $k \leftarrow k + 1$
-

From local view to global view. While the Algorithm 1 and the above description are from the local view of agent i in order to facilitate the understanding of the training process of R-FAST, we need a global iteration counter k to measure the progress of the entire system and raise theoretical convergence analysis. Algorithm 2 depicts the global view. The increase on the global iteration counter $k \leftarrow k + 1$ is triggered whenever any agent finishes one local iteration, and we use i^k to indicate such agent. $t_{i^k}^k$ is i^k 's local iteration counter. Posterior to the

asynchronous process, we define: i) $l : k \rightarrow (i, t)$, mapping the global iteration counter k to the associated active agent $i = i^k$ and its local iteration counter t as of the k -th global iteration; and ii) the inverse of l as $g : (i, t) \rightarrow k$. With these tools, we can measure the delayed extent of any received packet $v_j^{\tau_{v,ij}^t}$ in the global view: since $v_j^{\tau_{v,ij}^t}$ is generated at node j 's local iteration $\tau_{v,ij}^t - 1$ and equivalently the global iteration $g(j, \tau_{v,ij}^t - 1)$, the delay of the packet in global view is thus $d_{v,j}^k = k - g(j, \tau_{v,ij}^t - 1) - 1$, with $k = g(i, t)$. We define $d_{\rho,j}^k$ similarly for the ρ variables. We consider the following asynchronous model in this work.

Assumption 3 (On the asynchronous model).

- i) $\exists T \in \mathbb{N}$ and $T \geq n$ such that $\cup_{t=k}^{k+T-1} i^t = \mathcal{V}$, for all $k \in \mathbb{N}$;
- ii) $\exists D \in \mathbb{N}$ such that $0 \leq d_{v,j}^k, d_{\rho,j}^k \leq D$, for all $k \in \mathbb{N}$.

The above assumption rules out scenarios where some nodes have infinitely long inactive time and/or some transmission links fail for infinitely long time. The following remark shows that the synchronous counterpart of R-FAST, indeed, falls into our asynchronous model.

Remark 2. In Algorithm 1, if we have $\tau_{v,ij}^t = \tau_{\rho,ij}^t = t$ hold for $\forall i, j, t$, the algorithm reduces to a synchronous one. For example, to compute x_i^{t+1} , agent i needs to wait until all v_j^t from $\forall j \in \mathcal{N}_i^{\text{in}}(W)$ become available. The same coordination applies to the update of the z variable. To cast the synchronous scenario into the global view introduced above, one can set $i^k = (k \bmod n) + 1$, i.e., $\{i^k\}_{k=0}^\infty = \{1, 2, 3, \dots, n, 1, 2, \dots\}$. Therefore, we have $d_{v,j}^k = d_{\rho,j}^k = k - g(j, t - 1) - 1 = k - g(j, \lfloor \frac{k}{n} \rfloor - 1) - 1 = k - (\lfloor \frac{k}{n} \rfloor - 1)n - j < 2n - 2$. Clearly, synchronous updates satisfies Assumption 3 with $T = n$ and $D = 2n - 2$.

V. CONVERGENCE ANALYSIS

In this section, we present the theoretical convergence results of the proposed R-FAST algorithm. Beforehand, we denote $x^k \triangleq [x_1^k, x_2^k, \dots, x_n^k]^\top \in \mathbb{R}^{n \times p}$ as the concatenation of all local variables, and $\bar{x}^k \triangleq \frac{1}{n} \sum_{i=1}^n x_i^k \in \mathbb{R}^p$; we use $x^* \in \mathbb{R}^p$ to denote the optimal solution of problem (1) when F is strongly convex; $\|\cdot\|$ denotes the Frobenius norm and I denotes the identity matrix. Given a matrix $M \triangleq (M_{ij})_{i,j=1}^n$, $M_{i,:}$ and $M_{:,j}$ denote its i -th row vector and j -th column vector. Given the sequence $\{M^t\}_{t=s}^k$ with $k \geq s$, $M^{k:s} \triangleq M^k M^{k-1} \dots M^{s+1} M^s$ if $k > s$ and $M^{k:s} \triangleq M^s$ otherwise. $\|M\|_2$ denotes the spectral norm of matrix M and e_i denotes the i -th canonical vector. $[\cdot]_i$ represents the i -th component of a vector. In addition, we make the following blanket assumptions on the objectives.

Assumption 4 (Smoothness). Each $f_i(\cdot)$, $i = 1, \dots, n$ is L_i -Lipschitz differentiable. Define $C_L \triangleq \max \{L_i\}_{i=1}^n$, and $L \triangleq \sum_{i=1}^n L_i$.

Assumption 5 (Bounded variance). The stochastic gradient $\nabla f_i(x; \zeta_i)$, $\zeta_i \sim \mathcal{D}_i$ generated by each node is unbiased with bounded variance, i.e. $\mathbb{E}[\nabla f_i(x; \zeta_i)] =$

$\nabla f_i(x)$ and there exists a constant $\sigma \geq 0$ such that $\mathbb{E}[\|\nabla f_i(x; \zeta_i) - \nabla f_i(x)\|^2] \leq \sigma^2$.

A. Augmented System

In this section, we first recast the proposed R-FAST method as an **augmented system** to deal with the delays. In particular, leveraging *augmented* graphs, we can account for the delay by adding virtual nodes into the graph $\mathcal{G}(W)$ and $\mathcal{G}(A)$ to represent the value of delayed variables that are transmitted on the way, yielding an equivalent synchronous algorithm with augmented weight matrices \hat{W}^k (resp. \hat{A}^k), corresponding to W (resp. A), that governs the information exchange over the augmented graphs.

1) *An augmented system for consensus scheme: augmented graph of $\mathcal{G}(W)$* : We first add $D+1$ virtual nodes for each node i , denoted by $i[0], i[1], \dots, i[D]$, to store delayed information $v_i^k, v_i^{k-1}, \dots, v_i^{k-D}$. It should be noted that any virtual node $i[d], d = D, D-1, \dots, 1$ can only receive information from virtual node $i[d-1]$; besides, $i[0]$ can only receive information from the real node i or keep the value unchanged. Define $v^k \triangleq [v_1^k, \dots, v_n^k]^\top \in \mathbb{R}^{n \times p}$. Then, the consensus scheme can be rewritten as an augmented system as follows

$$h^{k+1} = \hat{W}^k (h^k - \gamma^k e_{ik} (z_{ik}^k)^\top), \quad (3)$$

where

$$h^k \triangleq [x^k; v^k; v^{k-1}; \dots; v^{k-D}] \in \mathbb{R}^{(D+2)n \times p}, \quad (4)$$

and $\hat{W}^k \in \mathbb{R}^{(D+2)n \times (D+2)n}$ denotes the row stochastic augmented matrix. For more details about the augmented system for consensus, the readers are referred to Appendix E.

The following lemma captures the asymptotic behavior of \hat{W}^k over spanning-tree graphs, whose proofs can be adapted from the proof of Lemma 17 in [25].

Lemma 1. Suppose Assumption 1, 2, and 3 hold. Define $K_1 \triangleq (2n-1) \cdot T + n \cdot D$, $C_2 \triangleq \frac{2\sqrt{(D+2)n(1+\bar{m}^{-K_1})}}{1-\bar{m}^{K_1}}$, $\eta \triangleq \bar{m}^{K_1}$ and $\rho \triangleq (1-\eta)^{\frac{1}{K_1}}$. We have for any $k \geq t \geq 0$: i) \hat{W}^k is row stochastic; ii) there exists a sequence of stochastic vectors $\{\psi^k\}_{k \geq 0}$ such that $\psi_i^k \geq \eta$ for all $i \in \mathcal{R}_W$, and

$$\|\hat{W}^{k:t} - 1(\psi^t)^\top\|_2 \leq C_2 \rho^{k-t}. \quad (5)$$

Next, we introduce an auxiliary variable

$$x_\psi^k \triangleq (\psi^k)^\top h^k \quad (6)$$

to construct a weighted average system corresponding to (3), whose evolution will be crucial to our subsequent analysis in upper-bounding the consensus error and optimization error. In particular, using (6), with (3) and the fact $(\psi^{k+1})^\top \hat{W}^k = (\psi^k)^\top$ [41], we get

$$x_\psi^{k+1} = x_\psi^k - \gamma^k (\psi^k)^\top e_{ik} (z_{ik}^k)^\top = x_\psi^k - \gamma^k \psi_{ik}^k (z_{ik}^k)^\top. \quad (7)$$

2) *An augmented system for gradient tracking scheme: augmented graph of $\mathcal{G}(A)$* : For the augmented system of gradient tracking scheme, different from that of the consensus scheme, we add $D + 1$ virtual nodes for each edge $(j, i) \in \mathcal{E}(A)$, denoted by $(j, i)^0, (j, i)^1, \dots, (j, i)^D$, to store the delayed information $z_{(j,i)^0}^k, z_{(j,i)^1}^k, \dots, z_{(j,i)^D}^k$ that has been generated by node $j \in \mathcal{N}_{\text{in}}^{\text{in}}(A)$ for node i but not received by node i yet. Then, we define the real and virtual nodes set as $\hat{\mathcal{V}} \triangleq \mathcal{V} \cup \{(j, i)^d \mid (j, i) \in \mathcal{E}(A), d = 0, 1, \dots, D\}$ and its cardinality as $S \triangleq |\hat{\mathcal{V}}| = n + (D + 1)|\mathcal{E}(A)|$. We use z_{sd}^k to denote $z_{(j,i)^d}^k$ if (j, i) is the s th edge of $\mathcal{E}(A)$. Define $z^k \triangleq [z_1^k, z_2^k, \dots, z_n^k]^\top \in \mathbb{R}^{n \times p}$ and $z_{\mathcal{E}(A)^d}^k \triangleq [z_{1d}^k, z_{2d}^k, \dots, z_{|\mathcal{E}(A)|d}^k]^\top \in \mathbb{R}^{|\mathcal{E}(A)| \times p}$. Then, the gradient tracking scheme can be rewritten as an augmented system as follows:

$$\hat{z}^{k+1} = \hat{A}^k \hat{z}^k + P^k e_{ik}(\epsilon^k)^\top, \quad (8)$$

where

$$\hat{z}^k \triangleq [z_i^k]_{i=1}^S = [z^k; z_{\mathcal{E}(A)^0}^k; z_{\mathcal{E}(A)^1}^k; \dots; z_{\mathcal{E}(A)^D}^k] \in \mathbb{R}^{S \times p} \quad (9)$$

denotes the concatenated tracking variables with initialization $z_i^0 = \nabla f_i(x_i^0; \zeta_i^0)$ for $i \in \mathcal{V}$ and $z_i^0 = 0$ for $i \in \hat{\mathcal{V}} \setminus \mathcal{V}$; $\hat{A}^k \in \mathbb{R}^{S \times S}$ and $P^k \in \mathbb{R}^{S \times S}$ are two column stochastic augmented matrices, and

$$\epsilon^k = \nabla f_{ik}(x_{ik}^{k+1}; \zeta_{ik}^{k+1}) - \nabla f_{ik}(x_{ik}^k; \zeta_{ik}^k). \quad (10)$$

More details about the augmented system for gradient tracking scheme can be found in Appendix F.

Similar to Lemma 1, the asymptotic behavior of \hat{A}^k is depicted in the following lemma.

Lemma 2. Suppose Assumption 1, 2, and 3 hold and define $C \triangleq 2 \frac{1+m-K_1}{1-mK_1}$. We have for any $k \geq t \geq 0$: i) \hat{A}^k is column stochastic; ii) there exists a sequence of stochastic vectors $\{\xi^k\}_{k \geq 0}$ such that $\xi_i^k \geq \eta$ for all $i \in \mathcal{R}_{A^\top}$, and

$$\|\hat{A}_{ij}^{k:t} - \xi_i^k\| \leq C \rho^{k-t} \quad (11)$$

for all $i, j \in \{1, \dots, S\}$.

The following Lemma provides the conservation property of the above gradient-tracking scheme.

Lemma 3. Suppose Assumption 1, 2, and 3 hold. Let $\{\hat{z}^k\}_{k=0}^\infty$ be the sequence generated by the system (8), we have for all $k \geq 0$,

$$\mathbf{1}^\top \hat{z}^k = \left(\sum_{i=1}^n \nabla f_i(x_i^k; \zeta_i^k) \right)^\top. \quad (12)$$

Proof. Applying (8) telescopically, yields: $\hat{z}^k = \hat{A}^{k-1:0} \hat{z}^0 + \sum_{l=1}^{k-1} \hat{A}^{k-1:l} P^{l-1} e_{il-1}(\epsilon^{l-1})^\top + P^{k-1} e_{ik-1}(\epsilon^{k-1})^\top$. Left

multiplying $\mathbf{1}^\top$ from both sides of the above equation, and using the column stochasticity of \hat{A}^k and P^k , we can get

$$\begin{aligned} \mathbf{1}^\top \hat{z}^k &= \mathbf{1}^\top \hat{z}^0 + \sum_{l=0}^{k-1} (\epsilon^l)^\top = \left(\sum_{i=1}^n \nabla f_i(x_i^0; \zeta_i^0) \right)^\top \\ &+ \left(\sum_{l=0}^{k-1} (\nabla f_{il}(x_{il}^{l+1}; \zeta_{il}^{l+1}) - \nabla f_{il}(x_{il}^l; \zeta_{il}^l)) \right)^\top \\ &\stackrel{(a)}{=} \left(\sum_{i=1}^n \nabla f_i(x_i^k; \zeta_i^k) \right)^\top, \end{aligned}$$

where in (a) we used $x_j^{l+1} = x_j^l$ and $\zeta_j^{l+1} = \zeta_j^l$ for $j \neq i^l$. \square

3) *Auxiliary sequence for tackling stochastic errors*: To tackle the stochastic error induced by random gradient sampling, we introduce an auxiliary sequence $\{\bar{z}_i^k\}_{i \in \mathcal{V}}$ (initialized as $\bar{z}_i^0 = \nabla f_i(x_i^0)$ for $i \in \mathcal{V}$), which resembles the recursion of tracking variable $\{z_i^k\}_{i \in \mathcal{V}}$ but uses the local full gradients for updating [38]. Let \bar{z}^k denote the augmented auxiliary variable corresponding to the tracking variables \hat{z}^k . Then, in view of (8), the recursion of the auxiliary variable \bar{z}^k can be rewritten in a compact form as follows:

$$\bar{z}^{k+1} = \hat{A}^k \bar{z}^k + P^k e_{ik}(\bar{\epsilon}^k)^\top, \quad (13)$$

where

$$\bar{\epsilon}^k = \nabla f_{ik}(x_{ik}^{k+1}) - \nabla f_{ik}(x_{ik}^k), \quad (14)$$

with x_{ik}^k being generated from Algorithm 2.

Remark 3. The auxiliary tracking variable $\{\bar{z}_i^k\}_{i \in \mathcal{V}}$ indeed acts the same as the real tracking variable $\{z_i^k\}_{i \in \mathcal{V}}$ except for employing local full gradients for updating. As we will show shortly, in a such design of the auxiliary sequence, the sum of gradients will be preserved over time, making it possible to quantify the difference between the auxiliary sequence and the real one. Clearly, this auxiliary sequence has no effect on the algorithm and, in fact, does not come into play when the algorithm runs, whose purpose is, instead, merely for convergence analysis.

Next we bound the variance of the tracking variable z_{ik}^k with respect to its deterministic counterpart \bar{z}_{ik}^k (auxiliary sequence) using the following Lemma.

Lemma 4. Suppose Assumption 1-3 and 5 hold. We have for $k \geq 0$,

$$\mathbb{E} \left[\|\bar{z}_{ik}^k - z_{ik}^k\|^2 \right] \leq n \sigma^2. \quad (15)$$

Proof. Similar to the proof of Lemma 3, the virtual variables has the following property:

$$\begin{aligned} \mathbf{1}^\top \bar{z}^k &= \left(\sum_{i=1}^n \nabla f_i(x_i^0) + \sum_{l=0}^{k-1} (\nabla f_{il}(x_{il}^{l+1}) - \nabla f_{il}(x_{il}^l)) \right)^\top \\ &= \left(\sum_{i=1}^n \nabla f_i(x_i^k) \right)^\top. \end{aligned}$$

Therefore, we have

$$\begin{aligned}
& \mathbb{E} \left[\left\| \mathbf{1}^\top \hat{z}^k - \mathbf{1}^\top \bar{z}^k \right\|^2 \right] \\
&= \mathbb{E} \left[\left\| \sum_{i=1}^n \nabla f_i(x_i^k; \zeta_i^k) - \sum_{i=1}^n \nabla f_i(x_i^k) \right\|^2 \right] \\
&= \sum_{i=1}^n \mathbb{E} \left[\left\| \nabla f_i(x_i^k; \zeta_i^k) - \nabla f_i(x_i^k) \right\|^2 \right] \\
&\quad + \sum_{i \neq i'}^n \mathbb{E} \left\langle \nabla f_i(x_i^k; \zeta_i^k) - \nabla f_i(x_i^k), \right. \\
&\quad \left. \nabla f_{i'}(x_{i'}^k; \zeta_{i'}^k) - \nabla f_{i'}(x_{i'}^k) \right\rangle \stackrel{(a)}{\leq} n\sigma^2,
\end{aligned}$$

where in (a) we have used Assumption 5 and the fact that the inner product equals to zero since the two terms of the inner product are independent of each other.

Additionally, knowing that

$$\mathbb{E} [\hat{z}^k - \bar{z}^k] = 0,$$

we then obtain

$$\mathbb{E} \left[\left\| z_{i^k}^k - \bar{z}_{i^k}^k \right\|^2 \right] \leq \mathbb{E} \left[\left\| \mathbf{1}^\top \hat{z}^k - \mathbf{1}^\top \bar{z}^k \right\|^2 \right] \leq n\sigma^2,$$

which completes the proof. \square

B. Strongly Convex: Geometric convergence

We first define the consensus error, gradient tracking error and optimization error on the augmented graph and our objective is to prove that these errors will converge to a ball with a linear rate. To this end, we derive recursions of these above error terms (c.f., Proposition 1) and, with the help of Lemma 5, build an equivalent linear system of inequalities for the obtained error dynamics. By using the generalized small gain theorem, the linear convergence of the above error terms can be obtained, leading to the main results as given in Theorem 1.

Let $\{x_i^k, v_i^k, z_i^k, \bar{z}_i^k\}_{k \geq 0, i \in [n]}$ be the sequence generated by R-FAST. Define the consensus error, gradient tracking error, the magnitude of the tracking variable and optimization error are $E_c^k \triangleq \mathbb{E} \left[\left\| h^k - \mathbf{1} x_\psi^k \right\|^2 \right]$, $E_t^k \triangleq \mathbb{E} \left[\left\| \bar{z}_{i^k}^k - \xi_{i^k}^{k-1}(\bar{z}^k)^\top \mathbf{1} \right\|^2 \right]$, $E_z^k \triangleq \mathbb{E} \left[\left\| \bar{z}_{i^k}^k \right\|^2 \right]$ and $E_o^k \triangleq \mathbb{E} \left[\left\| x_\psi^k - (x^*)^\top \right\|^2 \right]$ respectively. Then, the recursions of these above error terms are established in the following proposition.

Proposition 1. *Consider the R-FAST algorithm with a constant step-size γ . Suppose Assumption 1-5 hold. Then, we have for all $k \geq 0$,*

$$\begin{aligned}
E_c^{k+1} &\leq 2C_2^2 E_c^0 \cdot \rho^{2k} + \frac{4\gamma^2 C_2^2}{1-\rho} \sum_{l=0}^k \rho^{k-l} E_z^l \\
&+ \frac{4\gamma^2 C_2^2 n}{1-\rho} \sum_{l=0}^k \rho^{k-l} \cdot \sigma^2,
\end{aligned} \tag{16}$$

$$\begin{aligned}
E_t^{k+1} &\leq 3C_1^2 \|\bar{z}^0\|^2 \cdot \rho^{2k} \\
&+ \sum_{l=0}^k \rho^{k-l} \left(\frac{27C_1^2 C_L^2}{1-\rho} E_c^l + \frac{54\gamma^2 C_1^2 C_L^2}{1-\rho} E_z^l + \frac{54\gamma^2 C_1^2 C_L^2 n}{1-\rho} \sigma^2 \right),
\end{aligned} \tag{17}$$

$$E_z^k \leq 3E_t^k + 3C_L^2 n E_c^k + 3L^2 E_o^k, \tag{18}$$

$$\begin{aligned}
E_o^{k+1} &\leq 4\mathcal{L}(\gamma)^{-2r} E_o^0 \cdot \mathcal{L}(\gamma)^{\frac{2r}{T} \cdot (k+1)} \\
&+ \frac{4\mathcal{L}(\gamma)^{-2r} \gamma^2}{1-\mathcal{L}(\gamma)^{\frac{r}{T}}} \sum_{l=0}^k \mathcal{L}(\gamma)^{\frac{r}{T} \cdot (k-l)} (C_L^2 n E_c^l + E_t^l + n\sigma^2),
\end{aligned} \tag{19}$$

where

$$\mathcal{L}(\gamma) \triangleq 1 - \tau\eta^2\gamma, \quad C_1 \triangleq \frac{2\sqrt{2S}(1 + \bar{m}^{-K_1})}{\rho(1 - \bar{m}^{K_1})}. \tag{20}$$

Proof. See Appendix A for the detailed proofs. \square

Remark 4. Since the proposed method works on two spanning-tree graphs and runs in a totally asynchronous manner, it is not possible for the augmented system to have the contraction property at each single step, which renders the existing analytical techniques invalid [17], [25], [26]. We thus carry out the analysis over a properly designed time period in which r common root nodes will be activated at least once, guaranteeing the contraction property (c.f., (46) in the appendix).

In what follows, we show that each of the aforementioned error terms E_c^k , E_t^k , E_z^k and E_o^k will linearly converge to a neighborhood of zero with respect to the global iteration k . To this end, we introduce the following definition and the corresponding lemma which will be crucial to our subsequent analysis based on the small-gain theorem [42].

Definition 1. For given sequence $\{u^k\}_{k=0}^\infty$, constant $\lambda \in (0, 1)$ and $N \in \mathbb{N}$, we define

$$|u|^{\lambda, N} = \max_{k=0, 1, 2, \dots, N} \frac{|u^k|}{\lambda^k}. \tag{21}$$

Lemma 5. Consider non-negative sequences $\{u^k\}_{k=0}^\infty$, and $\{v_i^k\}_{k=0}^\infty$ for $i = 1, \dots, m$. If there exist constants $\lambda_0, \lambda_1, \dots, \lambda_m \in (0, 1)$, $R_0, R_1, \dots, R_m \in \mathbb{R}_+$, $\sigma > 0$, $\lambda_h \in (0, 1)$ and $R_h \in \mathbb{R}_+$ such that

$$u^{k+1} \leq R_0 (\lambda_0)^k + \sum_{i=1}^m R_i \sum_{l=0}^k (\lambda_i)^{k-l} v_i^l + R_h \sum_{l=0}^k (\lambda_h)^{k-l} \sigma^2,$$

then, there holds

$$|u|^{\lambda, N} \leq u^0 + \frac{R_0}{\lambda} + \sum_{i=1}^m \left(\frac{R_i}{\lambda - \lambda_i} \cdot |v_i|^{\lambda, N} \right) + \frac{R_h}{1 - \lambda_h} \cdot \frac{\sigma^2}{\lambda^N},$$

for any $\lambda \in \left(\max \left(\max_{i=0, 1, \dots, m} \lambda_i, \lambda_h \right), 1 \right)$ and $N \in \mathbb{N}$.

With these above supporting results, we are ready to derive the convergence property of the proposed algorithm for strongly convex objective function.

Theorem 1 (Geometric convergence). *Suppose Assumptions 1-5 hold, F is τ -strongly convex and the constant step size γ is sufficiently small. There exists $\lambda \in (\max(\rho, (1 - \tau\eta^2\gamma)^{\frac{r}{T}}), 1)$ such that for $\forall k \geq 0$,*

$$\mathbb{E} \left[\left\| x^k - \mathbf{1} (x^*)^\top \right\|^2 \right] \leq \mathcal{O}(\lambda^k) + \Xi(\gamma)\sigma^2, \quad (22)$$

where $\rho = (1 - \bar{m}^{(2n-1) \cdot T + n \cdot D})^{\frac{1}{(2n-1) \cdot T + n \cdot D}} \in (0, 1)$, $\eta = \bar{m}^{(2n-1) \cdot T + n \cdot D} \in (0, 1)$ and $\Xi(\gamma)$ is defined at (26).

Remark 5. In Theorem 1, we show that in expectation, the proposed algorithm converges to a neighborhood of the optimal solution with linear rate λ , which aligns with the convergence result of the synchronous stochastic distributed optimization algorithm S-AB [17] over directed network. The linear convergence rate $\lambda \in (\max(\rho, (1 - \tau\eta^2\gamma)^{\frac{r}{T}}), 1)$ increases as T and/or D increase, implying that the convergence rate gets slower when the degree of asynchrony gets larger or the message delay gets larger. In addition, according to Remark 2 and setting $T = n$ and $D = 2n - 2$, we obtain the convergence result for the synchronous R-FAST, which is, to the best of our knowledge, the first convergence result for the stochastic synchronous algorithms using the push-pull protocol. The geometric exact convergence result of the deterministic synchronous push-pull algorithm [26] is readily recovered by further setting $\sigma^2 = 0$.

Proof of Theorem 1. We reformulate the error dynamic system as established in Proposition 1 into a linear system using Lemma 5. Specifically, choosing $\lambda \in (\max(\rho, (1 - \tau\eta^2\gamma)^{\frac{r}{T}}), 1)$, for any $N \in \mathbb{N}$, and applying Lemma 5 to the inequalities (16)-(19) in Proposition 1 yields that

$$\begin{aligned} \begin{bmatrix} |E_z|^{\lambda, N} \\ |E_c|^{\lambda, N} \\ |E_t|^{\lambda, N} \\ |E_o|^{\lambda, N} \end{bmatrix} &\leq P \begin{bmatrix} |E_z|^{\lambda, N} \\ |E_c|^{\lambda, N} \\ |E_t|^{\lambda, N} \\ |E_o|^{\lambda, N} \end{bmatrix} + \underbrace{\begin{bmatrix} 0 \\ E_c^0 + \frac{2C_3^2 E_c^0}{\lambda} \\ E_t^0 + \frac{3C_1^2 \|\bar{z}^0\|^2}{\lambda} \\ E_o^0 + \frac{4(1-\tau\eta^2\gamma)^{-2r} E_o^0}{\lambda} \end{bmatrix}}_{\alpha} \\ &\quad + \frac{\sigma^2}{\lambda^N} \underbrace{\begin{bmatrix} 0 \\ \frac{4\gamma^2 C_2^2 n}{(1-\rho)^2} \\ \frac{54\gamma^2 C_1^2 C_L^2 n}{(1-\rho)^2} \\ \frac{4(1-\tau\eta^2\gamma)^{-2r} \gamma^2 n}{(1-(1-\tau\eta^2\gamma)^{\frac{r}{T}})^2} \end{bmatrix}}_{\beta}, \end{aligned} \quad (23)$$

where

$$P \triangleq \quad (24)$$

$$\begin{bmatrix} 0 & b_1 & 3 & 3L^2 \\ \frac{b_3\gamma^2}{(1-\rho)(\lambda-\rho)} & 0 & 0 & 0 \\ \frac{b_2\gamma^2}{(1-\rho)(\lambda-\rho)} & \frac{b_2}{(1-\rho)(\lambda-\rho)} & 0 & 0 \\ 0 & \frac{b_2\mathcal{L}(\gamma)^{-2r}\gamma^2}{(1-\mathcal{L}(\gamma)^{\frac{r}{T}})(\lambda-\mathcal{L}(\gamma)^{\frac{r}{T}})} & \frac{4\mathcal{L}(\gamma)^{-2r}\gamma^2}{(1-\mathcal{L}(\gamma)^{\frac{r}{T}})(\lambda-\mathcal{L}(\gamma)^{\frac{r}{T}})} & 0 \end{bmatrix}$$

, $b_1 \triangleq 3C_L^2 n$, $b_2 \triangleq 54C_1^2 C_L^2$, $b_3 \triangleq 4C_2^2$ and $\mathcal{L}(\gamma) = 1 - \tau\eta^2\gamma$. If the spectral radius $\rho(P) < 1$, then using (23) recursively yields

$$\begin{bmatrix} \frac{E_z^N}{\lambda^N} \\ \frac{E_c^N}{\lambda^N} \\ \frac{E_t^N}{\lambda^N} \\ \frac{E_o^N}{\lambda^N} \end{bmatrix} \leq \begin{bmatrix} |E_z|^{\lambda, N} \\ |E_c|^{\lambda, N} \\ |E_t|^{\lambda, N} \\ |E_o|^{\lambda, N} \end{bmatrix} \leq (I - P)^{-1} \alpha + \frac{\sigma^2}{\lambda^N} (I - P)^{-1} \beta.$$

Multiplying by λ^N on both sides, we have

$$\begin{bmatrix} E_z^N \\ E_c^N \\ E_t^N \\ E_o^N \end{bmatrix} \leq \underbrace{\lambda^N \cdot (I - P)^{-1} \alpha}_{\text{linearly converge to 0}} + \underbrace{(I - P)^{-1} \beta \sigma^2}_{\text{steady error}}. \quad (25)$$

We note that (25) holds for any $N \in \mathbb{N}$. In what follows we show that the spectral radius $\rho(P) < 1$. If $\max(\rho, \mathcal{L}(\gamma)^{\frac{r}{T}}) < \lambda < 1$, the characteristic polynomial $p_P(z)$ of P satisfies the conditions of Lemma 24 in [25], therefore $\rho(P) < 1$ if and only if $p_P(1) > 0$, that is

$$\begin{aligned} \mathcal{B}(\lambda, \gamma) &\triangleq \frac{3b_2\gamma^2}{(1-\rho)(\lambda-\rho)} + \frac{b_1b_3\gamma^2}{(1-\rho)(\lambda-\rho)} + \frac{3b_2b_3\gamma^2}{(1-\rho)^2(\lambda-\rho)^2} \\ &\quad + \frac{12L^2b_2\mathcal{L}(\gamma)^{-2r}\gamma^4 + 3L^2b_2b_3\mathcal{L}(\gamma)^{-2r}\gamma^4}{(1-\rho)(\lambda-\rho)\left(1-\mathcal{L}(\gamma)^{\frac{r}{T}}\right)\left(\lambda-\mathcal{L}(\gamma)^{\frac{r}{T}}\right)} \\ &\quad + \frac{12L^2b_2b_3\mathcal{L}(\gamma)^{-2r}\gamma^4}{(1-\rho)^2(\lambda-\rho)^2\left(1-\mathcal{L}(\gamma)^{\frac{r}{T}}\right)\left(\lambda-\mathcal{L}(\gamma)^{\frac{r}{T}}\right)} < 1. \end{aligned}$$

It is can be verified that $\mathcal{B}(\lambda; \gamma)$ is continuous at $\lambda = 1$ for fixed γ . Therefore, as long as

$$\begin{aligned} \mathcal{B}(1, \gamma) &\triangleq \frac{3b_2\gamma^2}{(1-\rho)^2} + \frac{b_1b_3\gamma^2}{(1-\rho)^2} + \frac{3b_2b_3\gamma^2}{(1-\rho)^4} \\ &\quad + \frac{12L^2b_2\mathcal{L}(\gamma)^{-2r}\gamma^4 + 3L^2b_2b_3\mathcal{L}(\gamma)^{-2r}\gamma^4}{(1-\rho)^2\left(1-\mathcal{L}(\gamma)^{\frac{r}{T}}\right)^2} \\ &\quad + \frac{12L^2b_2b_3\mathcal{L}(\gamma)^{-2r}\gamma^4}{(1-\rho)^4\left(1-\mathcal{L}(\gamma)^{\frac{r}{T}}\right)^2} < 1, \end{aligned}$$

it is sufficient to claim the existence of some $\lambda \in (\max(\rho, \mathcal{L}(\gamma)^{\frac{r}{T}}), 1)$ such that $\mathcal{B}(\lambda; \gamma) < 1$. We now show that $\mathcal{B}(1; \gamma) < 1$ for sufficiently small γ . We only need to prove boundedness of the $\frac{\gamma}{1-\mathcal{L}(\gamma)^{\frac{r}{T}}}$ when $\gamma \downarrow 0$. According to L'Hôpital's rule, we get

$$\begin{aligned} \lim_{\gamma \rightarrow 0} \frac{\gamma}{1-\mathcal{L}(\gamma)^{\frac{r}{T}}} &= \lim_{\gamma \rightarrow 0} \frac{\gamma}{1-(1-\tau\eta^2\gamma)^{\frac{r}{T}}} \\ &= \frac{1}{\frac{r}{T}(1-\tau\eta^2\gamma)^{\frac{r}{T}-1} \cdot \tau\eta^2} \Big|_{\gamma=0} = \frac{T}{\tau\eta^2 r} < \infty, \end{aligned}$$

we thus proved that for a sufficiently small γ , there exists $\lambda \in (\max(\rho, (1 - \tau\eta^2\gamma)^{\frac{r}{T}}), 1)$ and (25) holds for any $N \in \mathbb{N}$.

Now, we are ready to prove the main results in Theorem 1. With the help of (25), we get that

$$\begin{aligned}\mathbb{E} \left[\|x_\psi^k - (x^*)^\top\|^2 \right] &\leq \mathcal{O}(\lambda^k) + \left[(I - P)^{-1} \beta \right]_4 \sigma^2, \\ \mathbb{E} \left[\|h^k - \mathbf{1} x_\psi^k\|^2 \right] &\leq \mathcal{O}(\lambda^k) + \left[(I - P)^{-1} \beta \right]_2 \sigma^2.\end{aligned}$$

Therefore, we further have

$$\begin{aligned}\mathbb{E} \left[\|x^k - \mathbf{1} (x^*)^\top\|^2 \right] &= \mathbb{E} \left[\|x^k - \mathbf{1} x_\psi^k + \mathbf{1} x_\psi^k - \mathbf{1} (x^*)^\top\|^2 \right] \\ &\leq 2\mathbb{E} \left[\|x^k - \mathbf{1} x_\psi^k\|^2 \right] + 2n\mathbb{E} \left[\|x_\psi^k - (x^*)^\top\|^2 \right] \\ &\leq 2\mathbb{E} \left[\|h^k - \mathbf{1} x_\psi^k\|^2 \right] + 2n\mathbb{E} \left[\|x_\psi^k - (x^*)^\top\|^2 \right] \\ &\leq \mathcal{O}(\lambda^k) + \underbrace{\left(2 \left[(I - P)^{-1} \beta \right]_2 + 2n \left[(I - P)^{-1} \beta \right]_4 \right)}_{\Xi(\gamma)} \cdot \sigma^2,\end{aligned}\quad (26)$$

which is the result of Theorem 1. \square

C. Non-Convex: Sublinear convergence

In this section, we consider the scenario that the overall objective function F in (1) is only smooth (possibly non-convex). We use the following merit function to measure distance to the stationary point¹:

$$M_F(x^k) \triangleq \|\nabla F(\bar{x}^k)\|^2 + \|x^k - \mathbf{1}(\bar{x}^k)^\top\|^2. \quad (27)$$

The following Lemma provides an upper bound for the accumulative consensus error $\sum_{l=0}^k \mathbb{E} \|h^l - \mathbf{1} x_\psi^l\|^2$ and tracking error $\sum_{l=0}^k \mathbb{E} \|\bar{z}_{i^l}^l - \xi_{i^l}^{l-1}(\bar{z}^l)^\top \mathbf{1}\|^2$, using the accumulative magnitude of gradient $\sum_{l=0}^k \mathbb{E} \|\nabla F(x_\psi^l)\|^2$.

Lemma 6. Suppose Assumption 1-5 hold. Let the constant step-size γ satisfy

$$\gamma < \frac{1}{\sqrt{3\varrho_c C_L^2 n + 3\varrho_t}}, \quad (28)$$

then, for all $k \geq 0$, we have

$$\begin{aligned}\sum_{l=0}^k \mathbb{E} \|h^l - \mathbf{1} x_\psi^l\|^2 &\leq \frac{3\varrho_c \gamma^2}{1 - 3(\varrho_c C_L^2 n + \varrho_t) \gamma^2} \sum_{l=0}^k \mathbb{E} \|\nabla F(x_\psi^l)\|^2 \\ &+ \frac{(1 - 3\varrho_t \gamma^2) c_c + 3c_t \varrho_c \gamma^2}{1 - 3(\varrho_c C_L^2 n + \varrho_t) \gamma^2} + \frac{\varrho_c n \gamma^2 (k+1)}{1 - 3(\varrho_c C_L^2 n + \varrho_t) \gamma^2} \sigma^2,\end{aligned}\quad (29)$$

$$\begin{aligned}\text{and} \\ \sum_{l=0}^k \mathbb{E} \|\bar{z}_{i^l}^l - \xi_{i^l}^{l-1}(\bar{z}^l)^\top \mathbf{1}\|^2 &\leq \frac{\varrho_t n \gamma^2 (k+1)}{1 - 3(\varrho_c C_L^2 n + \varrho_t) \gamma^2} \sigma^2 \\ &+ \frac{3\varrho_t \gamma^2}{1 - 3(\varrho_c C_L^2 n + \varrho_t) \gamma^2} \sum_{l=0}^k \mathbb{E} \|\nabla F(x_\psi^l)\|^2 \\ &+ \frac{(1 - 3\varrho_c C_L^2 n \gamma^2) c_t + 3c_c \varrho_t C_L^2 n \gamma^2}{1 - 3(\varrho_c C_L^2 n + \varrho_t) \gamma^2},\end{aligned}\quad (30)$$

where c_c , ϱ_c , c_t and ϱ_t are constants given as below:

$$c_c \triangleq \left(1 + \frac{2C_2^2}{1 - \rho^2} \right) \|h^0 - \mathbf{1} x_\psi^0\|^2, \quad \varrho_c \triangleq \frac{4C_2^2}{(1 - \rho)^2}, \quad (31)$$

¹For brevity, in what follows we use $\mathbb{E} \|\cdot\|^2$ to denote $\mathbb{E} [\|\cdot\|^2]$

$$\begin{aligned}c_t &\triangleq \frac{3C_1^2 \|\bar{z}^0\|^2}{1 - \rho^2} + \frac{27C_1^2 C_L^2 (2C_2^2 + 1 - \rho^2)}{(1 - \rho)^4} \|h^0 - \mathbf{1} x_\psi^0\|^2 \\ &+ \|\bar{z}_{i^0}^0 - \xi_{i^0}^{-1}(\bar{z}^0)^\top \mathbf{1}\|^2, \varrho_t \triangleq \frac{54C_1^2 C_L^2 [4C_2^2 + (1 - \rho)^2]}{(1 - \rho)^4}.\end{aligned}\quad (32)$$

Proof. See Appendix B for the detailed proofs. \square

The following lemma provides an upper bound of $\sum_{k=0}^{\bar{k}T-1} \mathbb{E} \|\nabla F(x_\psi^k)\|^2$ for $\bar{k} \geq 1$.

Lemma 7. Suppose Assumption 1-5 hold. Let the constant step-size γ satisfy

$$\gamma \leq \min \left\{ \frac{2}{(2T^2 + r\eta^2 T) L}, \frac{1}{8L} \right\}, \quad (33)$$

then, for all $\bar{k} \geq 1$, we have

$$\begin{aligned}\left(\frac{\gamma r \eta^2}{8T} - \frac{\gamma^2}{2} \right) \sum_{k=0}^{\bar{k}T-1} \mathbb{E} \|\nabla F(x_\psi^k)\|^2 &\leq F(x_\psi^0) - F^* \\ &+ \frac{1 + \gamma}{2} \sum_{k=0}^{\bar{k}T-1} \mathbb{E} \|\bar{z}_{i^k}^k - \xi_{i^k}^{k-1}(\bar{z}^k)^\top \mathbf{1}\|^2 + \frac{1}{2} r \eta^2 L^2 \bar{k} T^2 n \gamma^3 \sigma^2 \\ &+ \frac{\gamma C_L^2 n}{2} \sum_{k=0}^{\bar{k}T-1} \mathbb{E} \|h^k - \mathbf{1} x_\psi^k\|^2 + L n \bar{k} T \gamma^2 \sigma^2 + L^2 \bar{k} T^3 n \gamma^3 \sigma^2.\end{aligned}\quad (34)$$

where $F^* \triangleq \min_{x \in \mathbb{R}^p} F(x)$.

Proof. See Appendix C for the detailed proofs. \square

Remark 6. For the same reason as mentioned in Remark 4 for strongly-convex cases, the decent lemma based on the smooth property is no long valid in our non-convex setting. We thus develop a new decent lemma leveraging two-time-scale techniques that allow us to build an inequality within a properly chosen time period, which ensures a valid decent (c.f., (63) and Lemma 10 in the appendix).

With the above supporting lemmas, we provide the sub-linear convergence result of the proposed algorithm.

Theorem 2 (Sub-linear convergence). Suppose Assumption 1-5 hold. For any $K > 0$ being a multiple of T , and any constant step size satisfying $\gamma \leq \bar{\gamma}$, we have for Algorithm 2

$$\begin{aligned}\frac{1}{K} \sum_{k=0}^{K-1} \mathbb{E} [M_F(x^k)] &\leq \frac{32T (F(x_\psi^0) - F^* + c_t)}{\gamma \eta^2 K r} \\ &+ \frac{T E_1}{K} + \frac{32T (n \varrho_t + n L)}{\eta^2} \gamma \sigma^2 + E_2 \gamma^2 \sigma^2,\end{aligned}\quad (35)$$

where $\bar{\gamma}$ and x_ψ^0 are constants defined in (39) and (6) respectively; constants E_1 and E_2 defined in (70) and (71) (c.f., Appendix D).

Remark 7. Most of the existing works under asynchronous settings, such as the AD-PSGD [22] and OSGP [23], suffer from the data heterogeneity among nodes, leading to a dependency of ς in the complexity (See Corollary 2 in [22], Theorem 1 in [23]), where ς satisfies

$\frac{1}{n} \sum_{i=1}^n \|\nabla f_i(x) - \frac{1}{n} \nabla F(x)\|^2 \leq \varsigma^2$. In contrast, our convergence result shows that the proposed R-FAST algorithm can effectively remove the impact of the data heterogeneity on the convergence rate (i.e., ς -free in the convergence rate), yielding the robustness to the data heterogeneity across devices.

Proof of Theorem 2. Consider (34) in Lemma 7. We first provide an upper bound for $\sum_{k=0}^{\bar{k}T-1} \mathbb{E} \|h^k - \mathbf{1}x_\psi^k\|^2$ and $\sum_{k=0}^{\bar{k}T-1} \mathbb{E} \|\bar{z}_{ik}^k - \xi_{ik}^{k-1}(\bar{z}^k)^\top \mathbf{1}\|^2$ in term of $\sum_{k=0}^{\bar{k}T-1} \mathbb{E} \|\nabla F(x_\psi^k)\|^2$, which can be easily obtained by invoking (29) and (30) in Lemma 6. Substituting these obtained bounds into (34) when γ satisfies (28) and (33), and rearranging terms yields

$$\begin{aligned} & \left(\frac{r\eta^2}{8} - \frac{T\gamma}{2} - \frac{3\varrho_t T + 3(\varrho_t + \varrho_c C_L^2 n) T \gamma}{2(1 - 3(\varrho_c C_L^2 n + \varrho_t) \gamma^2)} \gamma \right) \frac{1}{\bar{k}T} \\ & \sum_{k=0}^{\bar{k}T-1} \mathbb{E} \|\nabla F(x_\psi^k)\|^2 \leq \frac{1}{\bar{k}} \left\{ \frac{F(x_\psi^0) - F^*}{\gamma} + \frac{C_L^2 n}{2} \right. \\ & \quad \left. \frac{c_c + 3c_t \varrho_c \gamma^2}{1 - 3(\varrho_c C_L^2 n + \varrho_t) \gamma^2} + \frac{1 + \gamma}{2\gamma} \cdot \frac{c_t + 3c_c \varrho_t C_L^2 n \gamma^2}{1 - 3(\varrho_c C_L^2 n + \varrho_t) \gamma^2} \right\} \\ & \quad + \frac{(1 + \gamma) \varrho_t n T \gamma}{2(1 - 3(\varrho_c C_L^2 n + \varrho_t) \gamma^2)} \sigma^2 + \frac{1}{2} r \eta^2 L^2 T^2 n \gamma^2 \sigma^2 \\ & \quad + \frac{C_L^2 n}{2} \cdot \frac{\varrho_c n T \gamma^2}{1 - 3(\varrho_c C_L^2 n + \varrho_t) \gamma^2} \sigma^2 + L n T \gamma \sigma^2 + L^2 T^3 n \gamma^2 \sigma^2. \end{aligned}$$

If γ further satisfies

$$\gamma \leq \min \left\{ \frac{1}{\sqrt{6(\varrho_c C_L^2 n + \varrho_t)}}, \frac{1 + 6\varrho_t}{6(\varrho_t + \varrho_c C_L^2 n)}, \frac{r\eta^2}{16(1 + 6\varrho_t)T} \right\}, \quad (36)$$

we can further obtain that

$$\begin{aligned} & \frac{1}{\bar{k}T} \sum_{k=0}^{\bar{k}T-1} \mathbb{E} \|\nabla F(x_\psi^k)\|^2 \leq \frac{16(F(x_\psi^0) - F^* + c_t)}{r\eta^2 \gamma \bar{k}} \\ & \quad + \frac{16(C_L^2 n c_c + c_t) + 48c_c \varrho_t C_L^2 n \gamma + 48(c_t \varrho_c + c_c \varrho_t) C_L^2 n \gamma^2}{r\eta^2 \bar{k}} \\ & \quad + \frac{16}{r\eta^2} \left(\varrho_t n T + \varrho_c C_L^2 n^2 T + L^2 T^3 n + \frac{1}{2} r \eta^2 L^2 T^2 n \right) \gamma^2 \sigma^2 \\ & \quad + \frac{16}{r\eta^2} (\varrho_t n T + L n T) \gamma \sigma^2. \end{aligned} \quad (37)$$

Then, we move to bound $\frac{1}{\bar{k}T} \sum_{k=0}^{\bar{k}T-1} \mathbb{E} [M_F(x^k)]$. To this end, we first establish a relationship between $\mathbb{E} [M_F(x^k)]$ with $\mathbb{E} \|\nabla F(x_\psi^k)\|^2$ and $\mathbb{E} \|h^k - \mathbf{1}x_\psi^k\|^2$ as follows:

$$\begin{aligned} & \mathbb{E} [M_F(x^k)] \leq 2\mathbb{E} \|\nabla F(x_\psi^k)\|^2 + 2\mathbb{E} \|\nabla F(\bar{x}^k) - \nabla F(x_\psi^k)\|^2 \\ & \quad + 2\mathbb{E} \|x^k - \mathbf{1}x_\psi^k\|^2 + 2\mathbb{E} \|\mathbf{1}x_\psi^k - \mathbf{1}(\bar{x}^k)^\top\|^2 \\ & \stackrel{(a)}{\leq} 2\mathbb{E} \|\nabla F(x_\psi^k)\|^2 + \left(\frac{2L^2}{n} + 4 \right) \mathbb{E} \|x^k - \mathbf{1}x_\psi^k\|^2 \\ & \leq 2\mathbb{E} \|\nabla F(x_\psi^k)\|^2 + \left(\frac{2L^2}{n} + 4 \right) \mathbb{E} \|h^k - \mathbf{1}x_\psi^k\|^2, \end{aligned} \quad (38)$$

where in (a) we used

$$\begin{aligned} & \mathbb{E} \|\nabla F(\bar{x}^k) - \nabla F(x_\psi^k)\|^2 \leq L^2 \mathbb{E} \|(\bar{x}^k)^\top - x_\psi^k\|^2 = \\ & \frac{L^2}{n} \mathbb{E} \left\| \frac{\mathbf{1}\mathbf{1}^\top}{n} (\mathbf{1}x_\psi^k - x^k) \right\|^2, \quad \left\| \frac{\mathbf{1}\mathbf{1}^\top}{n} \right\|_2 = 1, \end{aligned}$$

$$\text{and } \mathbb{E} \|\mathbf{1}x_\psi^k - \mathbf{1}(\bar{x}^k)^\top\|^2 = \mathbb{E} \left\| \frac{\mathbf{1}\mathbf{1}^\top}{n} (\mathbf{1}x_\psi^k - x^k) \right\|^2.$$

When γ satisfies (28), (33) and (36), i.e.,

$$\gamma \leq \min \left\{ \frac{1}{\sqrt{6(\varrho_c C_L^2 n + \varrho_t)}}, \frac{2}{(2T^2 + r\eta^2 T) L}, \frac{1}{8L}, \frac{1 + 6\varrho_t}{6(\varrho_t + \varrho_c C_L^2 n)}, \frac{r\eta^2}{16(1 + 6\varrho_t)T} \right\} \triangleq \bar{\gamma}, \quad (39)$$

combining (38) and (29) in Lemma 6, we have

$$\begin{aligned} & \frac{1}{\bar{k}T} \sum_{k=0}^{\bar{k}T-1} \mathbb{E} [M_F(x^k)] \leq \frac{2}{\bar{k}T} \sum_{k=0}^{\bar{k}T-1} \mathbb{E} \|\nabla F(x_\psi^k)\|^2 \\ & \quad + \left(\frac{2L^2}{n} + 4 \right) \frac{1}{\bar{k}T} \left(\frac{3\varrho_c \gamma^2}{1 - 3(\varrho_c C_L^2 n + \varrho_t) \gamma^2} \sum_{k=0}^{\bar{k}T-1} \mathbb{E} \|\nabla F(x_\psi^k)\|^2 \right. \\ & \quad \left. + \frac{(1 - 3\varrho_t \gamma^2) c_c + 3c_t \varrho_c \gamma^2}{1 - 3(\varrho_c C_L^2 n + \varrho_t) \gamma^2} + \frac{\varrho_c n \bar{k} T \gamma^2}{1 - 3(\varrho_c C_L^2 n + \varrho_t) \gamma^2} \sigma^2 \right). \end{aligned}$$

Substituting $\gamma \leq \frac{1}{\sqrt{6(\varrho_c C_L^2 n + \varrho_t)}}$ in (39), into the above inequality, we further have

$$\begin{aligned} & \frac{1}{\bar{k}T} \sum_{k=0}^{\bar{k}T-1} \mathbb{E} [M_F(x^k)] \leq \frac{2}{\bar{k}T} \sum_{k=0}^{\bar{k}T-1} \mathbb{E} \|\nabla F(x_\psi^k)\|^2 \\ & \quad + \frac{12(L^2 + 2n) \varrho_c \gamma^2}{n} \frac{1}{\bar{k}T} \sum_{k=0}^{\bar{k}T-1} \mathbb{E} \|\nabla F(x_\psi^k)\|^2 \\ & \quad + \frac{4(L^2 + 2n)(c_c + 3c_t \varrho_c \gamma^2)}{n \bar{k}T} + 4(L^2 + 2n) \varrho_c \gamma^2 \sigma^2. \end{aligned}$$

Substituting the upper bound of $\frac{1}{\bar{k}T} \sum_{k=0}^{\bar{k}T-1} \mathbb{E} \|\nabla F(x_\psi^k)\|^2$ (c.f., (37)) into the above inequality, and plugging $\gamma \leq \frac{1}{8L}$ in (39), yields that

$$\begin{aligned} & \frac{1}{\bar{k}T} \sum_{k=0}^{\bar{k}T-1} \mathbb{E} [M_F(x^k)] \leq \frac{32(F(x_\psi^0) - F^* + c_t)}{r\eta^2 \gamma \bar{k}} \\ & \quad + \frac{E_1}{\bar{k}} + \frac{32T(n\varrho_t + nL)}{\eta^2} \gamma \sigma^2 + E_2 \gamma^2 \sigma^2, \end{aligned} \quad (40)$$

where the constants E_1 and E_2 are defined in (70) and (71) in Appendix D.

Let $K = \bar{k}T$, (40) becomes

$$\begin{aligned} & \frac{1}{K} \sum_{k=0}^{K-1} \mathbb{E} [M_F(x^k)] \leq \frac{32T(F(x_\psi^0) - F^* + c_t)}{\eta^2 \gamma K r} \\ & \quad + \frac{TE_1}{K} + \frac{32T(n\varrho_t + nL)}{\eta^2} \gamma \sigma^2 + E_2 \gamma^2 \sigma^2, \end{aligned}$$

which is the result in Theorem 2. \square

By carefully choosing the step size in Theorem 2, we further obtain the following corollary.

Corollary 1. *Under the conditions in Theorem 2, if we further set the constant step-size $\gamma = \frac{1}{\sigma\sqrt{Kr}+\bar{\gamma}^{-1}}$, we have*

$$\begin{aligned} & \frac{1}{K} \sum_{k=0}^{K-1} \mathbb{E} [M_F(x^k)] \\ & \leq \frac{32T \left(F(x_\psi^0) - F^* + c_t + n\varrho_t + nL \right) \sigma}{\eta^2 \sqrt{Kr}} \\ & + \frac{32r^{-1}\bar{\gamma}^{-1}T \left(F(x_\psi^0) - F^* + c_t \right) + \eta^2 T E_1 + r^{-1} \eta^2 E_2}{\eta^2 K}. \end{aligned}$$

Remark 8. *The above result suggests that the convergence rate for R-FAST is of $\mathcal{O}\left(\frac{\sigma}{\sqrt{K}} + \frac{1}{K}\right)$, matching the rate of centralized SGD for non-convex problems [8]. Additionally, when K is large enough, the $\frac{1}{K}$ term will be dominated by $\frac{1}{\sqrt{K}}$, leading to a rate of $\mathcal{O}\left(\frac{1}{\sqrt{K}}\right)$.*

VI. EXPERIMENTS

In this section, we validate our theoretical results and the efficacy of the proposed R-FAST algorithm on several large-scale machine learning tasks. We implement all the algorithms using the distributed communication package *torch.distributed* in PyTorch [43], where a process serves as a node. For *asynchronous setup* in our implementation, each process (node) runs its own code independently and the messages are transmitted between processes in a fully-asynchronous way without any blocking. By doing so, each process runs at its own pace without waiting to receive the messages from its in-neighbour process. Therefore, each process may receive the delayed message from its in-neighbours and delays are determined by different updating frequencies among nodes (i.e., degree of asynchrony) and the transmitting time of messages. For *packet losses*, we emulate it in such a way that each agent can decide whether to send out updated information for each out-neighbor at each iteration. An agent will not send information packet again to its out-neighbors until it receives the out-neighbor's receipt confirmation for the message it sent last time. Note that a) all communications including the receipt confirmation are carried out in an asynchronous non-blocking manner; and b) each agent, during its waking time, either sends out the newly-updated information packet, or simply discards it.

A. Regularized logistic regression

We consider a decentralized training problem over a network of $n \in \{3, 7, 15, 31\}$ nodes, respectively, and train a regularized logistic regression model on 12,000 images of two handwritten digits (0 and 1) from the MNIST dataset [44]. Note that the objective function is *smooth and strongly convex*. We deploy R-FAST on multiple CPU cores, each of which serves as a computing node. The hyperparameter setup is: i) mini-batch size: 32 per node; ii) learning rate: 0.001.

Training over general network architectures. To verify that the proposed R-FAST algorithm can work over general network architectures satisfying Assumption 2, we consider three different network structures, i.e., binary-tree (c.f., Figure 2(a)), line(c.f., Figure 2(c)), and directed ring (c.f., Figure 2(b)). For binary-tree or line structure, we design the

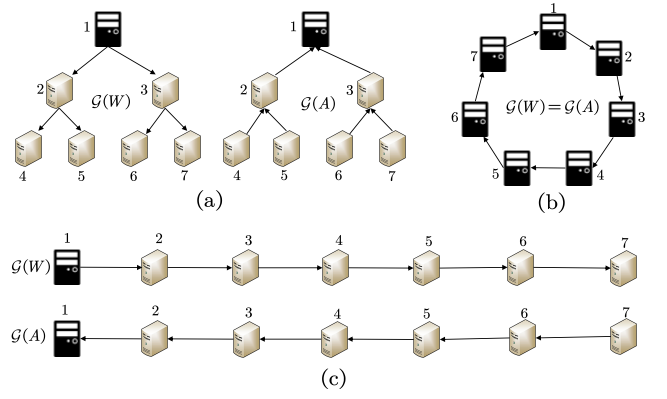


Figure 2. The underlying network architecture.

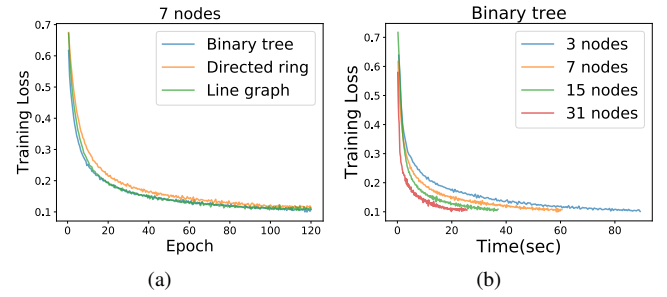


Figure 3. Performance of R-FAST in training logistic regression model over three different architectures (with 7 nodes) in terms of training loss versus epoch in subplot (a). The performance of R-FAST over binary tree architecture with different number of nodes is given in subplot (b).

specific two non-strongly-connected sub-graphs according to Assumption 2, that is, an oriented acyclic tree with one root as sub-graph $\mathcal{G}(W)$, and its inverse graph as sub-graph $\mathcal{G}(A)$. The corresponding row (resp. column) stochastic weight matrix W (resp. A) used for these three network architectures, along with the flexibility of architecture design, can be found in Appendix G.

It follows from Figure 3(a) that, the proposed R-FAST is able to converge for all the above three architectures. To the best of our knowledge, R-FAST is such an algorithm in the existing literature that can work on two spanning-tree graphs. Furthermore, we run R-FAST over the binary-tree structure for different number of nodes. Figure 3(b) shows that the time consumed for achieving a certain training loss (i.e., 0.105) is decreasing almost linearly with respect to the number of nodes, indicating that R-FAST can scale well with respect to the size of the network.

B. Large-scale image classification

We now report another experiment by training ResNet50 [45] on ImageNet dataset to verify the training efficiency and performance of our proposed R-FAST compared with the baselines. We randomly select 500 classes from the original ImageNet-1K [46] training set as our training set (thus containing 640,000 images), and select the same 500 classes from the original ImageNet-1K testing set as our testing set (thus containing 25,000 images).

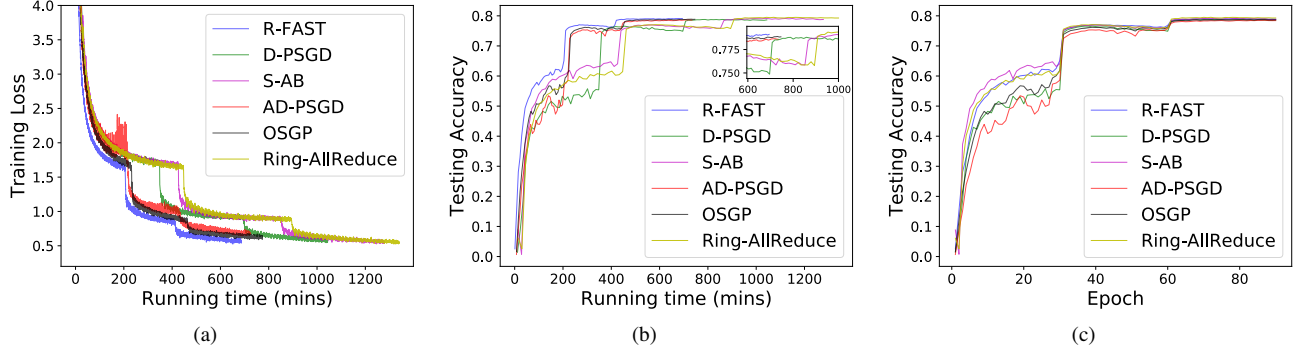


Figure 4. Performance comparison of R-FAST with D-PSGD, S-AB, AD-PSGD, OSGP and Ring-AllReduce in training ResNet50 when there is no straggler.

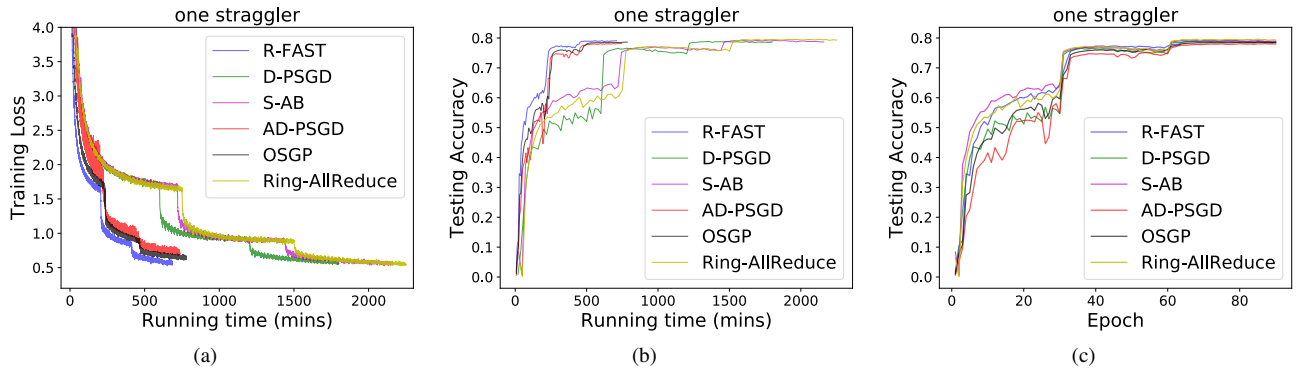


Figure 5. Performance comparison of R-FAST with D-PSGD, S-AB, AD-PSGD, OSGP and Ring-AllReduce in the presence of **one slow node/straggler**.

We compare the proposed R-FAST with the baselines: D-PSGD [14], S-AB [17], AD-PSGD [22], OSGP [23] and Ring-AllReduce [12]. All these algorithms are deployed on a high-performance server with 8 Nvidia RTX2080 Ti GPUs, i.e., each process (node) use a GPU to compute. We run D-PSGD and AD-PSGD over an undirected ring structure as they require undirected communication topology; and run R-FAST, S-AB and OSGP over a directed ring structure. In addition, for asynchronous algorithm R-FAST, AD-PSGD and OSGP, packet losses exist under our artificial settings as we have presented at the beginning of Section VI. All experiments are run for 90 epochs, and we use the following commonly used hyperparameter setup for the training process: i) mini-batch size: 32 per node; ii) learning rate: the initial value being 0.1 and decaying by a factor of 10 per 30 epochs; iii) Momentum: 0.9; and iv) weight decay: 10^{-4} .

Training efficiency. When there is no slow node (straggler) in the system, i.e., each node has the same computing speed, it follows from Figure 4(a), 4(b), 4(c) and Table 1 (column 2, 3) that R-FAST converges 1.5 times faster in running time than synchronous D-PSGD, S-AB and Ring-AllReduce while maintaining comparable testing accuracy (acc), thanks to the fully asynchronous training strategy and robust gradient tracking strategy. Furthermore, R-FAST enjoys higher testing accuracy (c.f., Table 1) comparing to asynchronous AD-PSGD and OSGP, mainly due to the robust gradient tracking strategy which is able to tackle the message losses.

Table 1
COMPARISON OF CONVERGENCE PERFORMANCE FOR R-FAST, D-PSGD, S-AB, AD-PSGD, OSGP AND RING-ALLREDUCE WHEN TRAINING RESNET50 UNDER TWO DIFFERENT SETTINGS: I) EACH NODE HAS THE SAME COMPUTING POWER (NO STRAGGLER); II) PRESENCE OF A STRAGGLER.

Algorithm	No straggler		Presence of a straggler	
	time(mins)	acc(%)	time(mins)	acc(%)
R-FAST	703	79.12	712	79.11
D-PSGD	1044	78.77	1800	78.71
S-AB	1278	79.14	2160	79.12
AD-PSGD	720	78.63	729	78.47
OSGP	753	78.86	768	78.68
Ring-AllReduce	1341	79.43	2250	79.43

Robustness against straggler. To verify the robustness of R-FAST against heterogeneous computing power among devices, we randomly select a GPU and allocate extra computing burden to slow down its computation to mimic the straggler. It follows from Figure 5(a), 5(b), 5(c) and Table 1(column 4, 5) that the training efficiency of the proposed R-FAST is barely affected and runs much faster than synchronous algorithms (e.g., 3 times faster than Ring-AllReduce) while maintaining comparable accuracy. Moreover, R-FAST can achieve much higher testing accuracy than asynchronous AD-PSGD and OSGP, meaning that R-FAST is much robust against stragglers considered in this work.

Table 2
COMPARISON OF CONVERGENCE PERFORMANCE IN TRAINING RESNET50
FOR R-FAST OVER 4, 8, AND 16 NODES.

node number	4	8	16
test accuracy(%)	79.29	79.12	79.01
time(mins)	1260	703	390

Scalability against the number of nodes. To explore the scalability of our proposed R-FAST on different numbers of nodes for the task of large-scale image classification, we implement R-FAST over a network of 4, 8, 16 nodes. We use a directed ring as the underlying network architecture for each of the above networks and the total epoch for training is 90. It can be observed from Figure 6 and Table 2 that the training speed of R-FAST increases almost linearly with the number of nodes while guaranteeing a small loss of accuracy, reflecting the good scalability of R-FAST.

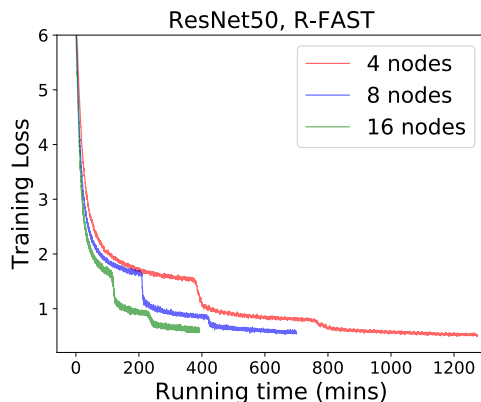


Figure 6. Comparison of convergence performance in training ResNet50 for R-FAST over 4, 8, and 16 nodes.

VII. CONCLUSION

In this paper, we proposed a new robust fully asynchronous method for solving large-scale distributed machine learning problems. We have provided the theoretical guarantee for the proposed R-FAST method both for both strongly convex and nonconvex cases. Experiments have shown that R-FAST can run much faster than the synchronous counterparts and achieve higher testing accuracy than the state-of-the-art asynchronous algorithms, especially in the presence of stragglers thanks to the introduced asynchronous mechanism and robust gradient tracking scheme. Most importantly, R-FAST can work on two spanning-tree graphs for training, which makes it flexible in the design of network architecture and is thus very suitable for scenarios where communication efficiency is a key concern and consensus protocols are difficult to design. It would be thus of great importance to explore new efficient communication architecture for message exchange.

REFERENCES

[1] Y. LeCun, Y. Bengio, and G. Hinton, “Deep learning,” *nature*, vol. 521, no. 7553, pp. 436–444, 2015.

[2] A. Voulodimos, N. Doulamis, A. Doulamis, and E. Protopapadakis, “Deep learning for computer vision: A brief review,” *Computational intelligence and neuroscience*, vol. 2018, 2018.

[3] J. Hirschberg and C. D. Manning, “Advances in natural language processing,” *Science*, vol. 349, no. 6245, pp. 261–266, 2015.

[4] K. Muhammad, A. Ullah, J. Lloret, J. Del Ser, and V. H. C. de Albuquerque, “Deep learning for safe autonomous driving: Current challenges and future directions,” *IEEE Transactions on Intelligent Transportation Systems*, vol. 22, no. 7, pp. 4316–4336, 2020.

[5] M. Langer, Z. He, W. Rahayu, and Y. Xue, “Distributed training of deep learning models: A taxonomic perspective,” *IEEE Transactions on Parallel and Distributed Systems*, vol. 31, no. 12, pp. 2802–2818, 2020.

[6] A. Nemirovski, A. Juditsky, G. Lan, and A. Shapiro, “Robust stochastic approximation approach to stochastic programming,” *SIAM Journal on optimization*, vol. 19, no. 4, pp. 1574–1609, 2009.

[7] E. Moulines and F. Bach, “Non-asymptotic analysis of stochastic approximation algorithms for machine learning,” *Advances in neural information processing systems*, vol. 24, 2011.

[8] S. Ghadimi and G. Lan, “Stochastic first-and zeroth-order methods for nonconvex stochastic programming,” *SIAM Journal on Optimization*, vol. 23, no. 4, pp. 2341–2368, 2013.

[9] J. Dean, G. Corrado, R. Monga, K. Chen, M. Devin, M. Mao, M. Ranzato, A. Senior, P. Tucker, K. Yang *et al.*, “Large scale distributed deep networks,” *Advances in neural information processing systems*, vol. 25, 2012.

[10] M. Zinkevich, M. Weimer, L. Li, and A. Smola, “Parallelized stochastic gradient descent,” *Advances in neural information processing systems*, vol. 23, 2010.

[11] B. McMahan, E. Moore, D. Ramage, S. Hampson, and B. A. y Arcas, “Communication-efficient learning of deep networks from decentralized data,” in *Artificial intelligence and statistics*. PMLR, 2017, pp. 1273–1282.

[12] A. Sergeev and M. Del Balso, “Horovod: fast and easy distributed deep learning in tensorflow,” *arXiv preprint arXiv:1802.05799*, 2018.

[13] P. Goyal, P. Dollár, R. Girshick, P. Noordhuis, L. Wesolowski, A. Kyrola, A. Tulloch, Y. Jia, and K. He, “Accurate, large minibatch sgd: Training imagenet in 1 hour,” *arXiv preprint arXiv:1706.02677*, 2017.

[14] X. Lian, C. Zhang, H. Zhang, C.-J. Hsieh, W. Zhang, and J. Liu, “Can decentralized algorithms outperform centralized algorithms? a case study for decentralized parallel stochastic gradient descent,” *Advances in Neural Information Processing Systems*, vol. 30, 2017.

[15] H. Tang, X. Lian, M. Yan, C. Zhang, and J. Liu, “D²: Decentralized training over decentralized data,” in *International Conference on Machine Learning*. PMLR, 2018, pp. 4848–4856.

[16] J. Zhang and K. You, “Decentralized stochastic gradient tracking for non-convex empirical risk minimization,” *arXiv preprint arXiv:1909.02712*, 2019.

[17] R. Xin, A. K. Sahu, U. A. Khan, and S. Kar, “Distributed stochastic optimization with gradient tracking over strongly-connected networks,” in *2019 IEEE 58th Conference on Decision and Control (CDC)*. IEEE, 2019, pp. 8353–8358.

[18] Q. Luo, J. He, Y. Zhuo, and X. Qian, “Prague: High-performance heterogeneity-aware asynchronous decentralized training,” in *Proceedings of the Twenty-Fifth International Conference on Architectural Support for Programming Languages and Operating Systems*, 2020, pp. 401–416.

[19] G. Nadiradze, A. Sabour, P. Davies, S. Li, and D. Alistarh, “Asynchronous decentralized sgd with quantized and local updates,” *Advances in Neural Information Processing Systems*, vol. 34, 2021.

[20] J. Verbracke, M. Wolting, J. Katzy, J. Kloppenburg, T. Verbelen, and J. S. Rellermeyer, “A survey on distributed machine learning,” *ACM Computing Surveys (CSUR)*, vol. 53, no. 2, pp. 1–33, 2020.

[21] S. S. Ram, A. Nedić, and V. V. Veeravalli, “Asynchronous gossip algorithms for stochastic optimization,” in *Proceedings of the 48th IEEE Conference on Decision and Control (CDC) held jointly with 2009 28th Chinese Control Conference*. IEEE, 2009, pp. 3581–3586.

[22] X. Lian, W. Zhang, C. Zhang, and J. Liu, “Asynchronous decentralized parallel stochastic gradient descent,” in *International Conference on Machine Learning*. PMLR, 2018, pp. 3043–3052.

[23] M. Assran, N. Loizou, N. Ballas, and M. Rabbat, “Stochastic gradient push for distributed deep learning,” in *International Conference on Machine Learning*. PMLR, 2019, pp. 344–353.

[24] J. Zhang and K. You, “Fully asynchronous distributed optimization with linear convergence in directed networks,” *arXiv preprint arXiv:1901.08215*, 2019.

- [25] Y. Tian, Y. Sun, and G. Scutari, "Achieving linear convergence in distributed asynchronous multiagent optimization," *IEEE Transactions on Automatic Control*, vol. 65, no. 12, pp. 5264–5279, 2020.
- [26] S. Pu, W. Shi, J. Xu, and A. Nedić, "Push-pull gradient methods for distributed optimization in networks," *IEEE Transactions on Automatic Control*, vol. 66, no. 1, pp. 1–16, 2020.
- [27] B. Recht, C. Re, S. Wright, and F. Niu, "Hogwild!: A lock-free approach to parallelizing stochastic gradient descent," *Advances in neural information processing systems*, vol. 24, 2011.
- [28] A. Agarwal and J. C. Duchi, "Distributed delayed stochastic optimization," *Advances in neural information processing systems*, vol. 24, 2011.
- [29] X. Lian, Y. Huang, Y. Li, and J. Liu, "Asynchronous parallel stochastic gradient for nonconvex optimization," *Advances in Neural Information Processing Systems*, vol. 28, 2015.
- [30] W. Zhang, S. Gupta, X. Lian, and J. Liu, "Staleness-aware async-sgd for distributed deep learning," *arXiv preprint arXiv:1511.05950*, 2015.
- [31] Z. Zhou, Y. Li, X. Ren, and S. Yang, "Towards efficient and stable k-asynchronous federated learning with unbounded stale gradients on non-IID data," *IEEE Transactions on Parallel and Distributed Systems*, 2022.
- [32] D. Kempe, A. Dobra, and J. Gehrke, "Gossip-based computation of aggregate information," in *44th Annual IEEE Symposium on Foundations of Computer Science, 2003. Proceedings.* IEEE, 2003, pp. 482–491.
- [33] A. Spiridonoff, A. Olshevsky, and I. C. Paschalidis, "Robust asynchronous stochastic gradient-push: Asymptotically optimal and network-independent performance for strongly convex functions," *Journal of Machine Learning Research*, vol. 21, no. 58, 2020.
- [34] X. Miao, X. Nie, Y. Shao, Z. Yang, J. Jiang, L. Ma, and B. Cui, "Heterogeneity-aware distributed machine learning training via partial reduce," in *Proceedings of the 2021 International Conference on Management of Data*, 2021, pp. 2262–2270.
- [35] P. Di Lorenzo and G. Scutari, "Next: In-network nonconvex optimization," *IEEE Transactions on Signal and Information Processing over Networks*, vol. 2, no. 2, pp. 120–136, 2016.
- [36] J. Xu, S. Zhu, Y. C. Soh, and L. Xie, "Augmented distributed gradient methods for multi-agent optimization under uncoordinated constant stepsizes," in *2015 54th IEEE Conference on Decision and Control (CDC)*. IEEE, 2015, pp. 2055–2060.
- [37] S. Pu and A. Nedić, "Distributed stochastic gradient tracking methods," *Mathematical Programming*, vol. 187, no. 1, pp. 409–457, 2021.
- [38] V. Kungurtsev, M. Morafah, T. Javidi, and G. Scutari, "Decentralized asynchronous non-convex stochastic optimization on directed graphs," *IEEE Transactions on Control of Network Systems*, 2023.
- [39] B. Gharesifard and J. Cortés, "When does a digraph admit a doubly stochastic adjacency matrix?" in *Proceedings of the 2010 American Control Conference*. IEEE, 2010, pp. 2440–2445.
- [40] K. Cai and H. Ishii, "Average consensus on general strongly connected digraphs," *Automatica*, vol. 48, no. 11, pp. 2750–2761, 2012.
- [41] Y. Tian, Y. Sun, and G. Scutari, "Asynchronous decentralized successive convex approximation," *arXiv preprint arXiv:1909.10144*, 2019.
- [42] A. Nedic, A. Olshevsky, and W. Shi, "Achieving geometric convergence for distributed optimization over time-varying graphs," *SIAM Journal on Optimization*, vol. 27, no. 4, pp. 2597–2633, 2017.
- [43] A. Paszke, S. Gross, S. Chintala, and G. Chanan, "Pytorch: Tensors and dynamic neural networks in python with strong gpu acceleration.(2017)," URL <https://github.com/pytorch/pytorch>, 2017.
- [44] L. Deng, "The mnist database of handwritten digit images for machine learning research [best of the web]," *IEEE signal processing magazine*, vol. 29, no. 6, pp. 141–142, 2012.
- [45] K. He, X. Zhang, S. Ren, and J. Sun, "Deep residual learning for image recognition," in *Proceedings of the IEEE conference on computer vision and pattern recognition*, 2016, pp. 770–778.
- [46] O. Russakovsky, J. Deng, H. Su, J. Krause, S. Satheesh, S. Ma, Z. Huang, A. Karpathy, A. Khosla, M. Bernstein *et al.*, "Imagenet large scale visual recognition challenge," *International journal of computer vision*, vol. 115, no. 3, pp. 211–252, 2015.

Appendix

CONTENTS

I	Introduction	1
II	RELATED WORK	2
II-A	On Asynchronous Model	2
II-B	On Robustness	2
III	PRELIMINARY	3
III-A	Network Model	3
III-B	Push-Pull Protocol	3
IV	The Proposed R-FAST Algorithm	3
V	Convergence Analysis	5
V-A	Augmented System	5
V-A1	An augmented system for consensus scheme: augmented graph of $\mathcal{G}(W)$	5
V-A2	An augmented system for gradient tracking scheme: augmented graph of $\mathcal{G}(A)$	6
V-A3	Auxiliary sequence for tackling stochastic errors	6
V-B	Strongly Convex: Geometric convergence	7
V-C	Non-Convex: Sublinear convergence	9
VI	Experiments	11
VI-A	Regularized logistic regression	11
VI-B	Large-scale image classification	11
VII	Conclusion	13
	References	13
	Appendix A: Proof of Proposition 1	15
	Appendix B: Proof of Lemma 6	19
	Appendix C: Proof of Lemma 7	23
	Appendix D: Definition of Constants	28
	Appendix E: Analysis of consensus scheme on augmented system	28
	Appendix F: Analysis of gradient tracking scheme on augmented system	29
	Appendix G: Used Weight Matrices and Architecture Design	31

APPENDIX A PROOF OF PROPOSITION 1

We first give a supporting lemma that we will use many times.

Lemma 8. *Let $\{v^k\}_{k=0}^{\infty}$ be non-negative sequence and $\lambda \in (0, 1)$. Then there holds that*

$$\left(\sum_{l=0}^k \lambda^{k-l} v^l \right)^2 \leq \frac{1}{1-\lambda} \sum_{l=0}^k \lambda^{k-l} (v^l)^2. \quad (41)$$

Proof.

$$\left(\sum_{l=0}^k \lambda^{k-l} v^l \right)^2 = \left(\sum_{l=0}^k \lambda^{\frac{k-l}{2}} \left(\lambda^{\frac{k-l}{2}} v^l \right) \right)^2 \stackrel{(a)}{\leq} \sum_{l=0}^k \left(\lambda^{\frac{k-l}{2}} \right)^2 \cdot \sum_{l=0}^k \left(\lambda^{\frac{k-l}{2}} v^l \right)^2 \leq \frac{1}{1-\lambda} \sum_{l=0}^k \lambda^{k-l} (v^l)^2,$$

where in (a) we have used Cauchy-Swarchz inequality. □

Now we restate the Proposition 1 in the main text:

Proposition 1. Consider the R-FAST algorithm with a constant step-size γ . Suppose Assumption 1-5 hold. Then, we have for all $k \geq 0$,

$$E_c^{k+1} \leq 2C_2^2 E_c^0 \cdot \rho^{2k} + \frac{4\gamma^2 C_2^2}{1-\rho} \sum_{l=0}^k \rho^{k-l} E_z^l + \frac{4\gamma^2 C_2^2 n}{1-\rho} \sum_{l=0}^k \rho^{k-l} \cdot \sigma^2, \quad (42a)$$

$$E_t^{k+1} \leq 3C_1^2 \|\bar{z}^0\|^2 \cdot \rho^{2k} + \sum_{l=0}^k \rho^{k-l} \left(\frac{27C_1^2 C_L^2}{1-\rho} E_c^l + \frac{54\gamma^2 C_1^2 C_L^2}{1-\rho} E_z^l + \frac{54\gamma^2 C_1^2 C_L^2 n}{1-\rho} \sigma^2 \right), \quad (42b)$$

$$E_z^k \leq 3E_t^k + 3C_L^2 n E_c^k + 3L^2 E_o^k, \quad (42c)$$

$$E_o^{k+1} \leq 4(1 - \tau\eta^2\gamma)^{-2r} E_o^0 \cdot (1 - \tau\eta^2\gamma)^{\frac{2r}{T} \cdot (k+1)} + \frac{4(1 - \tau\eta^2\gamma)^{-2r} \gamma^2}{1 - (1 - \tau\eta^2\gamma)^{\frac{r}{T}}} \sum_{l=0}^k (1 - \tau\eta^2\gamma)^{\frac{r}{T} \cdot (k-l)} (C_L^2 n E_c^l + E_t^l + n\sigma^2), \quad (42d)$$

where $C_1 = \frac{2\sqrt{2S}(1+\bar{m}^{-K_1})}{\rho(1-\bar{m}^{K_1})}$.

Proof. Our strategy is to bound these four errors in terms of linear combinations of their past values.

Bounding consensus error (c.f., (42a)) Applying (3) recursively, we get

$$h^{k+1} = \hat{W}^{k:0} h^0 - \sum_{l=0}^k \gamma^l \hat{W}^{k:l} e_{il} (z_{il}^l)^\top. \quad (43)$$

With (43), using (6) and the fact $(\psi^{t+1})^\top \hat{W}^t = (\psi^t)^\top$ [41], we have

$$x_\psi^{k+1} = x_\psi^0 - \sum_{l=0}^k \gamma^l (\psi^l)^\top e_{il} (z_{il}^l)^\top, \quad (44)$$

Using (43), (44), and Lemma 1, one can obtain that

$$\|h^{k+1} - \mathbf{1}x_\psi^{k+1}\| \leq C_2 \rho^k \|h^0 - \mathbf{1}x_\psi^0\| + C_2 \sum_{l=0}^k \rho^{k-l} \gamma \|z_{il}^l\|.$$

Using $(a+b)^2 \leq 2a^2 + 2b^2$ and Lemma 8, yields that

$$\begin{aligned} \|h^{k+1} - \mathbf{1}x_\psi^{k+1}\|^2 &\leq 2(C_2 \rho^k \|h^0 - \mathbf{1}x_\psi^0\|)^2 + 2\left(\gamma C_2 \sum_{l=0}^k \rho^{k-l} \|z_{il}^l\|\right)^2 \\ &\leq 2C_2^2 \rho^{2k} \|h^0 - \mathbf{1}x_\psi^0\|^2 + \frac{2\gamma^2 C_2^2}{1-\rho} \sum_{l=0}^k \rho^{k-l} \|z_{il}^l\|^2. \end{aligned}$$

Taking expectation on both sides, we get that

$$\begin{aligned} \mathbb{E} \left[\|h^{k+1} - \mathbf{1}x_\psi^{k+1}\|^2 \right] &\leq 2C_2^2 \rho^{2k} \|h^0 - \mathbf{1}x_\psi^0\|^2 + \frac{2\gamma^2 C_2^2}{1-\rho} \sum_{l=0}^k \rho^{k-l} \mathbb{E} [\|z_{il}^l\|^2] \\ &= 2C_2^2 \rho^{2k} \|h^0 - \mathbf{1}x_\psi^0\|^2 + \frac{2\gamma^2 C_2^2}{1-\rho} \sum_{l=0}^k \rho^{k-l} \mathbb{E} [\|z_{il}^l - \bar{z}_{il}^l + \bar{z}_{il}^l\|^2] \\ &\leq 2C_2^2 \rho^{2k} \|h^0 - \mathbf{1}x_\psi^0\|^2 + \frac{4\gamma^2 C_2^2}{1-\rho} \sum_{l=0}^k \rho^{k-l} \mathbb{E} [\|\bar{z}_{il}^l\|^2] + \frac{4\gamma^2 C_2^2}{1-\rho} \sum_{l=0}^k \rho^{k-l} \mathbb{E} [\|z_{il}^l - \bar{z}_{il}^l\|^2] \\ &\leq 2C_2^2 \rho^{2k} \|h^0 - \mathbf{1}x_\psi^0\|^2 + \frac{4\gamma^2 C_2^2}{1-\rho} \sum_{l=0}^k \rho^{k-l} \mathbb{E} [\|\bar{z}_{il}^l\|^2] + \frac{4\gamma^2 C_2^2 n}{1-\rho} \sum_{l=0}^k \rho^{k-l} \cdot \sigma^2, \end{aligned}$$

where we used (15) in the last inequality.

Bounding gradient tracking error (c.f., (42b)) Similar with [25] (Proposition 19, 41b), using (3), (13), (14) and Lemma 2, we can get that

$$\|\bar{z}_{ik+1}^{k+1} - \xi_{ik+1}^k (\bar{z}^{k+1})^\top \mathbf{1}\| \leq C_1 \rho^k \|\bar{z}^0\| + 3C_1 C_L \sum_{l=0}^k \rho^{k-l} (\|h^l - \mathbf{1}x_\psi^l\| + \gamma \|z_{il}^l\|).$$

Using $(a + b + c)^2 \leq 3a^2 + 3b^2 + 3c^2$ and Lemma 8, yields that

$$\begin{aligned}
& \left\| \bar{z}_{i^{k+1}}^{k+1} - \xi_{i^{k+1}}^k (\bar{z}^{k+1})^\top \mathbf{1} \right\|^2 \\
& \leq 3 \left(C_1 \rho^k \|\bar{z}^0\| \right)^2 + 3 \left(3C_1 C_L \sum_{l=0}^k \rho^{k-l} \|h^l - \mathbf{1} x_\psi^l\| \right)^2 + 3 \left(3\gamma C_1 C_L \sum_{l=0}^k \rho^{k-l} \|z_{i^l}^l\| \right)^2 \\
& \leq 3C_1^2 \rho^{2k} \|\bar{z}^0\|^2 + \frac{27C_1^2 C_L^2}{1-\rho} \sum_{l=0}^k \rho^{k-l} \|h^l - \mathbf{1} x_\psi^l\|^2 + \frac{27\gamma^2 C_1^2 C_L^2}{1-\rho} \sum_{l=0}^k \rho^{k-l} \|z_{i^l}^l\|^2.
\end{aligned}$$

Taking expectation on both sides, we get that

$$\begin{aligned}
& \mathbb{E} \left[\left\| \bar{z}_{i^{k+1}}^{k+1} - \xi_{i^{k+1}}^k (\bar{z}^{k+1})^\top \mathbf{1} \right\|^2 \right] \\
& \leq 3C_1^2 \rho^{2k} \|\bar{z}^0\|^2 + \frac{27C_1^2 C_L^2}{1-\rho} \sum_{l=0}^k \rho^{k-l} \mathbb{E} \left[\|h^l - \mathbf{1} x_\psi^l\|^2 \right] + \frac{27\gamma^2 C_1^2 C_L^2}{1-\rho} \sum_{l=0}^k \rho^{k-l} \mathbb{E} \left[\|z_{i^l}^l\|^2 \right] \\
& \leq 3C_1^2 \rho^{2k} \|\bar{z}^0\|^2 + \frac{27C_1^2 C_L^2}{1-\rho} \sum_{l=0}^k \rho^{k-l} \mathbb{E} \left[\|h^l - \mathbf{1} x_\psi^l\|^2 \right] + \frac{27\gamma^2 C_1^2 C_L^2}{1-\rho} \sum_{l=0}^k \rho^{k-l} \mathbb{E} \left[\|z_{i^l}^l - \bar{z}_{i^l}^l + \bar{z}_{i^l}^l\|^2 \right] \\
& \leq 3C_1^2 \rho^{2k} \|\bar{z}^0\|^2 + \frac{27C_1^2 C_L^2}{1-\rho} \sum_{l=0}^k \rho^{k-l} \mathbb{E} \left[\|h^l - \mathbf{1} x_\psi^l\|^2 \right] \\
& \quad + \frac{54\gamma^2 C_1^2 C_L^2}{1-\rho} \sum_{l=0}^k \rho^{k-l} \mathbb{E} \left[\|\bar{z}_{i^l}^l\|^2 \right] + \frac{54\gamma^2 C_1^2 C_L^2}{1-\rho} \sum_{l=0}^k \rho^{k-l} \mathbb{E} \left[\|z_{i^l}^l - \bar{z}_{i^l}^l\|^2 \right] \\
& \leq 3C_1^2 \rho^{2k} \|\bar{z}^0\|^2 + \frac{27C_1^2 C_L^2}{1-\rho} \sum_{l=0}^k \rho^{k-l} \mathbb{E} \left[\|h^l - \mathbf{1} x_\psi^l\|^2 \right] \\
& \quad + \frac{54\gamma^2 C_1^2 C_L^2}{1-\rho} \sum_{l=0}^k \rho^{k-l} \mathbb{E} \left[\|\bar{z}_{i^l}^l\|^2 \right] + \frac{54\gamma^2 C_1^2 C_L^2 n}{1-\rho} \sum_{l=0}^k \rho^{k-l} \cdot \sigma^2,
\end{aligned}$$

where we used (15) in the last inequality.

Bounding gradient tracking variable (c.f., (42c)) Using triangle inequality, we get that

$$\begin{aligned}
\|\bar{z}_{i^k}^k\| & \leq \|\bar{z}_{i^k}^k - \xi_{i^k}^{k-1} (\bar{z}^k)^\top \mathbf{1}\| + \xi_{i^k}^{k-1} \|\nabla F(x_\psi^k) - (\bar{z}^k)^\top \mathbf{1}\| + \xi_{i^k}^{k-1} \|\nabla F(x_\psi^k) - \nabla F(x^*)\| \\
& \stackrel{(a)}{\leq} \|\bar{z}_{i^k}^k - \xi_{i^k}^{k-1} (\bar{z}^k)^\top \mathbf{1}\| + \xi_{i^k}^{k-1} \left\| \sum_{i=1}^n (\nabla f_i(x_i^k) - \nabla f_i(x_\psi^k)) \right\| + \xi_{i^k}^{k-1} \|\nabla F(x_\psi^k) - \nabla F(x^*)\| \\
& \stackrel{(b)}{\leq} \|\bar{z}_{i^k}^k - \xi_{i^k}^{k-1} (\bar{z}^k)^\top \mathbf{1}\| + C_L \sqrt{n} \|x^k - \mathbf{1} x_\psi^k\| + L \|x_\psi^k - (x^*)^\top\| \\
& \leq \|\bar{z}_{i^k}^k - \xi_{i^k}^{k-1} (\bar{z}^k)^\top \mathbf{1}\| + C_L \sqrt{n} \|h^k - \mathbf{1} x_\psi^k\| + L \|x_\psi^k - (x^*)^\top\|,
\end{aligned}$$

where we used (16) in (a) and Assumption 4 in (b). Further, we have

$$\begin{aligned}
\mathbb{E} \left[\|\bar{z}_{i^k}^k\|^2 \right] & \leq \mathbb{E} \left[\left(\|\bar{z}_{i^k}^k - \xi_{i^k}^{k-1} (\bar{z}^k)^\top \mathbf{1}\| + C_L \sqrt{n} \|h^k - \mathbf{1} x_\psi^k\| + L \|x_\psi^k - (x^*)^\top\| \right)^2 \right] \\
& \leq 3\mathbb{E} \left[\|\bar{z}_{i^k}^k - \xi_{i^k}^{k-1} (\bar{z}^k)^\top \mathbf{1}\|^2 \right] + 3C_L^2 n \mathbb{E} \left[\|h^k - \mathbf{1} x_\psi^k\|^2 \right] + 3L^2 \mathbb{E} \left[\|x_\psi^k - (x^*)^\top\|^2 \right]
\end{aligned}$$

Bounding optimization error (c.f., (42d)) According to (7), we have that $x_\psi^{k+1} = x_\psi^k - \gamma \psi_{i^k}^k (z_{i^k}^k)^\top$. Thus, by triangle inequality, we further have,

$$\begin{aligned}
& \left\| x_\psi^{k+1} - (x^*)^\top \right\| = \left\| x_\psi^k - \gamma \psi_{i^k}^k (z_{i^k}^k)^\top - (x^*)^\top \right\| \\
& \leq \left\| x_\psi^k - \gamma \psi_{i^k}^k \xi_{i^k}^{k-1} \nabla F(x_\psi^k) - (x^*)^\top \right\| + \gamma \psi_{i^k}^k \xi_{i^k}^{k-1} \left\| \nabla F(x_\psi^k) - \mathbf{1}^\top \bar{z}^k \right\| \\
& \quad + \gamma \psi_{i^k}^k \left\| \bar{z}_{i^k}^k - \xi_{i^k}^{k-1} (\bar{z}^k)^\top \mathbf{1} \right\| + \gamma \psi_{i^k}^k \left\| z_{i^k}^k - \bar{z}_{i^k}^k \right\| \\
& \stackrel{(a)}{\leq} \underbrace{\left(1 - \tau \psi_{i^k}^k \xi_{i^k}^{k-1} \gamma\right)}_{\triangleq \omega^k} \left\| x_\psi^k - (x^*)^\top \right\| + \gamma C_L \sqrt{n} \|h^k - \mathbf{1} x_\psi^k\| \\
& \quad + \gamma \left\| \bar{z}_{i^k}^k - \xi_{i^k}^{k-1} (\bar{z}^k)^\top \mathbf{1} \right\| + \gamma \left\| z_{i^k}^k - \bar{z}_{i^k}^k \right\| \\
& \stackrel{(b)}{\leq} \prod_{t=0}^k \omega^t \left\| x_\psi^0 - (x^*)^\top \right\| + \gamma C_L \sqrt{n} \sum_{l=0}^k \prod_{t=l}^{k-1} \omega^t \|h^l - \mathbf{1} x_\psi^l\| \\
& \quad + \gamma \sum_{l=0}^k \prod_{t=l}^{k-1} \omega^t \left\| \bar{z}_{i^l}^l - \xi_{i^l}^{l-1} (\bar{z}^l)^\top \mathbf{1} \right\| + \gamma \sum_{l=0}^k \prod_{t=l}^{k-1} \omega^t \|z_{i^l}^l - \bar{z}_{i^l}^l\|,
\end{aligned} \tag{45}$$

where we used the property of τ -strongly convex of $F(\cdot)$ and Assumption 4 in (a), and (b) follows by applying the above inequality recursively.

With the help of Lemma 1 and Lemma 2, we get that if $i^k \in \mathcal{R}$, $\psi_{i^k}^k \geq \eta$ and $\xi_{i^k}^{k-1} \geq \eta$, then $\omega^k \leq 1 - \tau \eta^2 \gamma$. Besides, noticing that $r = |\mathcal{R}|$, we get that for any $k \geq 0$,

$$\prod_{t=k}^{k+T-1} \omega^t \leq (1 - \tau \eta^2 \gamma)^r, \tag{46}$$

and for any $s \geq 1$

$$\prod_{t=k}^{k+s-1} \omega^t \leq (1 - \tau \eta^2 \gamma)^{\lfloor \frac{s}{T} \rfloor r} \leq (1 - \tau \eta^2 \gamma)^{-r} (1 - \tau \eta^2 \gamma)^{\frac{r}{T} s},$$

where $(1 - \tau \eta^2 \gamma)^{\frac{r}{T}}$ indicates the contraction factor. Substituting this into (45) leads to

$$\begin{aligned}
\left\| x_\psi^{k+1} - (x^*)^\top \right\| & \leq (1 - \tau \eta^2 \gamma)^{-r} (1 - \tau \eta^2 \gamma)^{\frac{r}{T}(k+1)} \left\| x_\psi^0 - (x^*)^\top \right\| \\
& \quad + (1 - \tau \eta^2 \gamma)^{-r} \gamma C_L \sqrt{n} \sum_{l=0}^k (1 - \tau \eta^2 \gamma)^{\frac{r}{T}(k-l)} \|h^l - \mathbf{1} x_\psi^l\| \\
& \quad + (1 - \tau \eta^2 \gamma)^{-r} \gamma \sum_{l=0}^k (1 - \tau \eta^2 \gamma)^{\frac{r}{T}(k-l)} \left\| \bar{z}_{i^l}^l - \xi_{i^l}^{l-1} (\bar{z}^l)^\top \mathbf{1} \right\| \\
& \quad + (1 - \tau \eta^2 \gamma)^{-r} \gamma \sum_{l=0}^k (1 - \tau \eta^2 \gamma)^{\frac{r}{T}(k-l)} \|z_{i^l}^l - \bar{z}_{i^l}^l\|.
\end{aligned}$$

Using $(a + b + c + d)^2 \leq 4a^2 + 4b^2 + 4c^2 + 4d^2$ and Lemma 8, we have

$$\begin{aligned}
\left\| x_\psi^{k+1} - (x^*)^\top \right\|^2 & \leq 4 (1 - \tau \eta^2 \gamma)^{-2r} (1 - \tau \eta^2 \gamma)^{\frac{2r}{T}(k+1)} \left\| x_\psi^0 - (x^*)^\top \right\|^2 \\
& \quad + \frac{4 (1 - \tau \eta^2 \gamma)^{-2r} \gamma^2 C_L^2 n}{1 - (1 - \tau \eta^2 \gamma)^{\frac{r}{T}}} \sum_{l=0}^k (1 - \tau \eta^2 \gamma)^{\frac{r}{T}(k-l)} \|h^l - \mathbf{1} x_\psi^l\|^2 \\
& \quad + \frac{4 (1 - \tau \eta^2 \gamma)^{-2r} \gamma^2}{1 - (1 - \tau \eta^2 \gamma)^{\frac{r}{T}}} \sum_{l=0}^k (1 - \tau \eta^2 \gamma)^{\frac{r}{T}(k-l)} \left\| \bar{z}_{i^l}^l - \xi_{i^l}^{l-1} (\bar{z}^l)^\top \mathbf{1} \right\|^2 \\
& \quad + \frac{4 (1 - \tau \eta^2 \gamma)^{-2r} \gamma^2}{1 - (1 - \tau \eta^2 \gamma)^{\frac{r}{T}}} \sum_{l=0}^k (1 - \tau \eta^2 \gamma)^{\frac{r}{T}(k-l)} \|z_{i^l}^l - \bar{z}_{i^l}^l\|^2.
\end{aligned}$$

Taking expectation on both sides, get that

$$\begin{aligned}
\mathbb{E} \left[\left\| x_\psi^{k+1} - (x^*)^\top \right\|^2 \right] &\leq 4 (1 - \tau \eta^2 \gamma)^{-2r} (1 - \tau \eta^2 \gamma)^{\frac{2r}{T}(k+1)} \left\| x_\psi^0 - (x^*)^\top \right\|^2 \\
&\quad + \frac{4 (1 - \tau \eta^2 \gamma)^{-2r} \gamma^2 C_L^2 n}{1 - (1 - \tau \eta^2 \gamma)^{\frac{r}{T}}} \sum_{l=0}^k (1 - \tau \eta^2 \gamma)^{\frac{r}{T}(k-l)} \mathbb{E} \left[\left\| h^l - 1x_\psi^l \right\|^2 \right] \\
&\quad + \frac{4 (1 - \tau \eta^2 \gamma)^{-2r} \gamma^2}{1 - (1 - \tau \eta^2 \gamma)^{\frac{r}{T}}} \sum_{l=0}^k (1 - \tau \eta^2 \gamma)^{\frac{r}{T}(k-l)} \mathbb{E} \left[\left\| \bar{z}_{i^l}^l - \xi_{i^l}^{l-1} (\bar{z}^l)^\top \mathbf{1} \right\|^2 \right] \\
&\quad + \frac{4 (1 - \tau \eta^2 \gamma)^{-2r} \gamma^2}{1 - (1 - \tau \eta^2 \gamma)^{\frac{r}{T}}} \sum_{l=0}^k (1 - \tau \eta^2 \gamma)^{\frac{r}{T}(k-l)} \mathbb{E} \left[\left\| z_{i^k}^k - \bar{z}_{i^k}^k \right\|^2 \right] \\
&\leq 4 (1 - \tau \eta^2 \gamma)^{-2r} (1 - \tau \eta^2 \gamma)^{\frac{2r}{T}(k+1)} \left\| x_\psi^0 - (x^*)^\top \right\|^2 \\
&\quad + \frac{4 (1 - \tau \eta^2 \gamma)^{-2r} \gamma^2 C_L^2 n}{1 - (1 - \tau \eta^2 \gamma)^{\frac{r}{T}}} \sum_{l=0}^k (1 - \tau \eta^2 \gamma)^{\frac{r}{T}(k-l)} \mathbb{E} \left[\left\| h^l - 1x_\psi^l \right\|^2 \right] \\
&\quad + \frac{4 (1 - \tau \eta^2 \gamma)^{-2r} \gamma^2}{1 - (1 - \tau \eta^2 \gamma)^{\frac{r}{T}}} \sum_{l=0}^k (1 - \tau \eta^2 \gamma)^{\frac{r}{T}(k-l)} \mathbb{E} \left[\left\| \bar{z}_{i^l}^l - \xi_{i^l}^{l-1} (\bar{z}^l)^\top \mathbf{1} \right\|^2 \right] \\
&\quad + \frac{4 (1 - \tau \eta^2 \gamma)^{-2r} \gamma^2 n}{1 - (1 - \tau \eta^2 \gamma)^{\frac{r}{T}}} \sum_{l=0}^k (1 - \tau \eta^2 \gamma)^{\frac{r}{T}(k-l)} \sigma^2,
\end{aligned}$$

where we used (15) in the last inequality.

The proof of Proposition 1 is completed. \square

APPENDIX B PROOF OF LEMMA 6

We restate Lemma 6 in the main text:

Lemma 6. *Suppose Assumption 1-5 hold. Let the constant step-size γ satisfy*

$$\gamma < \frac{1}{\sqrt{3\varrho_c C_L^2 n + 3\varrho_t}}, \quad (47)$$

then, for all $k \geq 0$, we have

$$\begin{aligned}
\sum_{l=0}^k \mathbb{E} \left\| h^l - 1x_\psi^l \right\|^2 &\leq \frac{3\varrho_c \gamma^2}{1 - 3(\varrho_c C_L^2 n + \varrho_t) \gamma^2} \sum_{l=0}^k \mathbb{E} \left\| \nabla F(x_\psi^l) \right\|^2 \\
&\quad + \frac{(1 - 3\varrho_t \gamma^2) c_c + 3c_t \varrho_c \gamma^2}{1 - 3(\varrho_c C_L^2 n + \varrho_t) \gamma^2} + \frac{\varrho_c n \gamma^2 (k+1)}{1 - 3(\varrho_c C_L^2 n + \varrho_t) \gamma^2} \sigma^2,
\end{aligned} \quad (48)$$

and

$$\begin{aligned}
\sum_{l=0}^k \mathbb{E} \left\| \bar{z}_{i^l}^l - \xi_{i^l}^{l-1} (\bar{z}^l)^\top \mathbf{1} \right\|^2 &\leq \frac{\varrho_t n \gamma^2 (k+1)}{1 - 3(\varrho_c C_L^2 n + \varrho_t) \gamma^2} \sigma^2 \\
&\quad + \frac{3\varrho_t \gamma^2}{1 - 3(\varrho_c C_L^2 n + \varrho_t) \gamma^2} \sum_{l=0}^k \mathbb{E} \left\| \nabla F(x_\psi^l) \right\|^2 \\
&\quad + \frac{(1 - 3\varrho_c C_L^2 n \gamma^2) c_t + 3c_c \varrho_t C_L^2 n \gamma^2}{1 - 3(\varrho_c C_L^2 n + \varrho_t) \gamma^2},
\end{aligned} \quad (49)$$

where c_c , ϱ_c , c_t and ϱ_t are constants given as below:

$$c_c \triangleq \left(1 + \frac{2C_2^2}{1 - \rho^2} \right) \left\| h^0 - 1x_\psi^0 \right\|^2, \quad \varrho_c \triangleq \frac{4C_2^2}{(1 - \rho)^2}, \quad (50)$$

$$\begin{aligned}
c_t &\triangleq \frac{3C_1^2 \left\| \bar{z}^0 \right\|^2}{1 - \rho^2} + \frac{27C_1^2 C_L^2 (2C_2^2 + 1 - \rho^2)}{(1 - \rho)^4} \left\| h^0 - 1x_\psi^0 \right\|^2 + \left\| \bar{z}_{i^0}^0 - \xi_{i^0}^{-1} (\bar{z}^0)^\top \mathbf{1} \right\|^2, \\
\varrho_t &\triangleq \frac{54C_1^2 C_L^2 \left[4C_2^2 + (1 - \rho)^2 \right]}{(1 - \rho)^4}.
\end{aligned} \quad (51)$$

Proof. According to (42a), we know that for $l \geq 1$:

$$\mathbb{E} \left[\|h^l - \mathbf{1}x_\psi^l\|^2 \right] \leq 2C_2^2 \rho^{2(l-1)} \|h^0 - \mathbf{1}x_\psi^0\|^2 + \frac{4\gamma^2 C_2^2}{1-\rho} \sum_{t=0}^{l-1} \rho^{l-1-t} \mathbb{E} \left[\|\bar{z}_{i^t}^t\|^2 \right] + \frac{4\gamma^2 C_2^2 n \sigma^2}{(1-\rho)^2}. \quad (52)$$

Then, for $k \geq 0$, we have

$$\begin{aligned} \sum_{l=0}^k \mathbb{E} \left[\|h^l - \mathbf{1}x_\psi^l\|^2 \right] &= \|h^0 - \mathbf{1}x_\psi^0\|^2 + \sum_{l=1}^k \mathbb{E} \left[\|h^l - \mathbf{1}x_\psi^l\|^2 \right] \\ &\leq \|h^0 - \mathbf{1}x_\psi^0\|^2 + 2C_2^2 \|h^0 - \mathbf{1}x_\psi^0\|^2 \sum_{l=1}^k \rho^{2(l-1)} + \frac{4\gamma^2 C_2^2}{1-\rho} \sum_{l=1}^k \sum_{t=0}^{l-1} \rho^{l-1-t} \mathbb{E} \left[\|\bar{z}_{i^t}^t\|^2 \right] + \frac{4\gamma^2 C_2^2 n \sigma^2}{(1-\rho)^2} (k+1) \\ &\leq \|h^0 - \mathbf{1}x_\psi^0\|^2 + \frac{2C_2^2 \|h^0 - \mathbf{1}x_\psi^0\|^2}{1-\rho^2} + \frac{4\gamma^2 C_2^2}{1-\rho} \sum_{t=0}^{k-1} \sum_{l=t+1}^k \rho^{l-1-t} \mathbb{E} \left[\|\bar{z}_{i^t}^t\|^2 \right] + \frac{4\gamma^2 C_2^2 n \sigma^2}{(1-\rho)^2} (k+1) \\ &\leq \left(1 + \frac{2C_2^2}{1-\rho^2} \right) \|h^0 - \mathbf{1}x_\psi^0\|^2 + \frac{4\gamma^2 C_2^2}{(1-\rho)^2} \sum_{t=0}^{k-1} \mathbb{E} \left[\|\bar{z}_{i^t}^t\|^2 \right] + \frac{4\gamma^2 C_2^2 n \sigma^2}{(1-\rho)^2} (k+1) \\ &\leq \underbrace{\left(1 + \frac{2C_2^2}{1-\rho^2} \right) \|h^0 - \mathbf{1}x_\psi^0\|^2}_{c_c} + \underbrace{\frac{4C_2^2}{(1-\rho)^2}}_{\varrho_c} \cdot \gamma^2 \sum_{l=0}^k \mathbb{E} \left[\|\bar{z}_{i^l}^l\|^2 \right] + \underbrace{\frac{4C_2^2}{(1-\rho)^2}}_{\varrho_c} \gamma^2 n \sigma^2 (k+1). \end{aligned} \quad (53)$$

According to (42b), we know that for $l \geq 1$:

$$\begin{aligned} \mathbb{E} \left[\|\bar{z}_{i^l}^l - \xi_{i^l}^{l-1} (\bar{z}^l)^\top \mathbf{1}\|^2 \right] &\leq 3C_1^2 \rho^{2(l-1)} \|\bar{z}^0\|^2 + \frac{27C_1^2 C_L^2}{1-\rho} \sum_{t=0}^{l-1} \rho^{l-1-t} \mathbb{E} \left[\|h^t - \mathbf{1}x_\psi^t\|^2 \right] \\ &\quad + \frac{54\gamma^2 C_1^2 C_L^2}{1-\rho} \sum_{t=0}^{l-1} \rho^{l-1-t} \mathbb{E} \left[\|\bar{z}_{i^t}^t\|^2 \right] + \frac{54\gamma^2 C_1^2 C_L^2 n \sigma^2}{(1-\rho)^2}. \end{aligned} \quad (54)$$

Then, for $k \geq 0$, we have

$$\begin{aligned}
& \sum_{l=0}^k \mathbb{E} \left[\left\| \bar{z}_{i^l}^l - \xi_{i^l}^{l-1}(\bar{z}^l)^\top \mathbf{1} \right\|^2 \right] \\
&= \left\| \bar{z}_{i^0}^0 - \xi_{i^0}^{-1}(\bar{z}^0)^\top \mathbf{1} \right\|^2 + \sum_{l=1}^k \mathbb{E} \left[\left\| \bar{z}_{i^l}^l - \xi_{i^l}^{l-1}(\bar{z}^l)^\top \mathbf{1} \right\|^2 \right] \\
&\leq \left\| \bar{z}_{i^0}^0 - \xi_{i^0}^{-1}(\bar{z}^0)^\top \mathbf{1} \right\|^2 + 3C_1^2 \left\| \bar{z}^0 \right\|^2 \sum_{l=1}^k \rho^{2(l-1)} + \frac{27C_1^2 C_L^2}{1-\rho} \sum_{l=1}^k \sum_{t=0}^{l-1} \rho^{l-1-t} \cdot \mathbb{E} \left[\left\| h^t - \mathbf{1} x_\psi^t \right\|^2 \right] \\
&\quad + \frac{54\gamma^2 C_1^2 C_L^2}{1-\rho} \sum_{l=1}^k \sum_{t=0}^{l-1} \rho^{l-1-t} \cdot \mathbb{E} \left[\left\| \bar{z}_{i^t}^t \right\|^2 \right] + \frac{54\gamma^2 C_1^2 C_L^2 n \sigma^2}{(1-\rho)^2} (k+1) \\
&\leq \left\| \bar{z}_{i^0}^0 - \xi_{i^0}^{-1}(\bar{z}^0)^\top \mathbf{1} \right\|^2 + \frac{3C_1^2 \left\| \bar{z}^0 \right\|^2}{1-\rho^2} + \frac{27C_1^2 C_L^2}{1-\rho} \sum_{t=0}^{k-1} \sum_{l=t+1}^k \rho^{l-1-t} \cdot \mathbb{E} \left[\left\| h^t - \mathbf{1} x_\psi^t \right\|^2 \right] \\
&\quad + \frac{54\gamma^2 C_1^2 C_L^2}{1-\rho} \sum_{t=0}^{k-1} \sum_{l=t+1}^k \rho^{l-1-t} \cdot \mathbb{E} \left[\left\| \bar{z}_{i^t}^t \right\|^2 \right] + \frac{54\gamma^2 C_1^2 C_L^2 n \sigma^2}{(1-\rho)^2} (k+1) \\
&\leq \left\| \bar{z}_{i^0}^0 - \xi_{i^0}^{-1}(\bar{z}^0)^\top \mathbf{1} \right\|^2 + \frac{3C_1^2 \left\| \bar{z}^0 \right\|^2}{1-\rho^2} + \frac{27C_1^2 C_L^2}{(1-\rho)^2} \sum_{t=0}^{k-1} \mathbb{E} \left[\left\| h^t - \mathbf{1} x_\psi^t \right\|^2 \right] \\
&\quad + \frac{54\gamma^2 C_1^2 C_L^2}{(1-\rho)^2} \sum_{t=0}^{k-1} \mathbb{E} \left[\left\| \bar{z}_{i^t}^t \right\|^2 \right] + \frac{54\gamma^2 C_1^2 C_L^2 n \sigma^2}{(1-\rho)^2} (k+1) \tag{55} \\
&\leq \left\| \bar{z}_{i^0}^0 - \xi_{i^0}^{-1}(\bar{z}^0)^\top \mathbf{1} \right\|^2 + \frac{3C_1^2 \left\| \bar{z}^0 \right\|^2}{1-\rho^2} + \frac{27C_1^2 C_L^2}{(1-\rho)^2} \sum_{l=0}^k \mathbb{E} \left[\left\| h^l - \mathbf{1} x_\psi^l \right\|^2 \right] \\
&\quad + \frac{54\gamma^2 C_1^2 C_L^2}{(1-\rho)^2} \sum_{l=0}^k \mathbb{E} \left[\left\| \bar{z}_{i^l}^l \right\|^2 \right] + \frac{54\gamma^2 C_1^2 C_L^2 n \sigma^2}{(1-\rho)^2} (k+1) \\
&\stackrel{(a)}{\leq} \left\| \bar{z}_{i^0}^0 - \xi_{i^0}^{-1}(\bar{z}^0)^\top \mathbf{1} \right\|^2 + \frac{3C_1^2 \left\| \bar{z}^0 \right\|^2}{1-\rho^2} + \frac{54\gamma^2 C_1^2 C_L^2}{(1-\rho)^2} \sum_{l=0}^k \mathbb{E} \left[\left\| \bar{z}_{i^l}^l \right\|^2 \right] + \frac{54\gamma^2 C_1^2 C_L^2 n \sigma^2}{(1-\rho)^2} (k+1) \\
&\quad + \frac{27C_1^2 C_L^2}{(1-\rho)^2} \left\{ \left(1 + \frac{2C_2^2}{1-\rho^2} \right) \left\| h^0 - \mathbf{1} x_\psi^0 \right\|^2 + \frac{4\gamma^2 C_2^2}{(1-\rho)^2} \sum_{l=0}^k \mathbb{E} \left[\left\| \bar{z}_{i^l}^l \right\|^2 \right] + \frac{4\gamma^2 C_2^2 n \sigma^2}{(1-\rho)^2} (k+1) \right\} \\
&\leq \underbrace{\frac{3C_1^2 \left\| \bar{z}^0 \right\|^2}{1-\rho^2} + \frac{27C_1^2 C_L^2 (2C_2^2 + 1 - \rho^2)}{(1-\rho)^4} \left\| h^0 - \mathbf{1} x_\psi^0 \right\|^2 + \left\| \bar{z}_{i^0}^0 - \xi_{i^0}^{-1}(\bar{z}^0)^\top \mathbf{1} \right\|^2}_{c_t} \\
&\quad + \underbrace{\frac{54C_1^2 C_L^2 [2C_2^2 + (1-\rho)^2]}{(1-\rho)^4}}_{\varrho_t} \cdot \gamma^2 \sum_{l=0}^k \mathbb{E} \left[\left\| \bar{z}_{i^l}^l \right\|^2 \right] + \underbrace{\frac{54C_1^2 C_L^2 [2C_2^2 + (1-\rho)^2]}{(1-\rho)^4}}_{\varrho_t} \cdot \gamma^2 n \sigma^2 (k+1),
\end{aligned}$$

where in (a) we have used (53).

Further, with (53) and (55), using $\|a + b + c\|^2 \leq 3\|a\|^2 + 3\|b\|^2 + 3\|c\|^2$, we have

$$\begin{aligned}
& \sum_{l=0}^k \mathbb{E} \left[\|h^l - \mathbf{1}x_\psi^l\|^2 \right] \\
& \leq c_c + 3\varrho_c \gamma^2 \sum_{l=0}^k \mathbb{E} \left[\left\| \bar{z}_{i^l}^l - \xi_{i^l}^{l-1} (\bar{z}^l)^\top \mathbf{1} \right\|^2 \right] + 3\varrho_c \gamma^2 \sum_{l=0}^k (\xi_{i^l}^{l-1})^2 \mathbb{E} \left[\|\nabla F(x_\psi^l)\|^2 \right] \\
& \quad + 3\varrho_c \gamma^2 \sum_{l=0}^k (\xi_{i^l}^{l-1})^2 \mathbb{E} \left[\left\| \nabla F(x_\psi^l) - (\bar{z}^l)^\top \mathbf{1} \right\|^2 \right] + \varrho_c \gamma^2 \sum_{l=0}^k n\sigma^2 \\
& \stackrel{(a)}{\leq} c_c + 3\varrho_c \gamma^2 \sum_{l=0}^k \mathbb{E} \left[\left\| \bar{z}_{i^l}^l - \xi_{i^l}^{l-1} (\bar{z}^l)^\top \mathbf{1} \right\|^2 \right] + 3\varrho_c \gamma^2 \sum_{l=0}^k \mathbb{E} \left[\left\| \sum_{i=1}^n (\nabla f_i(x_i^k) - \nabla f_i(x_\psi^k)) \right\|^2 \right] \\
& \quad + \varrho_c \gamma^2 \sum_{l=0}^k \left(3\mathbb{E} \left[\|\nabla F(x_\psi^l)\|^2 \right] + n\sigma^2 \right) \\
& \stackrel{(b)}{\leq} c_c + 3\varrho_c \gamma^2 \sum_{l=0}^k \mathbb{E} \left[\left\| \bar{z}_{i^l}^l - \xi_{i^l}^{l-1} (\bar{z}^l)^\top \mathbf{1} \right\|^2 \right] + 3\varrho_c C_L^2 n \gamma^2 \sum_{l=0}^k \mathbb{E} \left[\|h^l - \mathbf{1}x_\psi^l\|^2 \right] \\
& \quad + \varrho_c \gamma^2 \sum_{l=0}^k \left(3\mathbb{E} \left[\|\nabla F(x_\psi^l)\|^2 \right] + n\sigma^2 \right),
\end{aligned}$$

and

$$\begin{aligned}
& \sum_{l=0}^k \mathbb{E} \left[\left\| \bar{z}_{i^l}^l - \xi_{i^l}^{l-1} (\bar{z}^l)^\top \mathbf{1} \right\|^2 \right] \\
& \leq c_t + 3\varrho_t \gamma^2 \sum_{l=0}^k \mathbb{E} \left[\left\| \bar{z}_{i^l}^l - \xi_{i^l}^{l-1} (\bar{z}^l)^\top \mathbf{1} \right\|^2 \right] + 3\varrho_t \gamma^2 \sum_{l=0}^k (\xi_{i^l}^{l-1})^2 \mathbb{E} \left[\|\nabla F(x_\psi^l)\|^2 \right] \\
& \quad + 3\varrho_t \gamma^2 \sum_{l=0}^k (\xi_{i^l}^{l-1})^2 \mathbb{E} \left[\left\| \nabla F(x_\psi^l) - (\bar{z}^l)^\top \mathbf{1} \right\|^2 \right] + \varrho_t \gamma^2 \sum_{l=0}^k n\sigma^2 \\
& \stackrel{(c)}{\leq} c_t + 3\varrho_t \gamma^2 \sum_{l=0}^k \mathbb{E} \left[\left\| \bar{z}_{i^l}^l - \xi_{i^l}^{l-1} (\bar{z}^l)^\top \mathbf{1} \right\|^2 \right] + 3\varrho_t \gamma^2 \sum_{l=0}^k \mathbb{E} \left[\left\| \sum_{i=1}^n (\nabla f_i(x_i^l) - \nabla f_i(x_\psi^l)) \right\|^2 \right] \\
& \quad + \varrho_t \gamma^2 \sum_{l=0}^k \left(3\mathbb{E} \left[\|\nabla F(x_\psi^l)\|^2 \right] + n\sigma^2 \right) \\
& \stackrel{(d)}{\leq} c_t + 3\varrho_t \gamma^2 \sum_{l=0}^k \mathbb{E} \left[\left\| \bar{z}_{i^l}^l - \xi_{i^l}^{l-1} (\bar{z}^l)^\top \mathbf{1} \right\|^2 \right] + 3\varrho_t C_L^2 n \gamma^2 \sum_{l=0}^k \mathbb{E} \left[\|h^l - \mathbf{1}x_\psi^l\|^2 \right] \\
& \quad + \varrho_t \gamma^2 \sum_{l=0}^k \left(3\mathbb{E} \left[\|\nabla F(x_\psi^l)\|^2 \right] + n\sigma^2 \right),
\end{aligned}$$

where we used (16) in (a) and (c), and used Assumption 4 in (b) and (d). Moreover, if we treat $\sum_{l=0}^k \mathbb{E} \left[\|h^l - \mathbf{1}x_\psi^l\|^2 \right]$ and $\sum_{l=0}^k \mathbb{E} \left[\left\| \bar{z}_{i^l}^l - \xi_{i^l}^{l-1} (\bar{z}^l)^\top \mathbf{1} \right\|^2 \right]$ as new variables x and y respectively, then the above two interconnected inequalities can be rewritten by

$$\begin{cases} x \leq c_c + 3\varrho_c \gamma^2 \cdot y + 3\varrho_c C_L^2 n \gamma^2 \cdot x + \varrho_c \gamma^2 \sum_{l=0}^k \left(3\mathbb{E} \left[\|\nabla F(x_\psi^l)\|^2 \right] + n\sigma^2 \right) \\ y \leq c_t + 3\varrho_t \gamma^2 \cdot y + 3\varrho_t C_L^2 n \gamma^2 \cdot x + \varrho_t \gamma^2 \sum_{l=0}^k \left(3\mathbb{E} \left[\|\nabla F(x_\psi^l)\|^2 \right] + n\sigma^2 \right) \end{cases}$$

Using simple calculation, we can easily know that when γ satisfies $\gamma < \frac{1}{\sqrt{3\varrho_c C_L^2 T + 3\varrho_t}}$, the intersection of 2 lines is exactly the upper bound of x and y , and the intersection is

$$\begin{aligned} x &= \frac{3\varrho_c \gamma^2}{1 - 3(\varrho_c C_L^2 n + \varrho_t) \gamma^2} \sum_{l=0}^k \mathbb{E} [\|\nabla F(x_\psi^l)\|^2] + \frac{(1 - 3\varrho_t \gamma^2) c_c + 3c_t \varrho_c \gamma^2}{1 - 3(\varrho_c C_L^2 n + \varrho_t) \gamma^2} \\ &\quad + \frac{\varrho_c n \gamma^2 (k+1)}{1 - 3(\varrho_c C_L^2 n + \varrho_t) \gamma^2} \sigma^2, \\ y &= \frac{3\varrho_t \gamma^2}{1 - 3(\varrho_c C_L^2 n + \varrho_t) \gamma^2} \sum_{l=0}^k \mathbb{E} \|\nabla F(x_\psi^l)\|^2 + \frac{(1 - 3\varrho_c C_L^2 n \gamma^2) c_t + 3c_c \varrho_t C_L^2 n \gamma^2}{1 - 3(\varrho_c C_L^2 n + \varrho_t) \gamma^2} \\ &\quad + \frac{\varrho_t n \gamma^2 (k+1)}{1 - 3(\varrho_c C_L^2 n + \varrho_t) \gamma^2} \sigma^2. \end{aligned}$$

The proof of Lemma 6 is thus completed. \square

APPENDIX C PROOF OF LEMMA 7

To prove Lemma 7, we resort to two supporting lemmas and give them first.

The first supporting lemma as follows provides the lower and upper bound of $\mathbb{E} \|\nabla F(x_\psi^k)\|^2$ within a time window of length T , in term of its value at the starting point in this window, up to certain errors.

Lemma 9. Suppose Assumption 1-5 hold. For $\forall k \geq 0$ and $t \in [1, T-1]$, $\mathbb{E} \|\nabla F(x_\psi^{kT+t})\|^2$ can be lower bounded by

$$\begin{aligned} \mathbb{E} [\|\nabla F(x_\psi^{kT+t})\|^2] &\geq \frac{1}{2} \mathbb{E} [\|\nabla F(x_\psi^{kT})\|^2] - 4\gamma^2 L^2 T \sum_{t=0}^{T-1} \mathbb{E} [\|\bar{z}_{ikT+t}^{kT+t} - \xi_{ikT+t}^{kT+t-1} (\bar{z}^{kT+t})^\top \mathbf{1}\|^2] \\ &\quad - 4\gamma^2 L^2 T \sum_{t=0}^{T-1} (\psi_{ikT+t}^{kT+t})^2 (\xi_{ikT+t}^{kT+t-1})^2 \mathbb{E} [\|\mathbf{1}^\top \bar{z}^{kT+t}\|^2] - 2\gamma^2 L^2 T^2 n \sigma^2, \end{aligned} \quad (56)$$

and can be upper bounded by

$$\begin{aligned} \mathbb{E} [\|\nabla F(x_\psi^{kT+t})\|^2] &\leq 2\mathbb{E} [\|\nabla F(x_\psi^{kT})\|^2] + 8\gamma^2 L^2 T \sum_{t=0}^{T-1} \mathbb{E} [\|\bar{z}_{ikT+t}^{kT+t} - \xi_{ikT+t}^{kT+t-1} (\bar{z}^{kT+t})^\top \mathbf{1}\|^2] \\ &\quad + 8\gamma^2 L^2 T \sum_{t=0}^{T-1} (\psi_{ikT+t}^{kT+t})^2 (\xi_{ikT+t}^{kT+t-1})^2 \mathbb{E} [\|\mathbf{1}^\top \bar{z}^{kT+t}\|^2] + 4\gamma^2 L^2 T^2 n \sigma^2. \end{aligned} \quad (57)$$

Proof. Applying (7) recursively, the update of x_ψ^{kT+t} can be written as

$$x_\psi^{kT+t} = x_\psi^{kT} - \gamma \sum_{j=0}^{t-1} \psi_{ikT+j}^{kT+j} (z_{ikT+j}^{kT+j})^\top.$$

Using the smoothness of $F(\cdot)$, we have

$$\begin{aligned}
& \mathbb{E} \left[\left\| \nabla F \left(x_{\psi}^{kT+t} \right) - \nabla F \left(x_{\psi}^{kT} \right) \right\|^2 \right] \leq L^2 \mathbb{E} \left[\left\| x_{\psi}^{kT+t} - x_{\psi}^{kT} \right\|^2 \right] = \gamma^2 L^2 \mathbb{E} \left[\left\| \sum_{j=0}^{t-1} \psi_{i^{kT+j}}^{kT+j} z_{i^{kT+j}}^{kT+j} \right\|^2 \right] \\
& \leq \gamma^2 L^2 (T-1) \sum_{j=0}^{T-2} \left(\psi_{i^{kT+j}}^{kT+j} \right)^2 \mathbb{E} \left[\left\| z_{i^{kT+j}}^{kT+j} \right\|^2 \right] \leq \gamma^2 L^2 T \sum_{t=0}^{T-1} \left(\psi_{i^{kT+t}}^{kT+t} \right)^2 \mathbb{E} \left[\left\| z_{i^{kT+t}}^{kT+t} \right\|^2 \right] \\
& = \gamma^2 L^2 T \sum_{t=0}^{T-1} \left(\psi_{i^{kT+t}}^{kT+t} \right)^2 \mathbb{E} \left[\left\| z_{i^{kT+t}}^{kT+t} - \bar{z}_{i^{kT+t}}^{kT+t} + \bar{z}_{i^{kT+t}}^{kT+t} \right\|^2 \right] \\
& \leq 2\gamma^2 L^2 T \sum_{t=0}^{T-1} \left(\psi_{i^{kT+t}}^{kT+t} \right)^2 \mathbb{E} \left[\left\| \bar{z}_{i^{kT+t}}^{kT+t} \right\|^2 \right] + 2\gamma^2 L^2 T n \sum_{t=0}^{T-1} \left(\psi_{i^{kT+t}}^{kT+t} \right)^2 \sigma^2 \\
& \leq 4\gamma^2 L^2 T \sum_{t=0}^{T-1} \mathbb{E} \left[\left\| \bar{z}_{i^{kT+t}}^{kT+t} - \xi_{i^{kT+t}}^{kT+t-1} (\bar{z}^{kT+t})^{\top} \mathbf{1} \right\|^2 \right] \\
& \quad + 4\gamma^2 L^2 T \sum_{t=0}^{T-1} \left(\psi_{i^{kT+t}}^{kT+t} \right)^2 \left(\xi_{i^{kT+t}}^{kT+t-1} \right)^2 \mathbb{E} \left[\left\| \mathbf{1}^{\top} \bar{z}^{kT+t} \right\|^2 \right] + 2\gamma^2 L^2 T^2 n \sigma^2.
\end{aligned}$$

Using $\|a + b\|^2 \leq 2\|a\|^2 + 2\|b\|^2$, we have

$$\begin{aligned}
& \mathbb{E} \left[\left\| \nabla F \left(x_{\psi}^{kT} \right) \right\|^2 \right] \\
& = \mathbb{E} \left[\left\| \nabla F \left(x_{\psi}^{kT} \right) - \nabla F \left(x_{\psi}^{kT+t} \right) + \nabla F \left(x_{\psi}^{kT+t} \right) \right\|^2 \right] \\
& \leq 2\mathbb{E} \left[\left\| \nabla F \left(x_{\psi}^{kT} \right) - \nabla F \left(x_{\psi}^{kT+t} \right) \right\|^2 \right] + 2\mathbb{E} \left[\left\| \nabla F \left(x_{\psi}^{kT+t} \right) \right\|^2 \right] \\
& \leq 8\gamma^2 L^2 T \sum_{t=0}^{T-1} \mathbb{E} \left[\left\| \bar{z}_{i^{kT+t}}^{kT+t} - \xi_{i^{kT+t}}^{kT+t-1} (\bar{z}^{kT+t})^{\top} \mathbf{1} \right\|^2 \right] \\
& \quad + 8\gamma^2 L^2 T \sum_{t=0}^{T-1} \left(\psi_{i^{kT+t}}^{kT+t} \right)^2 \left(\xi_{i^{kT+t}}^{kT+t-1} \right)^2 \mathbb{E} \left[\left\| \mathbf{1}^{\top} \bar{z}^{kT+t} \right\|^2 \right] + 4\gamma^2 L^2 T^2 n \sigma^2 + 2\mathbb{E} \left[\left\| \nabla F \left(x_{\psi}^{kT+t} \right) \right\|^2 \right].
\end{aligned}$$

Then we obtain the lower bound of $\mathbb{E} \left[\left\| \nabla F \left(x_{\psi}^{kT+t} \right) \right\|^2 \right]$ by rearranging the terms:

$$\begin{aligned}
\mathbb{E} \left[\left\| \nabla F \left(x_{\psi}^{kT+t} \right) \right\|^2 \right] & \geq \frac{1}{2} \mathbb{E} \left[\left\| \nabla F \left(x_{\psi}^{kT} \right) \right\|^2 \right] - 4\gamma^2 L^2 T \sum_{t=0}^{T-1} \mathbb{E} \left[\left\| \bar{z}_{i^{kT+t}}^{kT+t} - \xi_{i^{kT+t}}^{kT+t-1} (\bar{z}^{kT+t})^{\top} \mathbf{1} \right\|^2 \right] \\
& \quad - 4\gamma^2 L^2 T \sum_{t=0}^{T-1} \left(\psi_{i^{kT+t}}^{kT+t} \right)^2 \left(\xi_{i^{kT+t}}^{kT+t-1} \right)^2 \mathbb{E} \left[\left\| \mathbf{1}^{\top} \bar{z}^{kT+t} \right\|^2 \right] - 2\gamma^2 L^2 T^2 n \sigma^2.
\end{aligned}$$

Similarly, the upper bound of $\mathbb{E} \left[\left\| \nabla F \left(x_{\psi}^{kT+t} \right) \right\|^2 \right]$ can be obtained by

$$\begin{aligned}
& \mathbb{E} \left[\left\| \nabla F \left(x_{\psi}^{kT+t} \right) \right\|^2 \right] \\
& = \mathbb{E} \left[\left\| \nabla F \left(x_{\psi}^{kT+t} \right) - \nabla F \left(x_{\psi}^{kT} \right) + \nabla F \left(x_{\psi}^{kT} \right) \right\|^2 \right] \\
& \leq 2\mathbb{E} \left[\left\| \nabla F \left(x_{\psi}^{kT+t} \right) - \nabla F \left(x_{\psi}^{kT} \right) \right\|^2 \right] + 2\mathbb{E} \left[\left\| \nabla F \left(x_{\psi}^{kT} \right) \right\|^2 \right] \\
& \leq 2\mathbb{E} \left[\left\| \nabla F \left(x_{\psi}^{kT} \right) \right\|^2 \right] + 8\gamma^2 L^2 T \sum_{t=0}^{T-1} \mathbb{E} \left[\left\| \bar{z}_{i^{kT+t}}^{kT+t} - \xi_{i^{kT+t}}^{kT+t-1} (\bar{z}^{kT+t})^{\top} \mathbf{1} \right\|^2 \right] \\
& \quad + 8\gamma^2 L^2 T \sum_{t=0}^{T-1} \left(\psi_{i^{kT+t}}^{kT+t} \right)^2 \left(\xi_{i^{kT+t}}^{kT+t-1} \right)^2 \mathbb{E} \left[\left\| \mathbf{1}^{\top} \bar{z}^{kT+t} \right\|^2 \right] + 4\gamma^2 L^2 T^2 n \sigma^2.
\end{aligned}$$

The proof of Lemma 9 is completed. \square

The second supporting lemma as follows is obtained by applying the descent lemma recursively from $k = 0$ to a given total iteration.

Lemma 10. Suppose Assumption 1-5 hold. For the given total iteration of $\bar{k}T$, we have

$$\begin{aligned} & \frac{\gamma}{2} \sum_{k=0}^{\bar{k}-1} \sum_{t=0}^{T-1} \psi_{i^k T+t}^{kT+t} \xi_{i^k T+t}^{kT+t-1} \mathbb{E} \left[\left\| \nabla F(x_{\psi}^{kT+t}) \right\|^2 \right] - \frac{\gamma^2}{2} \sum_{k=0}^{\bar{k}T-1} \mathbb{E} \left[\left\| \nabla F(x_{\psi}^k) \right\|^2 \right] \\ & \leq F(x_{\psi}^0) - F^* + \frac{\gamma C_L^2 n}{2} \sum_{k=0}^{\bar{k}T-1} \mathbb{E} \left[\left\| h^k - \mathbf{1} x_{\psi}^k \right\|^2 \right] + \left(\frac{1}{2} + 2L\gamma^2 \right) \sum_{k=0}^{\bar{k}T-1} \mathbb{E} \left[\left\| \bar{z}_{i^k}^k - \xi_{i^k}^{k-1} (\bar{z}^k)^\top \mathbf{1} \right\|^2 \right] \\ & \quad + Ln\bar{k}T\gamma^2\sigma^2 - \sum_{k=0}^{\bar{k}T-1} \left(\frac{\gamma\psi_{i^k}^k \xi_{i^k}^{k-1}}{2} - 2L\gamma^2 (\psi_{i^k}^k)^2 (\xi_{i^k}^{k-1})^2 \right) \mathbb{E} \left[\left\| \mathbf{1}^\top \bar{z}^k \right\|^2 \right]. \end{aligned} \quad (58)$$

Proof. With (7), applying the descent lemma to F at x_{ψ}^k and x_{ψ}^{k+1} , gives that

$$\begin{aligned} & \mathbb{E} \left[F(x_{\psi}^{k+1}) \right] \leq \mathbb{E} \left[F(x_{\psi}^k) \right] + \gamma\psi_{i^k}^k \mathbb{E} \left[\left\langle \nabla F(x_{\psi}^k), -(\bar{z}_{i^k}^k)^\top \right\rangle \right] + \frac{L\gamma^2 (\psi_{i^k}^k)^2}{2} \mathbb{E} \left[\left\| \bar{z}_{i^k}^k \right\|^2 \right] \\ & \leq \mathbb{E} \left[F(x_{\psi}^k) \right] - \gamma\psi_{i^k}^k \mathbb{E} \left[\left\langle \nabla F(x_{\psi}^k), (\bar{z}_{i^k}^k)^\top \right\rangle \right] + \gamma\psi_{i^k}^k \mathbb{E} \left[\left\langle \nabla F(x_{\psi}^k), (\bar{z}_{i^k}^k)^\top - (z_{i^k}^k)^\top \right\rangle \right] \\ & \quad + L\gamma^2 (\psi_{i^k}^k)^2 \mathbb{E} \left[\left\| \bar{z}_{i^k}^k \right\|^2 \right] + L\gamma^2 (\psi_{i^k}^k)^2 \mathbb{E} \left[\left\| z_{i^k}^k - \bar{z}_{i^k}^k \right\|^2 \right] \\ & \stackrel{(a)}{\leq} \underbrace{\mathbb{E} \left[F(x_{\psi}^k) \right] - \gamma\psi_{i^k}^k \mathbb{E} \left[\left\langle \nabla F(x_{\psi}^k), (\bar{z}_{i^k}^k)^\top - \xi_{i^k}^{k-1} \mathbf{1}^\top \bar{z}^k \right\rangle \right]}_{T_1} - \underbrace{\gamma\psi_{i^k}^k \xi_{i^k}^{k-1} \mathbb{E} \left[\left\langle \nabla F(x_{\psi}^k), \mathbf{1}^\top \bar{z}^k \right\rangle \right]}_{T_2} \\ & \quad + 2L\gamma^2 (\psi_{i^k}^k)^2 \mathbb{E} \left[\left\| \bar{z}_{i^k}^k - \xi_{i^k}^{k-1} (\bar{z}^k)^\top \mathbf{1} \right\|^2 \right] + 2L\gamma^2 (\psi_{i^k}^k)^2 (\xi_{i^k}^{k-1})^2 \mathbb{E} \left[\left\| \mathbf{1}^\top \bar{z}^k \right\|^2 \right] \\ & \quad + \gamma\psi_{i^k}^k \mathbb{E} \left[\left\langle \nabla F(x_{\psi}^k), (\bar{z}_{i^k}^k)^\top - (z_{i^k}^k)^\top \right\rangle \right] + Ln\gamma^2\sigma^2, \end{aligned} \quad (59)$$

where in (a) we used Lemma 4. Using Cauchy's inequality, we can bound T_1 by

$$T_1 \leq \frac{\gamma^2 \psi_{i^k}^k}{2} \mathbb{E} \left[\left\| \nabla F(x_{\psi}^k) \right\|^2 \right] + \frac{\psi_{i^k}^k}{2} \mathbb{E} \left[\left\| \bar{z}_{i^k}^k - \xi_{i^k}^{k-1} (\bar{z}^k)^\top \mathbf{1} \right\|^2 \right]. \quad (60)$$

Using $\langle a, b \rangle = \frac{1}{2} (\|a\|^2 + \|b\|^2 - \|a - b\|^2)$, we can bound T_2 by

$$\begin{aligned} T_2 &= -\frac{\gamma\psi_{i^k}^k \xi_{i^k}^{k-1}}{2} \left(\mathbb{E} \left[\left\| \nabla F(x_{\psi}^k) \right\|^2 \right] + \mathbb{E} \left[\left\| \mathbf{1}^\top \bar{z}^k \right\|^2 \right] - \mathbb{E} \left[\left\| \nabla F(x_{\psi}^k) - \mathbf{1}^\top \bar{z}^k \right\|^2 \right] \right) \\ &= -\frac{\gamma\psi_{i^k}^k \xi_{i^k}^{k-1}}{2} \mathbb{E} \left[\left\| \nabla F(x_{\psi}^k) \right\|^2 \right] - \frac{\gamma\psi_{i^k}^k \xi_{i^k}^{k-1}}{2} \mathbb{E} \left[\left\| \mathbf{1}^\top \bar{z}^k \right\|^2 \right] + \frac{\gamma\psi_{i^k}^k \xi_{i^k}^{k-1}}{2} \mathbb{E} \left[\left\| \nabla F(x_{\psi}^k) - \mathbf{1}^\top \bar{z}^k \right\|^2 \right] \\ &\leq -\frac{\gamma\psi_{i^k}^k \xi_{i^k}^{k-1}}{2} \mathbb{E} \left[\left\| \nabla F(x_{\psi}^k) \right\|^2 \right] - \frac{\gamma\psi_{i^k}^k \xi_{i^k}^{k-1}}{2} \mathbb{E} \left[\left\| \mathbf{1}^\top \bar{z}^k \right\|^2 \right] + \frac{\gamma\psi_{i^k}^k \xi_{i^k}^{k-1}}{2} C_L^2 n \mathbb{E} \left[\left\| h^k - \mathbf{1} x_{\psi}^k \right\|^2 \right]. \end{aligned} \quad (61)$$

Substituting (60) and (61) into (59), yields that

$$\begin{aligned} & \mathbb{E} \left[F(x_{\psi}^{k+1}) \right] \leq \mathbb{E} \left[F(x_{\psi}^k) \right] - \frac{\gamma\psi_{i^k}^k \xi_{i^k}^{k-1}}{2} \mathbb{E} \left[\left\| \nabla F(x_{\psi}^k) \right\|^2 \right] + \frac{\gamma^2 \psi_{i^k}^k}{2} \mathbb{E} \left[\left\| \nabla F(x_{\psi}^k) \right\|^2 \right] \\ & \quad + \frac{\gamma\psi_{i^k}^k \xi_{i^k}^{k-1}}{2} C_L^2 n \mathbb{E} \left[\left\| h^k - \mathbf{1} x_{\psi}^k \right\|^2 \right] + \left(\frac{\psi_{i^k}^k}{2} + 2L\gamma^2 (\psi_{i^k}^k)^2 \right) \mathbb{E} \left[\left\| \bar{z}_{i^k}^k - \xi_{i^k}^{k-1} (\bar{z}^k)^\top \mathbf{1} \right\|^2 \right] \\ & \quad - \left(\frac{\gamma\psi_{i^k}^k \xi_{i^k}^{k-1}}{2} - 2L\gamma^2 (\psi_{i^k}^k)^2 (\xi_{i^k}^{k-1})^2 \right) \mathbb{E} \left[\left\| \mathbf{1}^\top \bar{z}^k \right\|^2 \right] + \gamma\psi_{i^k}^k \mathbb{E} \left[\left\langle \nabla F(x_{\psi}^k), (\bar{z}_{i^k}^k)^\top - (z_{i^k}^k)^\top \right\rangle \right] \\ & \quad + Ln\gamma^2\sigma^2 \\ & \leq \mathbb{E} \left[F(x_{\psi}^k) \right] - \frac{\gamma\psi_{i^k}^k \xi_{i^k}^{k-1}}{2} \mathbb{E} \left[\left\| \nabla F(x_{\psi}^k) \right\|^2 \right] + \frac{\gamma^2}{2} \mathbb{E} \left[\left\| \nabla F(x_{\psi}^k) \right\|^2 \right] + \frac{\gamma}{2} C_L^2 n \mathbb{E} \left[\left\| h^k - \mathbf{1} x_{\psi}^k \right\|^2 \right] \\ & \quad + \left(\frac{1}{2} + 2L\gamma^2 \right) \mathbb{E} \left[\left\| \bar{z}_{i^k}^k - \xi_{i^k}^{k-1} (\bar{z}^k)^\top \mathbf{1} \right\|^2 \right] - \left(\frac{\gamma\psi_{i^k}^k \xi_{i^k}^{k-1}}{2} - 2L\gamma^2 (\psi_{i^k}^k)^2 (\xi_{i^k}^{k-1})^2 \right) \mathbb{E} \left[\left\| \mathbf{1}^\top \bar{z}^k \right\|^2 \right] \\ & \quad + \gamma\psi_{i^k}^k \mathbb{E} \left[\left\langle \nabla F(x_{\psi}^k), (\bar{z}_{i^k}^k)^\top - (z_{i^k}^k)^\top \right\rangle \right] + Ln\gamma^2\sigma^2. \end{aligned}$$

Summing the above inequality over k from 0 to $\bar{k}T - 1$, taking full expectations we get

$$\begin{aligned}
& \frac{\gamma}{2} \sum_{k=0}^{\bar{k}-1} \sum_{t=0}^{T-1} \psi_{i^{kT+t}}^{kT+t} \xi_{i^{kT+t}}^{kT+t-1} \mathbb{E} \left[\left\| \nabla F \left(x_{\psi}^{kT+t} \right) \right\|^2 \right] - \frac{\gamma^2}{2} \sum_{k=0}^{\bar{k}T-1} \mathbb{E} \left[\left\| \nabla F \left(x_{\psi}^k \right) \right\|^2 \right] \\
& \leq F \left(x_{\psi}^0 \right) - F^* + \frac{\gamma C_L^2 n}{2} \sum_{k=0}^{\bar{k}T-1} \mathbb{E} \left[\left\| h^k - 1 x_{\psi}^k \right\|^2 \right] + \left(\frac{1}{2} + 2L\gamma^2 \right) \sum_{k=0}^{\bar{k}T-1} \mathbb{E} \left[\left\| \bar{z}_{i^k}^k - \xi_{i^k}^{k-1} \left(\bar{z}^k \right)^{\top} \mathbf{1} \right\|^2 \right] \\
& \quad + Ln\bar{k}T\gamma^2\sigma^2 - \sum_{k=0}^{\bar{k}T-1} \left(\frac{\gamma\psi_{i^k}^k \xi_{i^k}^{k-1}}{2} - 2L\gamma^2 \left(\psi_{i^k}^k \right)^2 \left(\xi_{i^k}^{k-1} \right)^2 \right) \mathbb{E} \left[\left\| \mathbf{1}^{\top} \bar{z}^k \right\|^2 \right].
\end{aligned}$$

The proof of Lemma 10 is completed. \square

With the above two supporting lemmas, we are ready to prove Lemma 7. According to (56) in Lemma 9, the lower bound of $\sum_{t=0}^{T-1} \psi_{i^{kT+t}}^{kT+t} \xi_{i^{kT+t}}^{kT+t-1} \mathbb{E} \left[\left\| \nabla F \left(x_{\psi}^{kT+t} \right) \right\|^2 \right]$ can be obtained by

$$\begin{aligned}
& \sum_{t=0}^{T-1} \psi_{i^{kT+t}}^{kT+t} \xi_{i^{kT+t}}^{kT+t-1} \mathbb{E} \left[\left\| \nabla F \left(x_{\psi}^{kT+t} \right) \right\|^2 \right] \\
& = \psi_{i^{kT}}^{kT} \xi_{i^{kT}}^{kT-1} \mathbb{E} \left[\left\| \nabla F \left(x_{\psi}^{kT} \right) \right\|^2 \right] + \sum_{t=1}^{T-1} \psi_{i^{kT+t}}^{kT+t} \xi_{i^{kT+t}}^{kT+t-1} \mathbb{E} \left[\left\| \nabla F \left(x_{\psi}^{kT+t} \right) \right\|^2 \right] \\
& \geq \frac{\psi_{i^{kT}}^{kT} \xi_{i^{kT}}^{kT-1}}{2} \mathbb{E} \left[\left\| \nabla F \left(x_{\psi}^{kT} \right) \right\|^2 \right] + \sum_{t=1}^{T-1} \frac{\psi_{i^{kT+t}}^{kT+t} \xi_{i^{kT+t}}^{kT+t-1}}{2} \mathbb{E} \left[\left\| \nabla F \left(x_{\psi}^{kT+t} \right) \right\|^2 \right] \\
& \quad - \left(4\gamma^2 L^2 T \sum_{t=0}^{T-1} \mathbb{E} \left[\left\| \bar{z}_{i^{kT+t}}^{kT+t} - \xi_{i^{kT+t}}^{kT+t-1} \left(\bar{z}^{kT+t} \right)^{\top} \mathbf{1} \right\|^2 \right] \right) \sum_{t=1}^{T-1} \psi_{i^{kT+t}}^{kT+t} \xi_{i^{kT+t}}^{kT+t-1} \\
& \quad - \left(4\gamma^2 L^2 T \sum_{t=0}^{T-1} \left(\psi_{i^{kT+t}}^{kT+t} \right)^2 \left(\xi_{i^{kT+t}}^{kT+t-1} \right)^2 \mathbb{E} \left[\left\| \mathbf{1}^{\top} \bar{z}^{kT+t} \right\|^2 \right] \right) \sum_{t=1}^{T-1} \psi_{i^{kT+t}}^{kT+t} \xi_{i^{kT+t}}^{kT+t-1} \\
& \quad - 2\gamma^2 L^2 T^2 n \sigma^2 \sum_{t=1}^{T-1} \psi_{i^{kT+t}}^{kT+t} \xi_{i^{kT+t}}^{kT+t-1} \\
& \stackrel{(a)}{\geq} \frac{\mathbb{E} \left[\left\| \nabla F \left(x_{\psi}^{kT} \right) \right\|^2 \right]}{2} \sum_{t=0}^{T-1} \psi_{i^{kT+t}}^{kT+t} \xi_{i^{kT+t}}^{kT+t-1} - \left(4\gamma^2 L^2 T \sum_{t=0}^{T-1} \mathbb{E} \left[\left\| \bar{z}_{i^{kT+t}}^{kT+t} - \xi_{i^{kT+t}}^{kT+t-1} \left(\bar{z}^{kT+t} \right)^{\top} \mathbf{1} \right\|^2 \right] \right) (T-1) \\
& \quad - \left(4\gamma^2 L^2 T \sum_{t=0}^{T-1} \left(\psi_{i^{kT+t}}^{kT+t} \right)^2 \left(\xi_{i^{kT+t}}^{kT+t-1} \right)^2 \mathbb{E} \left[\left\| \mathbf{1}^{\top} \bar{z}^{kT+t} \right\|^2 \right] \right) (T-1) - 2\gamma^2 L^2 T^2 n \sigma^2 (T-1) \\
& \stackrel{(b)}{\geq} \frac{r\eta^2 \mathbb{E} \left[\left\| \nabla F \left(x_{\psi}^{kT} \right) \right\|^2 \right]}{2} - 4\gamma^2 L^2 T^2 \sum_{t=0}^{T-1} \mathbb{E} \left[\left\| \bar{z}_{i^{kT+t}}^{kT+t} - \xi_{i^{kT+t}}^{kT+t-1} \left(\bar{z}^{kT+t} \right)^{\top} \mathbf{1} \right\|^2 \right] \\
& \quad - 4\gamma^2 L^2 T^2 \sum_{t=0}^{T-1} \left(\psi_{i^{kT+t}}^{kT+t} \right)^2 \left(\xi_{i^{kT+t}}^{kT+t-1} \right)^2 \mathbb{E} \left[\left\| \mathbf{1}^{\top} \bar{z}^{kT+t} \right\|^2 \right] - 2\gamma^2 L^2 T^3 n \sigma^2,
\end{aligned}$$

where we used

$$\sum_{t=1}^{T-1} \psi_{i^{kT+t}}^{kT+t} \xi_{i^{kT+t}}^{kT+t-1} \leq T-1, \tag{62}$$

and

$$\sum_{t=0}^{T-1} \psi_{i^{kT+t}}^{kT+t} \xi_{i^{kT+t}}^{kT+t-1} \geq r\eta^2 \tag{63}$$

in (a) and (b) respectively, according to Assumption 2 and 3, Lemma 1 and 2.

Further, with simple calculation, we can lower bound $\sum_{k=0}^{\bar{k}-1} \sum_{t=0}^{T-1} \psi_{ik^{T+t}}^k \xi_{ik^{T+t}}^{kT+t-1} \mathbb{E} \left[\left\| \nabla F \left(x_{\psi}^{kT+t} \right) \right\|^2 \right]$ by

$$\begin{aligned}
& \sum_{k=0}^{\bar{k}-1} \sum_{t=0}^{T-1} \psi_{ik^{T+t}}^k \xi_{ik^{T+t}}^{kT+t-1} \mathbb{E} \left[\left\| \nabla F \left(x_{\psi}^{kT+t} \right) \right\|^2 \right] \\
& \geq \sum_{k=0}^{\bar{k}-1} \frac{r\eta^2 \mathbb{E} \left[\left\| \nabla F \left(x_{\psi}^{kT} \right) \right\|^2 \right]}{2} - 4\gamma^2 L^2 T^2 \sum_{k=0}^{\bar{k}-1} \sum_{t=0}^{T-1} \mathbb{E} \left[\left\| \bar{z}_{ik^{T+t}}^{kT+t} - \xi_{ik^{T+t}}^{kT+t-1} (\bar{z}^{kT+t})^\top \mathbf{1} \right\|^2 \right] \\
& \quad - \sum_{k=0}^{\bar{k}-1} \sum_{t=0}^{T-1} 4\gamma^2 L^2 T^2 (\psi_{ik^{T+t}}^k)^2 (\xi_{ik^{T+t}}^{kT+t-1})^2 \mathbb{E} \left[\left\| \mathbf{1}^\top \bar{z}^{kT+t} \right\|^2 \right] - 2L^2 \bar{k} T^3 n \gamma^2 \sigma^2 \\
& = \frac{r\eta^2}{2} \sum_{k=0}^{\bar{k}-1} \mathbb{E} \left[\left\| \nabla F \left(x_{\psi}^{kT} \right) \right\|^2 \right] - 4\gamma^2 L^2 T^2 \sum_{k=0}^{\bar{k}-1} \mathbb{E} \left[\left\| \bar{z}_{ik}^k - \xi_{ik}^{k-1} (\bar{z}^k)^\top \mathbf{1} \right\|^2 \right] \\
& \quad - \sum_{k=0}^{\bar{k}-1} 4\gamma^2 L^2 T^2 (\psi_{ik}^k)^2 (\xi_{ik}^{k-1})^2 \mathbb{E} \left[\left\| \mathbf{1}^\top \bar{z}^k \right\|^2 \right] - 2L^2 \bar{k} T^3 n \gamma^2 \sigma^2.
\end{aligned}$$

Combining the above inequality with (58) in Lemma 10, gives that

$$\begin{aligned}
& \frac{\gamma r \eta^2}{4} \sum_{k=0}^{\bar{k}-1} \mathbb{E} \left[\left\| \nabla F \left(x_{\psi}^{kT} \right) \right\|^2 \right] - \frac{\gamma^2}{2} \sum_{k=0}^{\bar{k}-1} \mathbb{E} \left[\left\| \nabla F \left(x_{\psi}^k \right) \right\|^2 \right] \\
& \leq F(x_{\psi}^0) - F^* + \frac{\gamma C_L^2 n}{2} \sum_{k=0}^{\bar{k}-1} \mathbb{E} \left[\left\| h^k - \mathbf{1} x_{\psi}^k \right\|^2 \right] \\
& \quad + \left(\frac{1}{2} + 2L\gamma^2 + 2L^2 T^2 \gamma^3 \right) \sum_{k=0}^{\bar{k}-1} \mathbb{E} \left[\left\| \bar{z}_{ik}^k - \xi_{ik}^{k-1} (\bar{z}^k)^\top \mathbf{1} \right\|^2 \right] + Ln \bar{k} T \gamma^2 \sigma^2 + L^2 \bar{k} T^3 n \gamma^3 \sigma^2 \\
& \quad - \sum_{k=0}^{\bar{k}-1} \left(\frac{\gamma \psi_{ik}^k \xi_{ik}^{k-1}}{2} - 2L\gamma^2 (\psi_{ik}^k)^2 (\xi_{ik}^{k-1})^2 - 2\gamma^3 L^2 T^2 (\psi_{ik}^k)^2 (\xi_{ik}^{k-1})^2 \right) \mathbb{E} \left[\left\| \mathbf{1}^\top \bar{z}^k \right\|^2 \right].
\end{aligned} \tag{64}$$

Summing up (57) over k from 0 to $\bar{k} - 1$ and over t from 0 to $T - 1$, get that

$$\begin{aligned}
& \sum_{k=0}^{\bar{k}-1} \sum_{t=0}^{T-1} \mathbb{E} \left[\left\| \nabla F \left(x_{\psi}^{kT+t} \right) \right\|^2 \right] \\
& \leq 2 \sum_{k=0}^{\bar{k}-1} \sum_{t=0}^{T-1} \mathbb{E} \left[\left\| \nabla F \left(x_{\psi}^{kT} \right) \right\|^2 \right] + 8\gamma^2 L^2 T \sum_{k=0}^{\bar{k}-1} \sum_{t=0}^{T-1} \left(\sum_{t=0}^{T-1} \mathbb{E} \left[\left\| \bar{z}_{ik^{T+t}}^{kT+t} - \xi_{ik^{T+t}}^{kT+t-1} (\bar{z}^{kT+t})^\top \mathbf{1} \right\|^2 \right] \right) \\
& \quad + \sum_{k=0}^{\bar{k}-1} \sum_{t=0}^{T-1} \left(\sum_{t=0}^{T-1} 8\gamma^2 L^2 T (\psi_{ik^{T+t}}^k)^2 (\xi_{ik^{T+t}}^{kT+t-1})^2 \mathbb{E} \left[\left\| \mathbf{1}^\top \bar{z}^{kT+t} \right\|^2 \right] \right) + 4L^2 \bar{k} T^3 n \gamma^2 \sigma^2,
\end{aligned}$$

i.e.,

$$\begin{aligned}
& \sum_{k=0}^{\bar{k}-1} \mathbb{E} \left[\left\| \nabla F \left(x_{\psi}^k \right) \right\|^2 \right] \leq 2T \sum_{k=0}^{\bar{k}-1} \mathbb{E} \left[\left\| \nabla F \left(x_{\psi}^{kT} \right) \right\|^2 \right] + 8\gamma^2 L^2 T^2 \sum_{k=0}^{\bar{k}-1} \mathbb{E} \left[\left\| \bar{z}_{ik}^k - \xi_{ik}^{k-1} (\bar{z}^k)^\top \mathbf{1} \right\|^2 \right] \\
& \quad + \sum_{k=0}^{\bar{k}-1} 8\gamma^2 L^2 T^2 (\psi_{ik}^k)^2 (\xi_{ik}^{k-1})^2 \mathbb{E} \left[\left\| \mathbf{1}^\top \bar{z}^k \right\|^2 \right] + 4L^2 \bar{k} T^3 n \gamma^2 \sigma^2.
\end{aligned} \tag{65}$$

Computing (64) + $\frac{\gamma r \eta^2}{8T} \times (65)$, gives that

$$\begin{aligned}
& \left(\frac{\gamma r \eta^2}{8T} - \frac{\gamma^2}{2} \right) \sum_{k=0}^{\bar{k}T-1} \mathbb{E} \left[\|\nabla F(x_\psi^k)\|^2 \right] \leq F(x_\psi^0) - F^* + \frac{\gamma C_L^2 n}{2} \sum_{k=0}^{\bar{k}T-1} \mathbb{E} \left[\|h^k - \mathbf{1} x_\psi^k\|^2 \right] \\
& + \left(\frac{1}{2} + 2L\gamma^2 + (2T^2 + r\eta^2 T) L^2 \gamma^3 \right) \sum_{k=0}^{\bar{k}T-1} \mathbb{E} \left[\|\bar{z}_{i^k}^k - \xi_{i^k}^{k-1}(\bar{z}^k)^\top \mathbf{1}\|^2 \right] \\
& + Ln\bar{k}T\gamma^2\sigma^2 + L^2\bar{k}T^3n\gamma^3\sigma^2 + \frac{1}{2}r\eta^2L^2\bar{k}T^2n\gamma^3\sigma^2 \\
& - \sum_{k=0}^{\bar{k}T-1} \left(\frac{\gamma\psi_{i^k}^k \xi_{i^k}^{k-1}}{2} - 2L\gamma^2 (\psi_{i^k}^k)^2 (\xi_{i^k}^{k-1})^2 - (2T^2 + r\eta^2 T) L^2 \gamma^3 (\psi_{i^k}^k)^2 (\xi_{i^k}^{k-1})^2 \right) \mathbb{E} \left[\|\mathbf{1}^\top \bar{z}^k\|^2 \right],
\end{aligned} \tag{66}$$

and if the constant step size γ satisfies (33), i.e., $\gamma \leq \min \left\{ \frac{2}{(2T^2 + r\eta^2 T)L}, \frac{1}{8L} \right\}$, we have

$$\frac{1}{2} + 2L\gamma^2 + (2T^2 + r\eta^2 T) L^2 \gamma^3 \leq \frac{1+\gamma}{2}, \tag{67}$$

and

$$\frac{\gamma\psi_{i^k}^k \xi_{i^k}^{k-1}}{2} - 2L\gamma^2 (\psi_{i^k}^k)^2 (\xi_{i^k}^{k-1})^2 - (2T^2 + r\eta^2 T) L^2 \gamma^3 (\psi_{i^k}^k)^2 (\xi_{i^k}^{k-1})^2 \geq 0, \tag{68}$$

then (66) can be relaxed as

$$\begin{aligned}
& \left(\frac{\gamma r \eta^2}{8T} - \frac{\gamma^2}{2} \right) \sum_{k=0}^{\bar{k}T-1} \mathbb{E} \left[\|\nabla F(x_\psi^k)\|^2 \right] \\
& \leq F(x_\psi^0) - F^* + \frac{1+\gamma}{2} \sum_{k=0}^{\bar{k}T-1} \mathbb{E} \left[\|\bar{z}_{i^k}^k - \xi_{i^k}^{k-1}(\bar{z}^k)^\top \mathbf{1}\|^2 \right] + \frac{1}{2} r \eta^2 L^2 \bar{k} T^2 n \gamma^3 \sigma^2 \\
& + \frac{\gamma C_L^2 n}{2} \sum_{k=0}^{\bar{k}T-1} \mathbb{E} \left[\|h^k - \mathbf{1} x_\psi^k\|^2 \right] + Ln\bar{k}T\gamma^2\sigma^2 + L^2\bar{k}T^3n\gamma^3\sigma^2,
\end{aligned} \tag{69}$$

which is the result of Lemma 7.

APPENDIX D DEFINITION OF CONSTANTS

$$\begin{aligned}
E_1 \triangleq & \frac{32(C_L^2 n c_c + c_t)}{r\eta^2} + \frac{4(L^2 + 2n)c_c}{nT} + \frac{12c_c \varrho_t C_L^2 n}{r\eta^2 L} + \frac{24(F(x_\psi^0) - F^* + c_t)(L^2 + 2n)\varrho_c}{nr\eta^2 L} \\
& + \frac{3(c_t \varrho_c + c_c \varrho_t) C_L^2 n}{2r\eta^2 L^2} + \frac{3(C_L^2 n c_c + c_t)(L^2 + 2n)\varrho_c}{nr\eta^2 L^2} + \frac{3(L^2 + 2n)c_t \varrho_c}{16nTL^2} \\
& + \frac{9(L^2 + 2n)c_c \varrho_c \varrho_t C_L^2}{8r\eta^2 L^3} + \frac{9(L^2 + 2n)(c_t \varrho_c + c_c \varrho_t)\varrho_c C_L^2}{64r\eta^2 L^4}.
\end{aligned} \tag{70}$$

$$\begin{aligned}
E_2 \triangleq & \frac{3(L^2 + 2n)\varrho_c}{r\eta^2 L^2} \left(\varrho_t T + \varrho_c C_L^2 n T + L^2 T^3 + \frac{1}{2} r \eta^2 L^2 T^2 \right) + 4(L^2 + 2n)\varrho_c \\
& + \frac{24}{r\eta^2 L} (L^2 + 2n)\varrho_c (\varrho_t T + LT) + \frac{32}{r\eta^2} \left(\varrho_t n T + \varrho_c C_L^2 n^2 T + L^2 T^3 n + \frac{1}{2} r \eta^2 L^2 T^2 n \right).
\end{aligned} \tag{71}$$

APPENDIX E ANALYSIS OF CONSENSUS SCHEME ON AUGMENTED SYSTEM

The results in this section and Appendix F are similar to that of [25], although we are working with more general underlying topology. We include them for completeness.

It follows from Algorithm 2 that the recursions of v_i^k and x_i^k , $i \in \mathcal{V}$, can be described as follows:

$$v_{i^k}^{k+1} = x_{i^k}^k - \gamma^k z_{i^k}^k, \tag{72a}$$

$$x_{i^k}^{k+1} = w_{i^k i^k} v_{i^k}^{k+1} + \sum_{j \in \mathcal{N}_{i^k}^{\text{in}}(W)} w_{i^k j} v_j^{k-d_{v,j}^k}, \tag{72b}$$

$$v_j^{k+1} = v_j^k, \quad x_j^{k+1} = x_j^k, \quad \forall j \in \mathcal{V} \setminus \{i^k\}. \tag{72c}$$

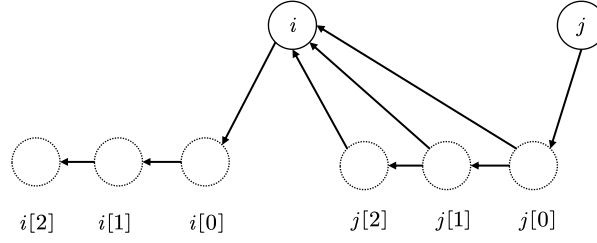


Figure 7. Illustration of constructing an augmented graph when the maximum delay $D = 2$. The above shows that three non-computing *virtual* nodes are added for each node.

We add $D+1$ virtual nodes for each node i , denoted by $i[0], i[1], \dots, i[D]$ (see Figure 7) and used for storing delayed information $v_i^k, v_i^{k-1}, \dots, v_i^{k-D}$. Any virtual node $i[d], d = D, D-1, \dots, 1$ can only receive information from virtual node $i[d-1]$; $i[0]$ can only receive information from the real node i or doesn't change the value. We give an example to illustrate the dynamics: at iteration k , any virtual node $i[d]$ for $i \in \mathcal{V}$ and $d = D, D-1, \dots, 1$ receives the information from $i[d-1]$ and replaces its own value with the received one; virtual node $i^k[0]$ replaces its own value with the information $x_{i^k}^k - \gamma^k z_{i^k}^k$ received from the real node i^k ; virtual nodes $j[0]$ for $j \neq i^k$ keep the value unchanged; the value of real node i^k becomes a weighted average of the $x_{i^k}^k - \gamma^k z_{i^k}^k$ and $v_j^{k-d_{v,j}^k}$ received from the virtual nodes $j[d_{v,j}^k]$ for $j \in \mathcal{N}_i^{\text{in}}(W)$; and the other real nodes keep the value unchanged.

Define $v^k \triangleq [v_1^k, \dots, v_n^k]^\top \in \mathbb{R}^{n \times p}$. Construct the $(D+2)n \times p$ dimensional concatenated variables of augmented system as

$$h^k \triangleq [x^k; v^k; v^{k-1}; \dots; v^{k-D}] \in \mathbb{R}^{(D+2)n \times p}, \quad (73)$$

and the augmented matrix $\hat{W}^k \in \mathbb{R}^{(D+2)n \times (D+2)n}$, defined as

$$\hat{W}_{rm}^k \triangleq \begin{cases} w_{i^k i^k}, & \text{if } r = m = i^k; \\ w_{i^k j}, & \text{if } r = i^k, m = j + (d_{v,j}^k + 1)n; \\ 1, & \text{if } r = m \in \{1, 2, \dots, 2n\} \setminus \{i^k, i^k + n\}; \\ 1, & \text{if } r \in \{2n+1, 2n+2, \dots, (D+2)n\} \\ & \cup \{i^k + n\} \text{ and } m = r - n; \\ 0, & \text{otherwise.} \end{cases} \quad (74)$$

The update of the augmented system can be rewritten in a compact form as

$$h^{k+1} = \hat{W}^k (h^k - \gamma^k e_{i^k} (z_{i^k}^k)^\top). \quad (75)$$

APPENDIX F

ANALYSIS OF GRADIENT TRACKING SCHEME ON AUGMENTED SYSTEM

In what follows, we call the real nodes in $\mathcal{G}(A)$ *computing nodes* and call the virtual nodes *noncomputing nodes*. Each Computing node $j \in \mathcal{V}$ can only send information to the noncomputing nodes $(j, i)^0$, for $i \in \mathcal{N}_j^{\text{out}}(A)$; each noncomputing node $(j, i)^d$ can either send information to the next noncomputing node $(j, i)^{d+1}$, or to the computing node i ; see Figure 8.

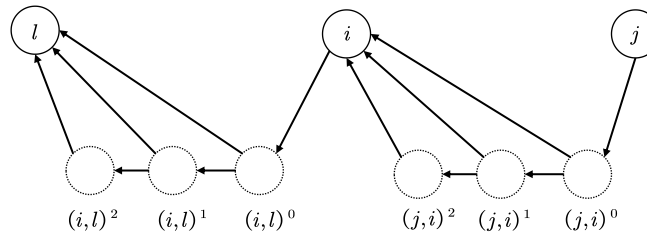


Figure 8. When the maximum delay $D = 2$, three noncomputing node are added for each edges $(j, i) \in \mathcal{E}(A)$ and $(i, l) \in \mathcal{E}(A)$.

For further description, we define $\mathcal{T}_i \triangleq \{k \mid i^k = i, k \in \mathbb{N}_0\}$ and it denotes the set of global iteration counter at which the computing node $i \in \mathcal{V}$ wakes up; let $\mathcal{T}_i^k \triangleq \{t \in \mathcal{T}_i \mid t \leq k\}$, it follows from (S.2 b,c) and (S.4) in Algorithm 2 that

$$\rho_{ij}^k = \sum_{t \in \mathcal{T}_j^{k-1}} a_{ij} z_j^{t+1/2} \text{ and } \tilde{\rho}_{ij}^k = \rho_{ij}^{k-1-d_{\rho,j}^{k-1}}, \quad (j, i) \in \mathcal{E}(A). \quad (76)$$

Remember that each computing node i stores z_i^0 at $k = 0$, and the values of the noncomputing agents are initialized to 0. At the beginning of iteration k , every computing agent i will store z_i^k whereas every noncomputing agent $(j, i)^d$ for $0 \leq d \leq D-1$, stores the mass $a_{ij}z_j$ (if any) generated by j for i at iteration $k-d-1$ (thus $k-d-1 \in \mathcal{T}_j^{k-1}$), i.e., $a_{ij}z_j^{k-(d+1)+1/2}$ (cf. (S.2 b,c) in Algorithm 2), and not been used by i yet; otherwise it stores 0. Formally, we have

$$z_{(j,i)^d}^k \triangleq a_{ij}z_j^{t+1/2} \cdot 1[t = k-d-1 \in \mathcal{T}_j^{k-1} \ \& \ t+1 > k-1-d_{\rho,j}^{k-1}].$$

The virtual node $(j, i)^D$ cumulates all the masses $a_{ij}z_j^{k-(d+1)+1/2}$ with $d \geq D$, not received by i yet:

$$z_{(j,i)^D}^k \triangleq \sum_{t \in \mathcal{T}_j^{k-D-1}, t+1 > k-1-d_{\rho,j}^{k-1}} a_{ij}z_j^{t+1/2}. \quad (77)$$

Next we write the update of the z -variables of both the computing and noncomputing nodes, absorbing the $(\rho, \tilde{\rho})$ -variables using (76)-(77).

The update of augmented system can be divided into two steps: sum-step and push-step. In the sum-step, the update of the z -variables of the computing nodes can be written as:

$$z_{i^k}^{k+\frac{1}{2}} = z_{i^k}^k + \sum_{j \in \mathcal{N}_{i^k}^{\text{in}}(A)} \left(\rho_{i^k j}^{k-d_{\rho,j}^k} - \tilde{\rho}_{i^k j}^k \right) + \epsilon^k \stackrel{(76)-(77)}{=} z_{i^k}^k + \sum_{j \in \mathcal{N}_{i^k}^{\text{in}}(A)} \sum_{d=d_{\rho,j}^k}^D z_{(j,i^k)^d}^k + \epsilon^k; \quad (78a)$$

$$z_j^{k+\frac{1}{2}} = z_j^k, \quad j \in \mathcal{V} \setminus \{i^k\}. \quad (78b)$$

i.e., node i^k builds the update $z_{i^k}^k \rightarrow z_{i^k}^{k+\frac{1}{2}}$ based upon the masses transmitted by the noncomputing agents $(j, i^k)^{d_{\rho,j}^k}, (j, i^k)^{d_{\rho,j}^k+1}, \dots, (j, i^k)^D$ [cf. (78a)]. And the other computing nodes keep their masses unchanged [cf. (78b)]. The updates of the noncomputing agents is set to

$$z_{(j,i^k)^d}^{k+\frac{1}{2}} \triangleq 0, \quad d = d_{\rho,j}^k, \dots, D, \quad j \in \mathcal{N}_{i^k}^{\text{in}}(A); \quad (78c)$$

$$z_{(j',i)^{\tau}}^{k+\frac{1}{2}} \triangleq z_{(j',i)^{\tau}}^k, \quad \text{for all the other } (j', i)^{\tau} \in \widehat{\mathcal{V}}. \quad (78d)$$

The noncomputing agents in (78c) set their variables to zero (as they transferred their masses to i^k) while the other noncomputing agents keep their variables unchanged [cf. (78d)].

In the push-step, the update of the z -variables of the computing nodes are as follows:

$$z_{i^k}^{k+1} = a_{i^k i^k} z_{i^k}^{k+\frac{1}{2}}; \quad (79a)$$

$$z_j^{k+1} = z_j^{k+\frac{1}{2}}, \quad \text{for } j \in \mathcal{V} \setminus \{i^k\}. \quad (79b)$$

i.e., agent i^k keeps the portion $a_{i^k i^k} z_{i^k}^{k+\frac{1}{2}}$ of the new generated mass [cf. (79a)] whereas the other computing agents do not change their variables [cf. (79b)]. The noncomputing nodes update as:

$$z_{(i^k, \ell)^0}^{k+1} \triangleq a_{\ell i^k} z_{i^k}^{k+\frac{1}{2}}, \quad \ell \in \mathcal{N}_{i^k}^{\text{out}}(A); \quad (79c)$$

$$z_{(i,j)^0}^{k+1} \triangleq 0, \quad (i, j) \in \mathcal{E}, \quad i \neq i^k; \quad (79d)$$

$$z_{(i,j)^d}^{k+1} \triangleq z_{(i,j)^{d-1}}^{k+\frac{1}{2}}, \quad d = 1, \dots, D-1, \quad (i, j) \in \mathcal{E}; \quad (79e)$$

$$z_{(i,j)^D}^{k+1} \triangleq z_{(i,j)^D}^{k+\frac{1}{2}} + z_{(i,j)^{D-1}}^{k+\frac{1}{2}}, \quad (i, j) \in \mathcal{E}. \quad (79f)$$

i.e., the computing agent i^k pushes its masses $a_{\ell i^k} z_{i^k}^{k+\frac{1}{2}}$ to the noncomputing agents $(i^k, \ell)^0$, with $\ell \in \mathcal{N}_{i^k}^{\text{out}}(A)$ [cf. (79c)]. The other noncomputing nodes $(i, j)^0$, $i \neq i^k$ set their variables to zero [cf. (79d)]. The noncomputing nodes $(i, j)^d$ for $0 \leq d \leq D-1$, transfers their mass to the next noncomputing node $(j, i)^{d+1}$ [cf. (79f), (79e)].

Remember that the $S \times p$ dimensional concatenated tracking variables \hat{z}^k is defined in (9). The transition matrix S^k of the sum step is defined as

$$S_{hm}^k \triangleq \begin{cases} 1, & \text{if } m \in \{(j, i^k)^d \mid d_{\rho,j}^k \leq d \leq D\} \\ & \text{and } h = i^k; \\ 1, & \text{if } m \in \widehat{\mathcal{V}} \setminus \{(j, i^k)^d \mid d_{\rho,j}^k \leq d \leq D\} \\ & \text{and } h = m; \\ 0, & \text{otherwise.} \end{cases}$$

Therefore, the sum-step can be written in compact form as

$$\hat{z}^{k+\frac{1}{2}} = S^k \hat{z}^k + e_{i^k} (\epsilon^k)^\top. \quad (80)$$

Define the transition matrix P^k of the push step as

$$P_{hm}^k \triangleq \begin{cases} a_{ji^k}, & \text{if } m = i^k \text{ and } h = (j, i^k)^0, j \in \mathcal{N}_{i^k}^{\text{out}}(A); \\ a_{i^k i^k}, & \text{if } m = h = i^k; \\ 1, & \text{if } m = h \in \mathcal{V} \setminus i^k; \\ 1, & \text{if } m = (i, j)^d, h = (i, j)^{d+1}, (i, j) \in \mathcal{E}(A), 0 \leq d \leq D-1; \\ 1, & \text{if } m = h = (i, j)^D, (i, j) \in \mathcal{E}(A); \\ 0, & \text{otherwise} \end{cases} \quad (81)$$

Then, the push-step can be written as

$$\hat{z}^{k+1} = P^k \hat{z}^{k+\frac{1}{2}}. \quad (82)$$

Combing (80) and (82), yields

$$\hat{z}^{k+1} = \hat{A}^k \hat{z}^k + P^k e_{i^k} (\epsilon^k)^\top, \quad \hat{A}^k = P^k S^k. \quad (83)$$

with initialization: $z_i^0 \in \mathbb{R}^p$ for $i \in \mathcal{V}$ and $z_i^0 = 0$ for $i \in \hat{\mathcal{V}} \setminus \mathcal{V}$.

APPENDIX G USED WEIGHT MATRICES AND ARCHITECTURE DESIGN

In this section, we present the specific weight matrices used in the experiments in the main text and provide some other possible topologies to illustrate the flexibility of architecture design.

Weight matrices used in experiments. The corresponding row (resp. column) stochastic weight matrix W (resp. A) satisfying Assumption 1 can be easily designed by knowing the number of in-neighbors (resp. out-neighbors).

For binary tree structure, the corresponding weight matrices are designed as Figure 9.

For directed ring structure, the corresponding weight matrices are designed as Figure 10.

For line structure, the corresponding weight matrices are designed as Figure 11.

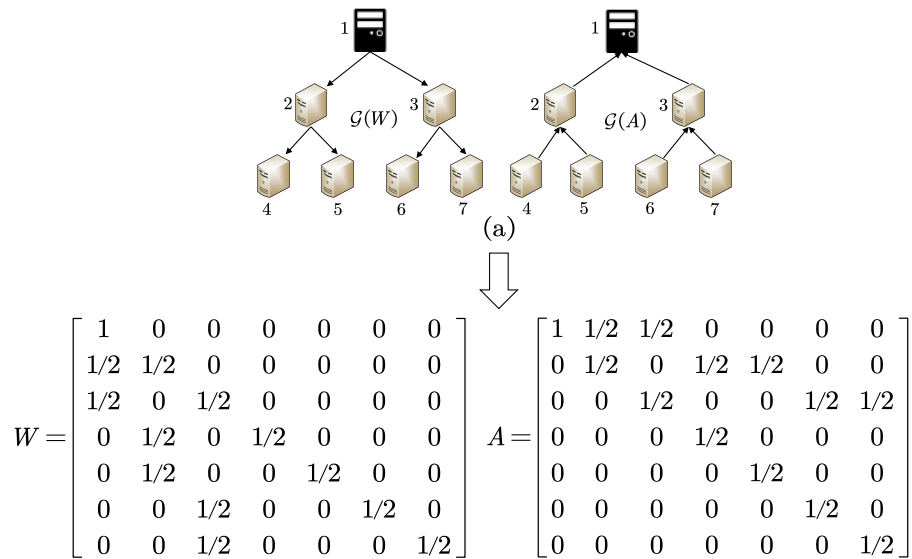


Figure 9. Weight matrices for binary tree structure.

Furthermore, we report several other possible graphs to illustrate the simplicity and flexibility of our proposed R-FAST algorithm for communication topology design.

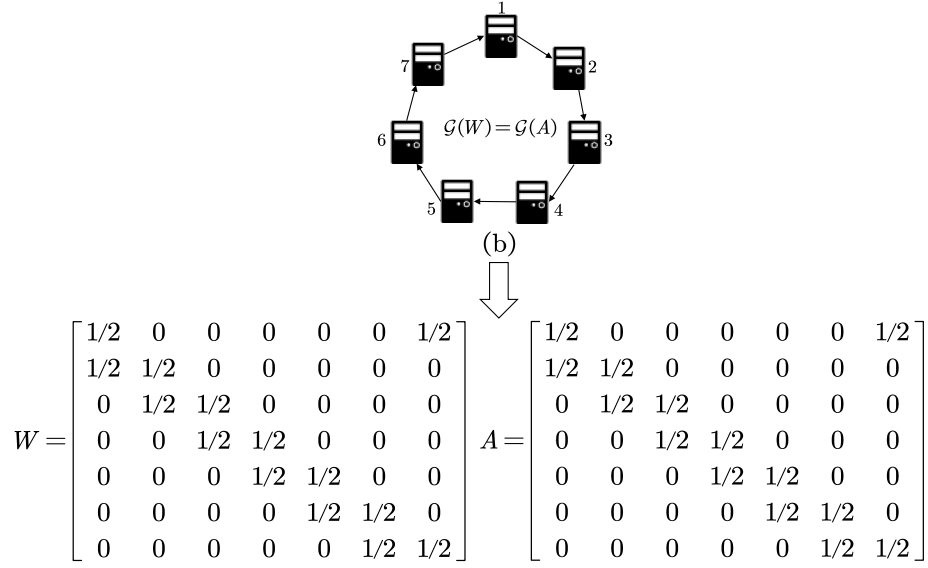


Figure 10. Weight matrices for directed ring structure.

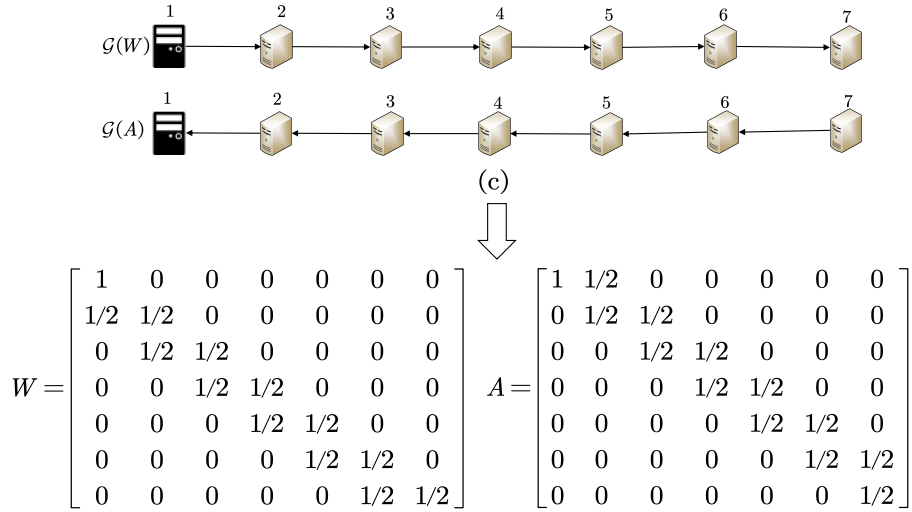


Figure 11. Weight matrices for line structure.

Flexibility of communication topology design. We present three different strategies of topology design based on an *unbalanced* strongly connected graph \mathcal{G} in Figure 12, where each row of subfigures indicates a way to splitting the original topology \mathcal{G} into two non-strongly-connected sub-graphs $\mathcal{G}(W)$ and $\mathcal{G}(A)$ with different sets of common root nodes satisfying Assumption 2. It follows that the minimum assumption of the proposed R-FAST algorithm imposed on the topology allows us to freely design the topologies of sub-graphs and the corresponding weight matrices of R-FAST. For instance, we can see from the bottom row of subfigures that nodes $\{1, 2, 3\}$ are chosen as common roots of sub-graphs $\mathcal{G}(W)$ and $\mathcal{G}(A)$, which resembles the group of servers in the Pramater-Server structure [11] that have higher computing power and communication bandwidth while other nodes serve as workers (clients) to provide training data and calculated gradient vectors. As such, our proposed R-FAST algorithm enjoys great flexibility of communication topology design to account for ad-hoc requirement in real training environments.

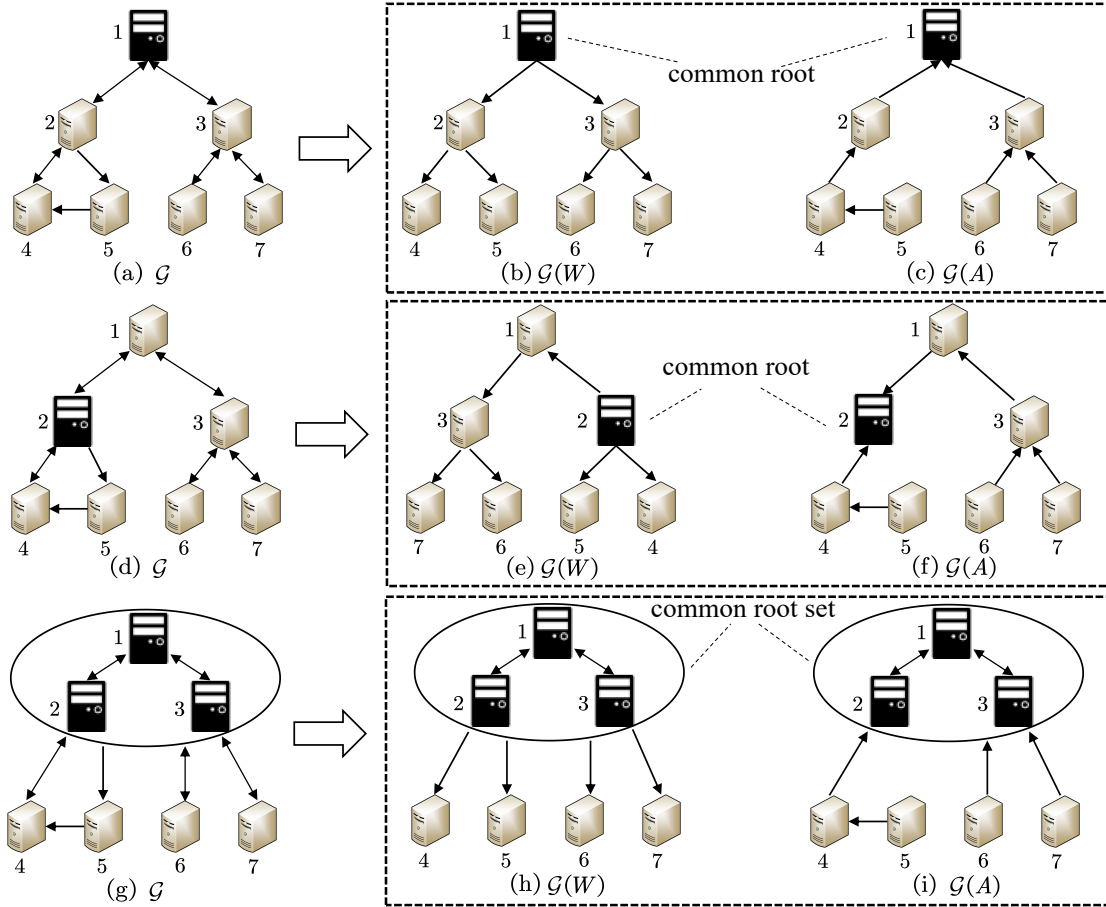


Figure 12. Illustration of the simplicity and flexibility of topology design. The left sub-figures (a), (d) and (g) denote the original topology and the middle ((b),(e), (h)) and right subfigures ((c),(f), (i)) represent the two non-strongly-connected sub-graphs